Charles University in Prague
1st faculty of medicine
Institute of Experimental Medicine, The Czech Academy of Sciences

PhD Programme in Biomedicine
Study discipline: Neuroscience

MUDr. Tetyana Chumak

Role of Islet1, BDNF and nanoparticles in development, function and regeneration of the auditory system.

Úloha Islet1, BDNF a nanočástic ve vývoji, funkci a regeneraci sluchového systému

PhD thesis

Supervisor: Prof. MUDr. Josef Syka, DrSc.

Prague 2016

Prohlášení:

Prohlašuji, že jsem závěrečnou práci zpracovala samostatně a že jsem řádně uvedla a citovala všechny použité prameny a literaturu. Současně prohlašuji, že práce nebyla využita k získání jiného nebo stejného titulu.

Souhlasím s trvalým uložením elektronické verze mé práce v databázi systému meziuniverzitního projektu Theses.cz za účelem soustavné kontroly podobnosti kvalifikačních prací.

V Praze, 16. 6. 2016

Indentifikacní záznam (Referencing):

CHUMAK, Tetyana. Úloha Islet1, BDNF a nanočástic ve vývoji, funkci a regeneraci sluchového systému. [Role of Islet 1, BDNF and nanoparticles in development, function and regeneration of the auditory system.] Praha, 2016. 139 stran, 3 přílohy. Disertační práce (Ph.D.). Univerzita Karlova v Praze, 1. lékařská fakulta, Ústav experimentální medicíny, AV ČR. Školitel prof. MUDr. Josef Syka, DrSc.

ACKNOWELEDGEMENT

First off I want to thank my supervisor, Prof. MUDr. Josef Syka, DrSc., for giving me the opportunity to conduct my PhD research in the pleasant and well equipped environment of his laboratory. I greatly appreciate his wise guidance and trust in my abilities. I would also like to express my gratitude to Dr. Popelář, whose help, patience and kindness have accompanied all the years of my study. Special thanks go to the members of our research group for being a source of friendships as well as excellent advice and collaboration.

Last but not least I would like to thank my family and close friends for their love, patience and support.

ABSTRACT

Detailed knowledge of the role that particular genes and factors play during the development and in the normal function of the auditory system is necessary to develop successful regenerative inner ear therapies. Islet1 transcription factor and brain derived neurothrophic factor (BDNF) have great potential to play a role in regenerative inner ear therapy as both have been shown to be sufficient for self-repair regeneration in cochlea in animal studies. In this study we looked at the roles these two factors play in the development and function of the auditory system.

In the transgenic mice used in the study, overexpression of Isl1 affected cell specification during embryonic development, leading to enlargement of the cochleovestibular ganglion and accelerated nerve fiber extension and branching in mutant embryos. The hearing of young transgenic mice was not affected. However, it started to decline in 1-month-old animals. This early onset of age-related hearing loss was found to be a consequence of the neurodegeneration of the olivocochlear system caused by Pax2-driven Isl1 misexpression in the hindbrain. Our data provide the first evidence that the alternation of the olivocochlear system efferent system accelerates the age-related functional decline of hearing without the loss of OHCs.

The functional role of BDNF in the mature auditory system was studied using mutant mice with conditional deletion of BDNF in the lower parts of the auditory pathway. The deletion of BDNF impaired frequency and intensity coding, and affected the inhibitory circuitry in the inferior colliculus, suggesting the importance of BDNF for normal sound processing in the ascending auditory pathway.

Another important step in regenerative therapy is the atraumatic delivery of an active agent to the specific cochlear tissue for targeted action. We tested three types of nanoparticles (NPs; liposomes, polymersomes and polylysine) as a potential tool for minimally invasive intracochlear drug delivery after middle ear application in adult animals. All NPs penetrated the round window membrane and were identified in the spiral ganglion, the organ of Corti and the lateral wall, producing no distinct morphological or functional damage to the inner ear. Using a model neurotoxic drug, liposomes and polymersomes were shown to be capable of carrying into the inner ear an active drug that elicits a detectable biological effect.

Results presented in this thesis contribute to knowledge about the role of Islet1 and BDNF in the development and function of the auditory system. Together with results of nanoparticle testing these data may contribute to the development of regenerative therapy for the inner ear.

Key words: Islet1, BDNF, cochlea, inferior colliculus, regeneration, development, drug delivery, nanoparticles

ABSTRAKT

Podmínkou úspěšného vývoje regenerační terapie ztráty sluchu je detailní znalost funkce jednotlivých genů a faktorů uplatňujících se během vývoje sluchového systému. Mezi faktory důležité pro vyvolání procesů regenerace ve vnitřním uchu patří transkripční faktor Islet1 a mozkový neurotrofní faktor BDNF. V předkládané dizertační práci je studována role obou faktorů ve vývoji a funkci sluchového systému a také možnosti využití nanočástic jako možného bezpečného prostředku pro jejich cílené doručení do kochley.

U embryí transgenních myší se zvýšenou expresí Islet1 (s Pax2 promotorem) bylo pozorováno větší kochleovestibulární ganglium a indukoval se zrychlený růst a větvení nervových vláken u embryí. Funkční testy měření kmenových potenciálů a otoakustických emisí ukázaly, že u mladých transgenních myší byla sluchová funkce na úrovni kontrolních myší, ale byl pozorován brzký nástup sluchové ztráty způsobené stárnutím. Tato sluchová ztráta souvisela s degenerací zakončení eferentních kochleárních vláken mediálního olivokochleárního systému, která byla způsobena misexpresí Islet1 v zadním mozku. Tyto výsledky poprvé ukázaly, že poškození mediálního olivokochleárního systému může urychlit vznik sluchové ztráty během stárnutí bez ztráty vnějších vláskových buněk.

Úloha BDNF ve sluchovém systému byla studována na modelu mutantních myších s podmíněnou delecí BDNF v nižších oddílech sluchové dráhy. Měření odpovědi neuronů v colliculus inferior ukázalo, že u myší s delecí BDNF došlo k narušení kódování intenzitních a frekvenčních vlastností zvukových stimulů. Výsledky tak ukazují, že přítomnost BDNF v nižších částech sluchové dráhy je nezbytná pro správnou funkci celého sluchového systému při zpracování behaviorálně významných zvuků.

Důležitým předpokladem úspěšné regenerativní léčby je atraumatické a cílené dodání aktivní látky specificky do příslušné části vnitřního ucha. Testovali jsme 3 typy nanočástic (NP) jako možného prostředku doručení aktivní látky: liposomy, polymersomy a polylysiny. NP byly aplikovány u dospělých myší na membránu okrouhlého okénka a byla analyzována jejich distribuce ve vnitřním uchu. Všechny tři typy NP úspěšně pronikaly do vnitřního ucha a byly nalezeny ve spirálním gangliu, Cortiho orgánu i laterální stěně a to bez morfologického nebo funkčního poškození vnitřního ucha. Na příkladu NP plněných neurotoxickou látkou disulfiramem byla ukázána možnost využít liposomů a polymersomů jako nosičů aktivní látky, která vyvolá ve vnitřním uchu biologický efekt měřitelný funkčním testem.

Předkládaná práce přináší nové poznatky o funkci transkripčního faktoru Islet1 a mozkového neurotrofního faktoru BDNF ve sluchovém systému. Spolu s diskutovanými možnostmi cíleného doručení (targeted drug delivery) mohou výsledky přispět k vývoji regenerativní léčby senzorineurálních poruch sluchu.

Klíčová slova: Islet1, BDNF, kochlea, colliculus inferior, regenerace, vývoj, přenos léků, nanočástice

LIST OF ABBREVIATIONS

°C	The degree Celsius
ABR	Auditory brainstem response
AC	Auditory cortex
AMPA	A-amino-3-hydroxy-5-methyl-4-isoxazolepropionic acid
AT	Acoustic trauma
BBN	Broadband noise
BDNF	Brain derived neurotrophic factor
Bs	Brain stem
Cb	Cerebellum
cDNA	Complementary deoxyribonucleic acid
CF	Characteristic frequency
CIC	Central nucleus of inferior colliculus
CN	Cochlear nucleus
CNS	Central nervous system
Cp	Threshold cycles
Cy3	Cyanic dye
DAB	Diaminobenzidine
DAPI	4',6-diamidino-2-phenylindole
dB	Decibel
DCIC	Dorsal cortex of inferior colliculus
DCN	Dorsal cochlear nucleus
DCs	Deiters' cells
DiI	1,1′-dioctadecyl-3,3,3′3′ tetramethylindocarbocyanine perchlorate
DNA	Deoxyribonucleic acid
DNase	Deoxyribonuclease
DPOAE	Distortion product of the otoacoustic emission
E	Embryonic day
eGFP	Enhanced green fluorescent protein
FL	Fluorescein
g	Grams
GABA	Gamma-aminobutyric acid
GAD67	Glutamic acid decarboxylase

GAPDH	Glyceraldehyde 3-phosphate dehydrogenase
h	Hour, hours
H2O2	Hydrogen peroxide
HC	Hair cells
Hprt1	Hypoxanthine phosphoribosyltransferase 1
HRP	Horseradish peroxidase
ChA	Choline acetyltransferase
IC	Inferior colliculus
IgG	Immunoglobulin G
IHC	Inner hair cell
IsI1	Islet 1
kg	Kilogram
kHz	Kilohertz
KO	Knock-out, bdnfpax2-KO
LCIC	Lateral cortex of inferior colliculus
LLN	Lateral lemniscus nuclei
M	Molar
m	Meter, meters
Mdn	Median
mFSL	Minimum first-spike latency
mg	Milligram
min	Minute, minutes
mM	Millimole
mm	Millimeter
Mn	Molar mass
MOC	Mideal olivocohlear bundle
mRNA	Messenger ribonucleic acid
Myo7a	Myosin 7a
n	Number
ns	Non-significant
NF200	200-kda neurofilament
nm	Nanometer
NMDA	N-methyl-D-aspartate

NT3	Neurotrophic factor 3
OAE	Otoacoustic emissions
OC	Organ of Corti
OHC	Outer hair cell
osl	Osseous spiral lamina
OW	Oval window
P	Postnatal day
p	Calculated probability
PBS	Phosphate-buffered saline
Pc	Posterior canal
PFA	Paraformaldehyde
pH	Logarithmic measure of hydrogen ion concentration
pl	Plasmid
PV	Parvalbumin
qPCR	Quantitative polymerase chain reaction
RIF	Rate-intensity function
RNA	Ribonucleic acid
ROSA26R	ROSA26 reporter mouse
RT-qPCR	Real-time quantitative polymerase chain reaction
RW	Round window
RWM	Round window membrane
s	Second, seconds
S	Saccule
SD	Standard deviation
SEM	Standard error of the mean
SG	Spiral ganglion
SGN	Spiral ganglion neuron
SM	Scala media
SNHL	Sensorineural hearing loss
SOC	Superior olivary complex
SPL	Sound pressure level
SR	Spontaneous rate
ST	Scala tympani

SV	Scala vestibuli
Tg	Transgenic
$Tg^{+/-}$	Pax2-Isl1 transgenic mice
Trk	Tyrosine kinase
VCN	Ventral cochlear nucleus
VG	Vestibular ganglion
WHO	World health organization
WT	Wild type
β-gal	B-galactosidase
µl	Microliter
µm	Micrometer

TABLE OF CONTENTS

1. Introduction

Hearing is a process of sound conversion into neural impulses in the inner ear and its interpretation by the central nervous system. Normal hearing is important for language development, learning and interpersonal communication. Loss of hearing is linked to feeling of social isolation, depression and possesses devastating impact on human well-being, education and employment. 360 million of people (over 5% of the world's population) have disabling hearing loss. Approximately one third of people over 65 years of age are affected by hearing loss and about 1.1 billion of youngsters are at risk of hearing loss due to the unsafe use of personal audio devices and exposure to damaging levels of recreational noise, according to World Health Organization. Appetite to recreational noise among the young people and demographic aging of the society will lead to increased population suffering age-related hearing loss (ARHL) and even higher social and economic demand to develop regenerative treatment for the cochlea.

Most often hearing loss is caused by damage to the inner ear or the VIII cerebral nerve (auditory nerve). This type of hearing loss is called sensorineural hearing loss (SNHL); it is accounted for 90% of all hearing loss and represents the most common sensory disorder in humans. In contrast to lower vertebrates, mammalian inner ear is not capable of spontaneous regeneration after damage. At present, people, suffering from hearing loss can benefit from a range of hearing aids and cochlear implants that recently significantly improved. However, a regeneration of damaged parts of the cochlea with full restoration of hearing would be the ideal scenario.

Recent development in the field of biotechnology and gene therapy opens new perspectives for the development of the inner ear regenerative therapy. First experimental attempts to initiate inner ear regeneration via activation of genes having protective and regenerative effect or deactivation of proapoptotic or damaging genes in the inner ear have been successful. However, to coordinate regenerative processes resulting in creation of morphologically and functionally mature cell a detailed understanding of mechanisms of inner ear development, maturation and degeneration is required.

Islet1 transcription factor and brain derived neurothrophic factor (BDNF) have a great potential to play a role in regenerative inner ear therapy. Both factors have been shown to be sufficient in self-repair regeneration in cochlea. The role of Islet1 in the development of the auditory system is largely unknown, however its overexpression in hair cells has been recently shown to protect cochlea from damage caused by noise or age (Huang et al., 2013).

BDNF is well known as a factor, responsible for development and maintenance of the spiral ganglion neurons and cochlear innervation. It has been also reported to protect spiral ganglion against degeneration in damaged cochlea (Shibata et al., 2010, Havenith et al., 2011, Pettingill et al., 2011, Fukui et al., 2012), and it's cochlear levels decrease with age (Ruttiger et al., 2007). The functional role of BDNF in the auditory system after onset of hearing, however, is still not fully understood.

In this study we will address the roles of these two factors in the development and function of the auditory system.

We will show that overexpression of Islet1 during early embryonic development is accompanied by increased number of precursors of sensory and neuronal cochlear cells and accelerated fiber growth in the brainstem supporting the idea of Islet1 importance during inner ear development and potential regenerative role. Unfortunately, this effect does not persist after birth and adult transgenic animals are, instead, more prone to age-related hearing loss. As we will show, hearing deterioration in transgenic animals is facilitated by degeneration of efferent fiber most likely caused by Islet1 misexpression in the brainstem. This finding suggests possible role of central neurodegeneration in age-related hearing loss and is supported by recent reports from the Bao and Maison laboratories (Fu et al., 2010, Liberman et al., 2014b).

In another mouse model we will investigate the impact of “peripheral” BDNF in function of the lower auditory brain structures. We will show that BDNF deletion in the lower parts of the auditory system leads to improper function of neurons in the inferior colliculus - one of the most important centers in the auditory brain. Our results suggest that after onset of hearing BDNF in the lower parts of the auditory system drives auditory fidelity along the entire ascending pathway up to the cortex by increasing inhibitory strength in behaviorally relevant frequency regions.

To trigger regenerative mechanisms in the damaged inner ear there is a need in a minimally invasive targeted delivery of therapeutic agents such as transcription factors, neurotrophic factors or genes inside cochlea. Nanoparticles are among the recently developed drug delivery technologies and are proposed as a suitable tool for cochlear regenerative therapy. In the present work we will discuss the results of application of three types of nanoparticles: liposomes, polymersomes and hyperbranched polylysine. We will show that all three types penetrate inside cochlea and cause by themselves no toxic effect and, in addition to that, lyposomes and polymersomes are capable of sufficient drug delivery inside the cochlea after round window membrane application.

1.1. Anatomy and function of the auditory system

1.1.1. Cochlea

The ear contains three partitions: outer, middle and inner ear (Figure 1). Outer ear (pinna and ear canal) collect sound and direct it toward tympanic membrane lying in its bottom and separating it from the middle ear. Middle ear is represented by an air-filled cavity connected with the nasopahrynx via Eustachian tube. It contains a chain of ossicles (the malleus, the incus, the stapes), thanks to which sound is amplified enough to be transformed from air filled middle ear cavity into the fluid filled inner ear cavity.

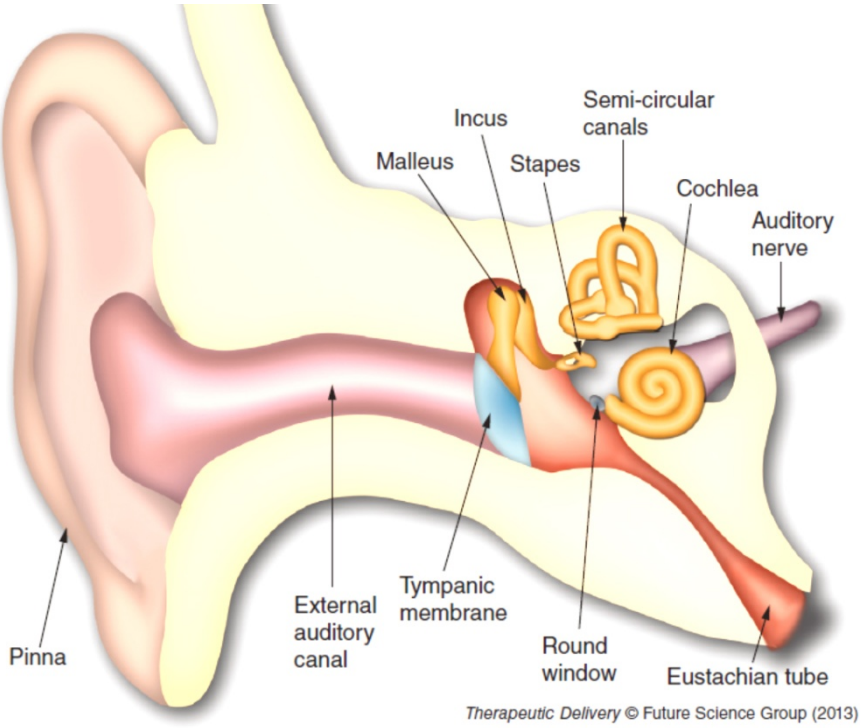

Figure 1. Coronal view of the ear.

See description in the text. Modified from (Hoskison et al., 2013).

Inner ear is divided into vestibular and auditory parts. Cochlea, the auditory part of the inner ear is located deep in the temporal bone and represented by a coiled tube that in mouse makes 1.75-2 turns around modiolus - the spongy bone in the center (Figure 2A). This bonny tube (bonny labyrinth) contains membranous labyrinth inside (Figure 2A). The membranous labyrinth (cochlear duct, scala media, SM) is filled with endolymph and houses the cochlear sensory organ- organ of Corti (OC) (Figure 2B, C). SM lies between two chambers: scala tympani (ST) below and scala vestibuli (SV) above. These chambers contain perilymph and communicate in the cochlear apex via a small hole- helicotrema. They both

end in the cochlear base each with a window: SV ends with oval window (OW) closed by the footplate of the stapes and ST ends with the round window (RW) closed by round window membrane (RWM). ST and SV serve for the transmission of pressure, caused by the sound wave coming from the middle ear through the footplate of stapes. When the pressure wave travels through the ST and SV from the oval window towards the round window it causes the vibrations to the walls of SM stimulating the cells of the OC.

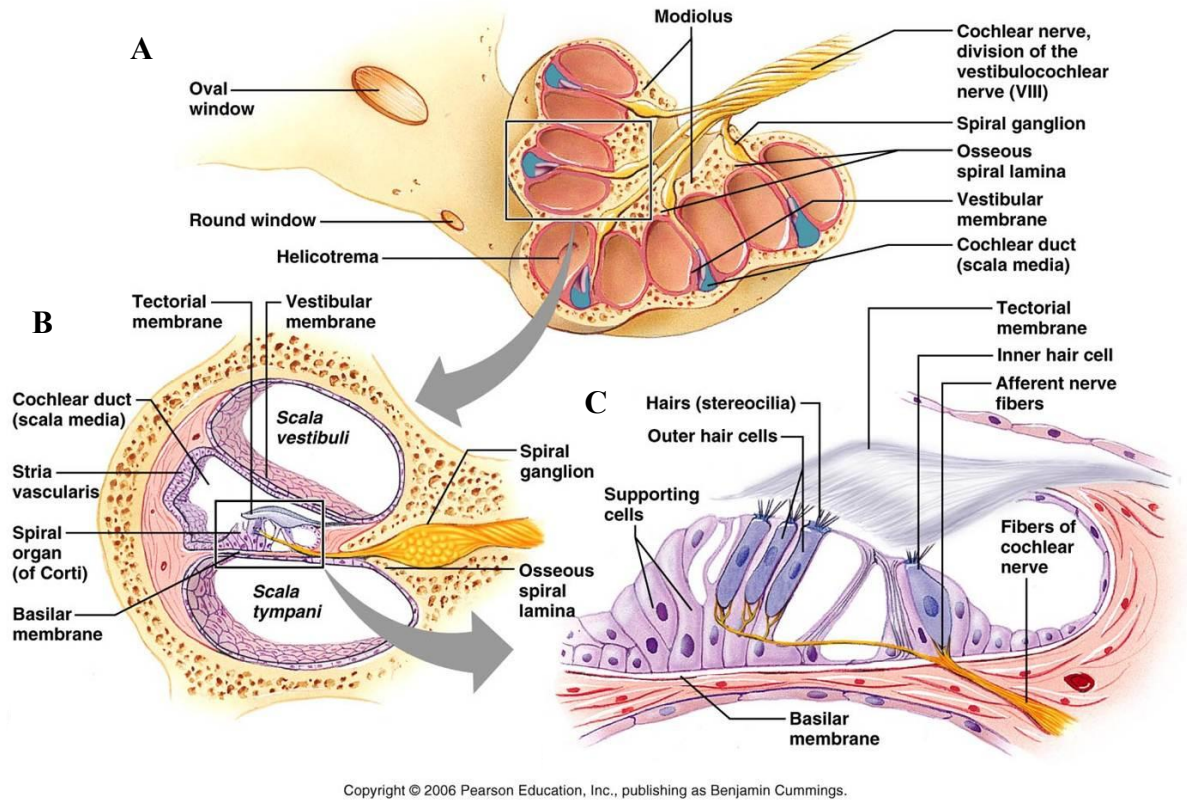

Figure 2. Crossection through cochlea

A. Schema of transmodiolar section trough all cochlear turns. B. A cochlear fragment showing section through one cochlear turn. C. Organ of Corti. Modified from Pearson Education, Inc., publishing as Benjamin Cummings.

Principal sensory cells of the OC - inner and outer hair cells (IHCs and OHCs, Figure 2C, Figure 3) are responsible for sound amplification and transduction. They received their name after stereocilia - "hair bundles" located on their apical surface (Figure 2C, Figure 3). Having stretch receptors, stereocilia can sense vibrations of the surrounding environment and transform them into electrical current. Pressure waves, evoked by sound, travel through the SM creating shearing forces between basilar and tectorial membranes (Figure 2C), that make stereocilia to move and bend. This causes ion channels in stereocilia to open and depolarize

the hair cells. Stereocilia on top of the cell is the only similarity between IHCs and OHCs – anatomy and function of these cells are rather distinct (Figure 3).

IHCs make one raw that extends along the cochlea from the base to the apex. They have pear shape and their stereocilia lie free in the endolymphatic space. Depolarization, triggered by IHCs stereocilia leads to release of neurotransmitter in the basilar part of cell, where it is densely contacted by afferent fibers (Figure 3). IHCs are contacted by 95% of afferent fibers representing main stream of the afferent information to the brain auditory centers. They receive also feedback innervation from the auditory brainstem- the efferent fibers synapse on the terminals of the contacting IHC afferent fibers (Figure 3). At the level of the IHCs coding of sound frequency and intensity occurs.

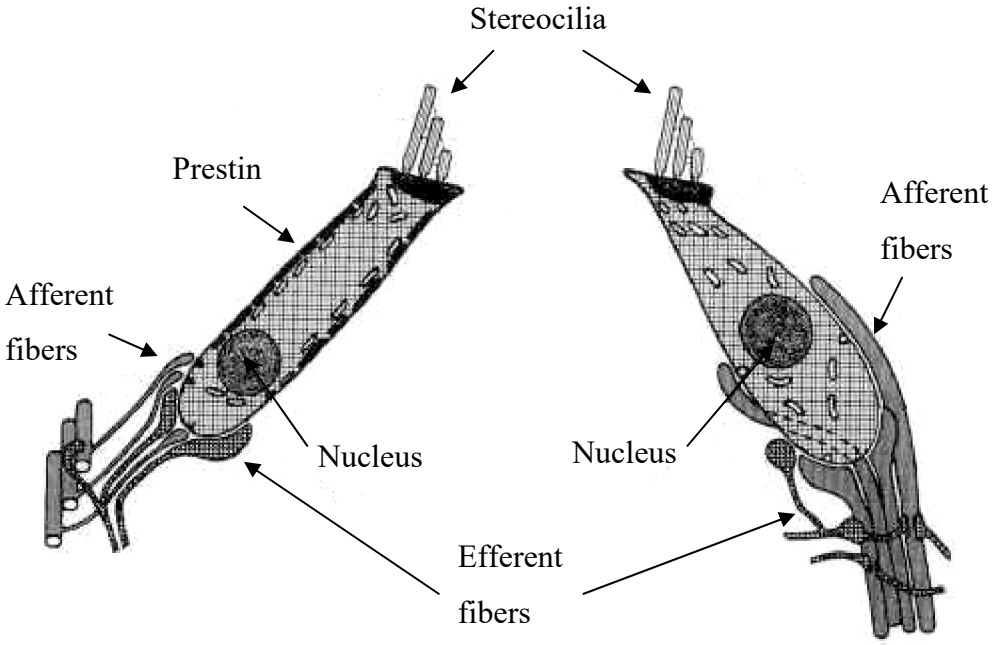

Figure 3. Innervation of the cochlear hair cells

IHCs receive abundant afferent innervation while OHCs are innervated mostly by efferent fibers. OHC: outer hair cell, IHC: inner hair cell.
Modified from http://www.eah-jena.de/~gitter/tut_hoer.html.

OHCs outnumber IHCs by about 3:1 and are arranged into 3 rows that lay on the cochlear basilar membrane laterally to the IHC row (Figure 2C). OHCs have cylindrical shape and their lateral wall contains motor protein – prestin (Figure 3). Stereocilia on top of the OHCs are embedded in the tectorial membrane. Depolarization, caused by stereocilia bending, activates prestin that makes OHC to contract. Active contraction of the OHCs increases the movements of the basilar membrane evoked by vibration of the perilymph in response to sound. This function is called cochlear amplification representing the main role of

the OHCs. OHC function is particularly important for perception of soft sounds and absence of OHCs leads to 40 to 60 dB hearing loss. They also improve sound perception when background noise is introduced. In contrast to IHCs the main source of OHCs innervation are efferent fibers from the brain (Figure 3). Affecting function of OHCs brain modulates cochlear sensitivity. OHCs receive also afferent innervation by remaining 5% of the afferent fibers coming to the cochlea. Role of this innervation is not fully understood yet.

Hair cells are surrounded and interdigitated by supporting cells. Altogether 5 types of supporting cells in the cochlea are distinguished. Two of them- inner and outer (Deiters') phalangeal cells come into direct contact with the IHCs and OHCs respectively. They play an active role in maintaining the hair cells structure, function and protection. There is also evidence that supporting cells receive synaptic connections (Eybalin et al., 1988, Merchanperez et al., 1993, Fechner et al., 2001, Huang et al., 2013) suggesting functions of these cells that are uncovered yet.

Afferent fiber and hair cell form a special type of contact – ribbon synapse. Presynaptic structure in this synapse – ribbon – docks vesicles with neurotransmitter (glutamate) enabling its gradual and fast multivesicular release. The afferent innervation that hair cells receive comes from the sensory neurons of the spiral ganglion (SG). SG sits in the modiolus and its neurons send their peripheral processes (dendrites) to the hair cells and central projections (axons) to the cochlear nucleus in the brainstem, starting ascending (afferent) auditory pathways. Two types of SGN neurons are distinguished: i) type I neurons make 90–95% of neuronal population and innervate IHCs, always one SGN contacts only one IHC, each hair cell is contacted by 10–20 SGNs depending on species and the particular position along the cochlea length; ii) type II neurons make remaining 5–10% of SGNs and contact exclusively OHCs, one neuron innervates 3–10 target cells. Accordingly, auditory nerve composed of central processes of the SGNs contains mostly axons of type I SGNs. Among them two subpopulation of fibers can be distinguished according to their physiological characteristics: fibers with low threshold and high spontaneous rate (SR>20 sp/s, sensitive fibers) and fibers with high threshold and low spontaneous rate (SR<20 sp/s) (Liberman, 1978). High-SR rate low-threshold fibers are activated in response to weak sound, but become saturated rapidly. More intense stimulation engages fibers with higher threshold and lower spontaneous rate. These fibers are important for hearing in a noisy environment due to their resistance to continuous background noise (Costalupes et al., 1984). Such progressive recruitment of nerve fibers from different populations can explain the extent of cochlear dynamics from perceptual threshold to the pain threshold.

Cochlear sensory cells and spiral ganglion neurons are tonotopically organized meaning that cells in different parts of the cochlea are sensitive to sounds of particular frequencies. Sounds of high frequencies are transduced at the cochlear base, while low frequency sounds are processed in the apex. This so called tonotopical organization persists in all auditory centers in the brain.

1.1.2. Afferent pathway, inferior colliculus

Cochlear part of the VIII nerve made of central SGN processes enters the brainstem and synapses on the neurons of the ipsilateral cochlear nucleus.

Cochlear nucleus initiates few parallel ascending pathways through the auditory centers in the lower brainstem that segregate auditory information coming from the cochlea and analyze different its parameters such as spectrum, timing and location of sound. Inferior colliculus (IC), as a center obligatory for almost all ascending auditory pathways, then integrates this information before sending it to the auditory thalamus and eventually auditory cortex for more complex analysis. Simplified schema of ascending auditory pathways is represented in Figure 4. Cochlear nucleus (CN) consists of two portions: dorsal (DCN) and ventral (VCN) cochlear nucleus. Each fiber coming from SG bifurcates as it enters the CN so that it sends a branch to both, DCN and VCN. Then this main branch sends numerous collaterals and synapse in different types of CN neurons. Axons of these CN neurons form few parallel ascending auditory pathways mentioned above. In the CN occurs decoding of sound temporal parameters such as stimulus duration, start and end of the stimulus (Schneggenburger and Forsythe, 2006, Golding and Oertel, 2012). Most of the fibers, leaving CN cross to the opposite side of the brainstem and either contact contralateral superior olivary complex (SOC) or ascend directly to the IC. Some of the fibers contact nuclei of the ipsilateral SOC. Thus some neurons in SOC obtain innervations from CNs from both sides enabling transfer and processing of information from two ears. This makes SOC an important auditory center in localization of sound by comparing difference in time and intensity between signals coming from different ears (Tollin et al., 2008, Grothe et al., 2010). On the way to the IC axons from the CN and SOC form lateral lemniscus. Some of them make a synaptic connection on the lateral lemniscus nuclei (LLN) that play a role in binaural hearing and analyses temporal pattern of the complex sound (Covey and Casseday, 1991).

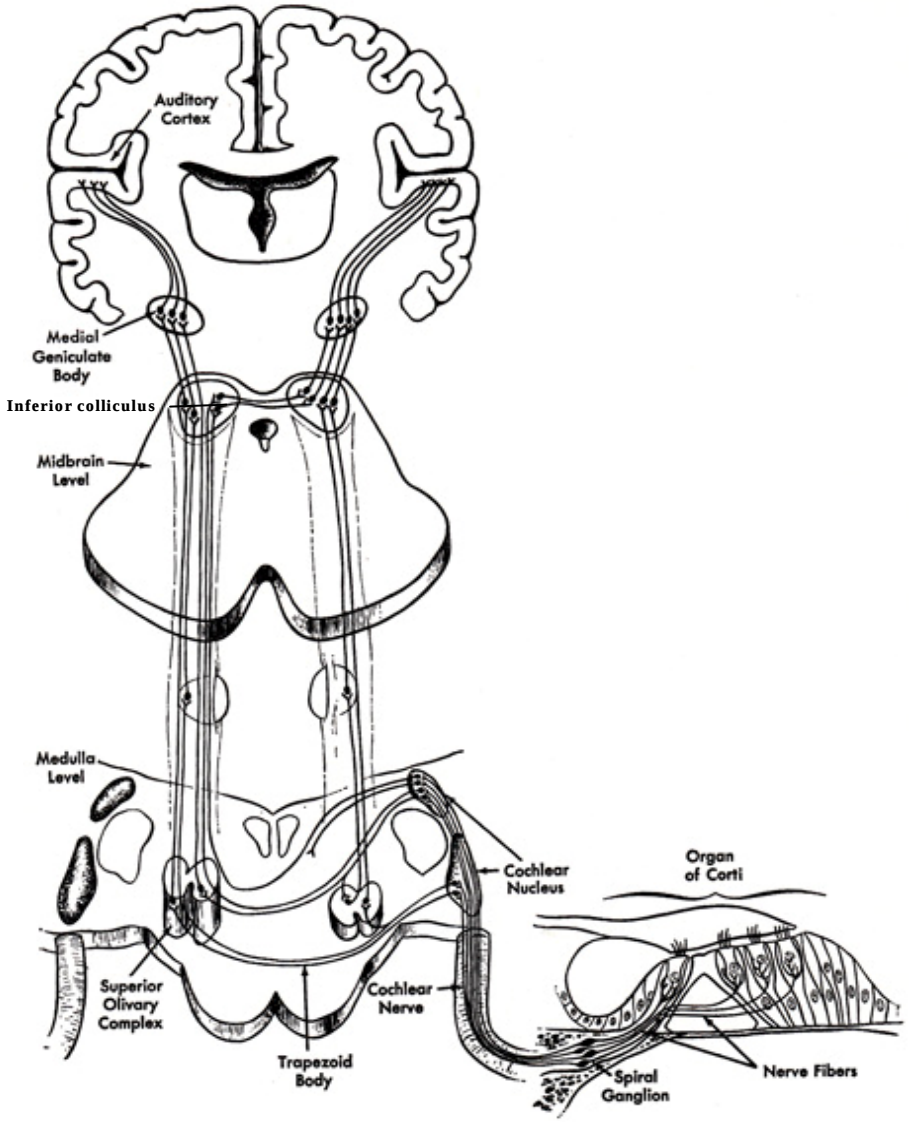

Figure 4. Simplified schema of the afferent auditory pathway

Description see in the text. Modified from http://gopixdatabase.com/gallery/auditory+pathway+animation/9.

IC is subdivided into 3 nuclei – central nucleus (CIC), and dorsal (DCIC) and lateral (LCIC) cortex (Fayelund and Osen, 1985) (Figure 5A).

The CIC represents a mainly ascending part of the primary auditory pathway. Afferent lemniscal fibers and IC neurons in CIC are organized in parallel laminae (Figure 5A) representing a structural basis for tonotopy in the IC (Stiebler and Ehret, 1985, Meininger et al., 1986, Reimer, 1993, Malmierca et al., 1995) (Figure 5B). Two main types of neurons are distinguished in the CIC based on the shape and orientation of the dendritic tree – bipolar and less common stellate neurons (Meininger et al., 1986). Most of the CIC neurons possess

NMDA and AMPA receptors and are thought to be represented predominantly by bipolar neurons (Merchan et al., 2005), about 25% of neurons are GABAergic (Kelly and Caspary, 2005) and are thought to be stellate neurons. Inhibition plays an important role in CIC (Pollak et al., 2011) as IC neuronal responses change dramatically when inhibition is inactivated (Faingold et al., 1991, Faingold et al., 1993, Palombi and Caspary, 1996, Casseday et al., 2000, Davis et al., 2003, Malmierca et al., 2003, Nataraj and Wenstrup, 2005, Sanchez et al., 2008).

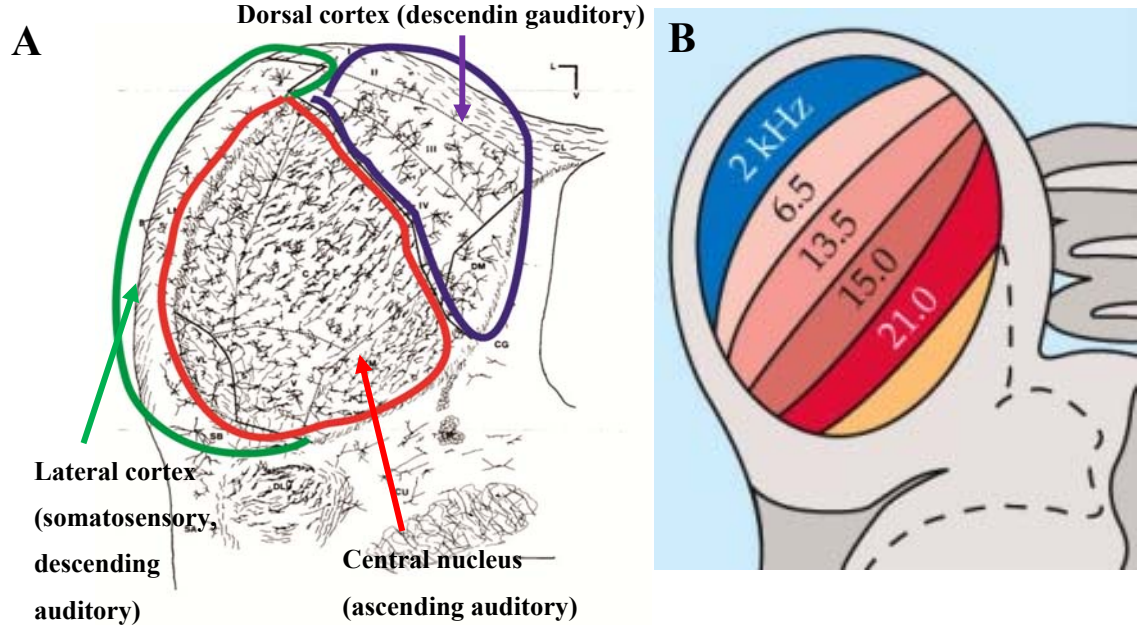

Figure 5. Structure of inferior colliculus.

A. Main subdevisions of the IC with main input to each part mentioned in brackets. Modified from http://www.physiology.wisc.edu/phys675lab/lab4_notes.htm. B. Schema of tonotopic organization in the I. Modified from (Serviere et al., 1984)

GABAergic inhibitory system in the IC modulates the spectral, temporal and binaural properties of IC responses sharpening the responses to rapid complex sounds (Le Beau et al., 1996, Sivaramakrishnan et al., 2004, Ingham and McAlpine, 2005). IC receives excitatory afferent input from DCN (Semple and Aitkin, 1980, Davis, 2002, Malmierca et al., 2005) and medial superior olive (Semple and Aitkin, 1980, Glendenning et al., 1992, Davis, 2002), while projections from LSO and LLN are a mixture of excitatory and inhibitory fibers (Adams and Mugnaini, 1984, Glendenning et al., 1992, Bajo et al., 1999, Riquelme et al., 2001). The CIC functional role in sound processing is complex and is still under investigation (Syka et al., 2000). After convergence of the excitatory and inhibitory inputs and interaction

between them in the IC a variety of new response properties are either formed de novo in the CIC or response properties that have been formed in lower nuclei are sharpened or further modified (Pollak et al., 2011).

Dorsomedial and caudal surface of the CIC is covered by DCIC, lateral surface by LCIC. Distinct feature of DCIC and LCIC neurons is presence of NO (Druga and Syka, 1993, Coote and Rees, 2008). Second layer of LCIC is particularly rich in acetylcholine and GABAergic neurons. DCIC receives afferent input similar to CIC; besides that together with LCIC it receives input from the auditory cortex and non-auditory structures (Druga and Syka, 1984b, a, Saldana et al., 1996, Druga et al., 1997, Winer et al., 1998, Malmierca, 2003, Schofield, 2009). LCIC receives relatively heavy input from somatosensory system (Robards, 1979, Zhou and Shore, 2006).

All IC subdivisions send projection to the thalamus and to the contralateral colliculus. Besides ascending fibers, IC receives heavy input from the auditory cortex, projections from the contralateral colliculus and possess dense intrinsic network of connections (Malmierca and Ryugoy, 2012).

LCIC seems to play a role in multisensory integration (Aitkin et al., 1978) and influence the function of the descending auditory system (Groff and Liberman, 2003, Ota et al., 2004). It may also provide auditory input to visual-motor areas that direct head and eye movements involved in gaze initiation (Loftus et al., 2008). DCIC is strongly influenced by bilateral descending pathways from the AC (Diamond et al., 1969, Druga and Syka, 1984a, b, Syka and Popelar, 1984, Fayelund, 1985, Syka et al., 1988, Druga et al., 1997, Yan and Ehret, 2001, Popelar et al., 2003, Winer, 2005a, b, Ayala et al., 2015, Popelar et al., 2016) suggesting that it is involved in attention to sound. Together with LCIC it possess neurons that respond selectively to novel stimuli and show rapid and pronounced habituation to identical stimuli suggesting their possible contribution to a rapid subcortical pathway for directing attention and/or orienting responses to novel sounds (Perez-Gonzalez et al., 2005).

1.1.3. Efferent control of the cochlea, olivocochlear system

Activity of the cochlear hair cells is modulated directly from the brain via efferent medial (MOC) and lateral (LOC) olivocochlear bundles. MOC neurons are large cholinergic cells located medioventrally within SOC (Campbell and Henson, 1988, Brown and Levine, 2008). They send thick myelinated axons to the OHCs of contralateral cochlea mainly where they form axosomatic synapses.

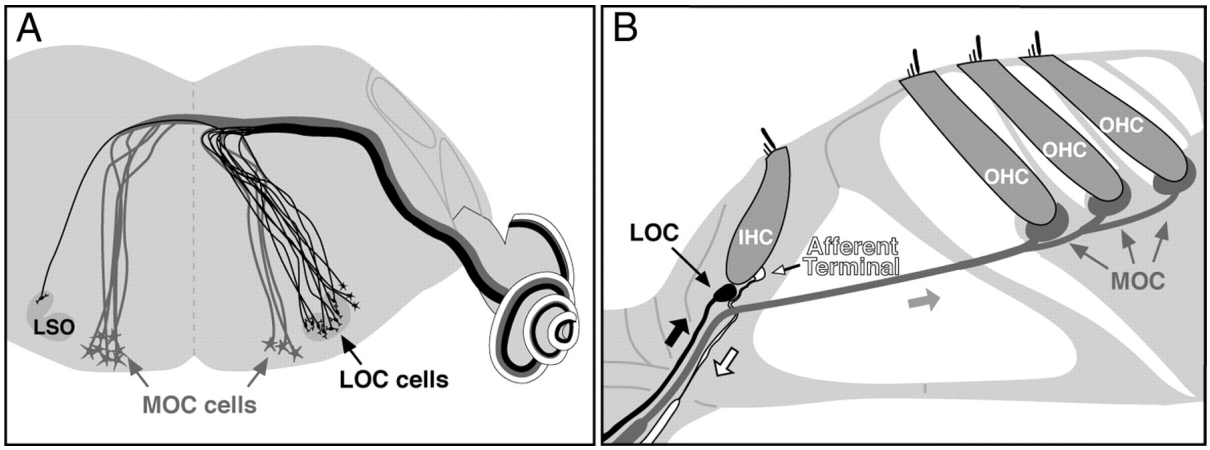

Figure 6. Schematic illustration of the cochlear efferent innervation.

A. Schema of brainstem slice at the level where sources of efferent innervation (LOC fibers are shown in black, MOC fibers in gray) of the cochlea are located. B. Efferent synapses in cochlear hair cells: LOC innervate of IHCs, MOC innervate OHCs. LSO: lateral superior olive, MOC: medial olivocochlear bundle, LOC: lateral olivocochlear bundle, IHC: inner hair cell, OHC: outer hair cell. Modified from (Darrow et al., 2007).

When MOC fibers are activated they hyperpolarize OHCs suppressing their ability to amplify the vibrations of the basilar membrane, leading by this way to decreased cochlear responses (Guinan and Stankovic, 1996). MOC may receive descending projections from the ipsilateral IC and bilateral ascending input from the VCN (Malmierca and Ryugoy, 2012).

LOC neurons lie within LSO and innervate dendrites, contacting IHCs. LOC neurons can possess cholin-, GABA-, dopamin- and peptidergic neurotransmission (Safieddine and Eybalin, 1992, Safieddine et al., 1997, Darrow et al., 2006). Their axons are unmyelinated and project mostly to ipsilateral cochlea.

Physiological studies show that MOC system possesses a protective role reducing cochlear damage in response to noise overstimulation (Handrock and Zeisberg, 1982, Kujawa and Liberman, 1997, Rajan, 2000, Maison et al., 2002b, Taranda et al., 2009, Maison et al., 2013). The MOC system role in “unmasking” biologically significant acoustic stimuli by reducing the response of the cochlea to simultaneous low-level noise has been proposed (Eggermont, 2001, Kirk and Smith, 2003). MOC terminals have been shown to degenerate with age (Fu et al., 2010) and surgical deefferentation accelerated age-related loss of cochlear nerve synapses (Liberman et al., 2014b) suggesting its protective role in age-related hearing loss. The functional role of the LOC is even less clear. Its cytochemical heterogenity sugests

that one of the LOC roles is modulation of afferents' excitability (Groff and Liberman, 2003, Darrow et al., 2007). LOC has been recently shown to participate in cochlear protection from noise exposure (Darrow et al., 2007) and ageing (Liberman et al., 2014b) together with MOC.

To conclude, olivocochlear system seems to play an important role in modulation of cochlear function and cochlear protection.

1.2. Development of mammalian inner ear

Early inner ear development is similar in all vertebrates. The cochlea, including organ of Corti and spiral ganglion, derive from non-neural ectoderm; the cells of spiral ligament, otic capsule and modiolus evolve from the surrounding mesenchyme; melanocyte-like cells of stria vascularis and Schwann cells in the spiral ganglion originate from neural crest (Magariños, 2014) .

The earliest morphological evidence of inner ear development in mouse appear at embryonic day E7.5 when pre-placodal region of ectoderm adjacent to hindbrain thickens and form otic placode (Figure 7A). At E8–9 otic placode invaginates to form otic cup (E9.5, Figure 7B) that later converts into a hollow sphere- the otic vesicle (otocyst, Figure 7C). Otic vesicle is a transient embryonic structure, containing all information to develop autonomously into the inner ear (Torres and Giraldez, 1998). Neural precursors delaminate from its ventral epithelium and migrate to form the cochleovestibular ganglion (Figure 7B, D) that will further split into spiral (Figure 7E–L) and vestibular ganglia. Otocyst undergoes intensive cell proliferation in this period. Ventro-medial part of the otocyst evaginates to form a cochlear duct. Together with the spiral ganglion it elongate and grow to form a coiled tube- future scala media (Figure 7E). Two cavities, scala tympani below and scala vestibuli above the cochlear duct form from the surrounding mesenchyme (Figure 7F–H). Cells in the cochlear duct undergo differentiation and reorganization and through the stage of lesser and greater epithelial ridge formation (Figure 7I, J) develop the inner sulcus, the spiral limbus, the sensory and supporting cells of organ of Corti (Figure 7K, L).

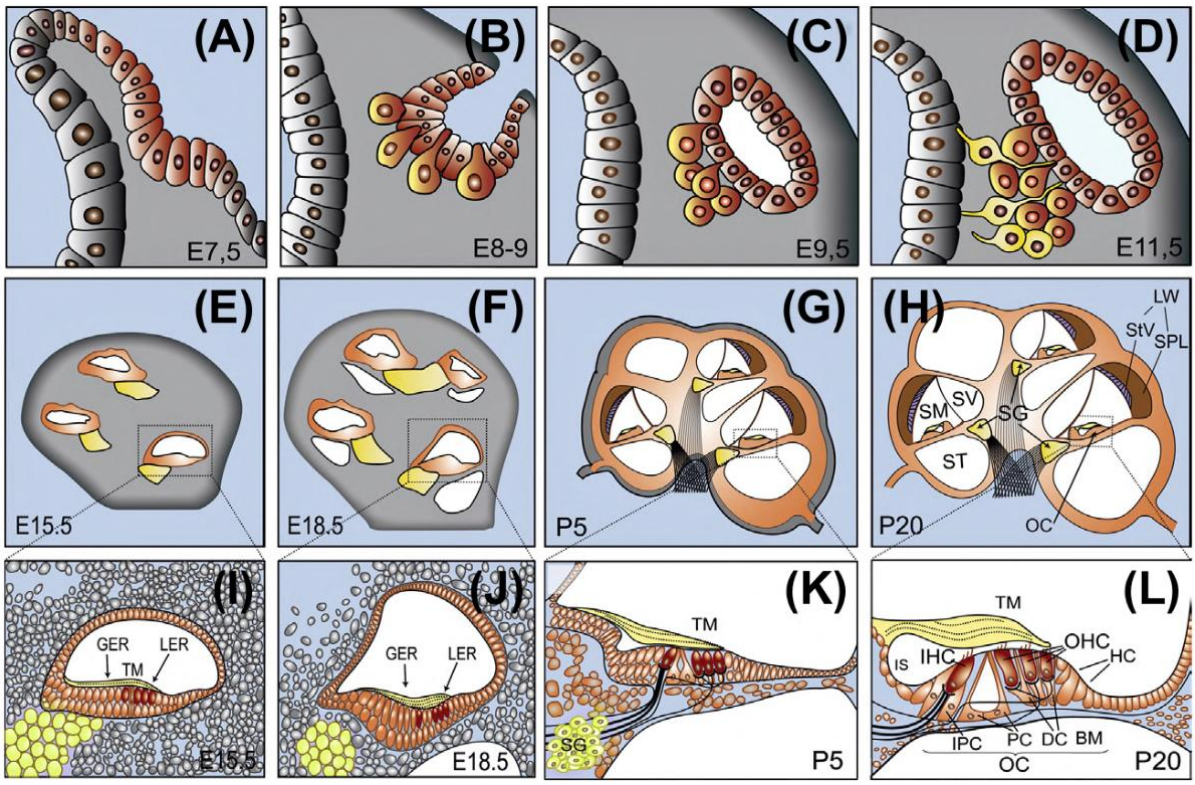

Figure 7. Stages of cochlear development in mouse

(A) Formation of otic placode. (B) Otic cup. (C) Otocyst. (B-D) Delamination of neural precursors. (E)Coiled cochlear duct and (I) primitive organ of Corti. (F) Formation of scala tympany and scala vestibul and cell differentiation in the organ of Corti. (G) Cochlea and (K) organ of Corti before onset of hearing. (H) Adult cochlea and (L) organ of Corti. LW: lateral wall, StV: stria vascularis, SPL: spiral ligament, SM: scala media, SV: scala vestibuli, ST: scala tympani, SG: spiral ganglion, OC: organ of Corti, GER: greater epithelial ridge, LER: lesser epithelial ridge, TM: tectorial membrane, IS: inner sulcus, IHC: inner hair cells, OHC: outer hair cells, IPC inner phalangeal cells:, PC: pillar cells, DC: Deiter's cells, BM: basilar membrane, HC: Hensen's cells. Modified from Development of Auditory and Vestibular Systems edited by Raymond Romand, Isabel Varela-Nieto, Academic Press, May 23, 2014.

Important step in the inner ear development is establishment of contacts between the sensory cells and neurons of the spiral ganglion. After differentiation of neurons in spiral ganglion between E9.5 and E13.5 (starting in the cochlear base and progressing toward the apex) they begin to send their peripheral processes toward forming cochlear epithelium. Extension of peripheral processes is initiated by intrinsic SG regulators. Once these projections reach cochlear epithelium their growth and reorganization and differentiation and maturation of hair and supporting cells become interdependent.

By the end of gestation the wiring pattern of cochlear innervation is roughly established. However, SGN afferents project simultaneously to both, IHCs and OHCs sending to them collaterals that will be refined and retracted during the first postnatal week. In the place of nerve fiber contacts with HC immature ribbon synapses have been observed prior to birth. To establish functional connections with SGN during development before onset of hearing hair cells fire periodic bursts of action potentials (Wang and Bergles, 2015). After birth number of ribbons in IHC increases from P0 to P6 and subsequently decrease by 50% from P6 to onset of hearing at P12 (for review see (Delacroix and Malgrange, 2015).

Development of such highly specialized and complex sensory organ from simple non-specific epithelium requires an action of temporally and spatially synchronized expression cascades of transcription factors (Chen and Streit, 2013). Transcription factors are proteins that regulate transcription - the first step of gene expression in which information is copied from DNA to the messenger RNA for further protein synthesis. Transcription factors bind specifically to DNA sequences and control their ability to be transcribed (converted) into mRNA (Latchman, 1997). Combination of transcription factors such as *Gata3*, *Pax2/8*, *Tbx1*, *Foxg1*, *Foxi1*, *Eya1*/*Six1*, and *Oct4* (Fritzsch et al., 2006, Kelley, 2006, Bouchard et al., 2010b) provides a necessary context for the switch from epidermal to proneurosensory fate during development of inner ear sensory epithelium. Developing prosensory cells express a number of genes that have functional roles in prosensory specification, including *Tbx1*, *Bmp4, Jag1*, and SRY-box containing gene 2 (*Sox2*). Differentiation of sensory epithelia into hair cells and supporting cells is regulated by temporally expressed transcription factors (Kiernan et al., 2005, Kelley, 2006, Jahan et al., 2013). However, the complete functional and molecular composition of the transcriptional network that controls neurosensory development remains unclear.

1.2.1. Role of Islet 1 in development and potential for cochlear regeneration

Islet 1 belongs to LIM-homeodomain (LIM-HD) family of transcription factors. It is a subfamily of homeobox genes that play fundamental roles in development. Primary structure of LIM-HD proteins has been remarkably conserved through evolution and they are prominently involved in tissue patterning and differentiation, especially neural patterning in nematodes, flies and vertebrates (Hobert and Westphal, 2000). LIM-HD transcription factors are characterized by two zinc finger motifs: the LIM domain for protein - protein interactions

and a homeodomain for binding to the DNA control elements of target genes (Karlsson et al., 1990, Hobert and Westphal, 2000).

Few transcription factors from LIM-homeodomain family are expressed during early inner ear development. *Lmx1a* (Nichols et al., 2008), has been found to be essential for normal ear morphogenesis as well as normal neurosensory development whereas eliminating Lmo4 results in formation of extra sensory epithelia (Deng et al., 2014). Like *Lmx1a*, *Islet1* (*Isl1*) is a LIM-HD transcription factor that can bind to DNA in the form of monomeric or heteromultimeric transcription factor complexes (Bhati et al., 2008). ISL1 acts in a context-dependent fashion, requiring other factors to achieve specificity, and it has a unique potential for combinatorial interaction with other transcription regulators in a homomeric or heteromeric fashion (Hobert and Westphal, 2000). Embryos lacking the *Isl1* gene die by embryonic day E10.5, indicating an essential requirement for ISL1 during normal embryonic development (Pfaff et al., 1996). Loss- of- function studies in the mouse have revealed crucial roles for ISL1 in motor neuron, pancreatic, cardiac, and eye development (Cai et al., 2003, Lin et al., 2006, Elshatory et al., 2007, Sun et al., 2008, Whitney et al., 2011). Thus, ISL1 contributes to the development of neuronal and non-neuronal cell types, suggesting that its activity is context dependent. The dose-dependent requirement for Isl1 is an interesting aspect of ISL1 regulation, which affects the specification of motor neurons (Liang et al., 2011) and modulates horizontal cell number in the mouse retina (Whitney et al., 2011). Overexpression of Isl1 in chick retina suppressed Lim1 increasing type II horizontal cells number by the cost of Lim1-dependent type I cells (Suga et al., 2009). During normal ear development, ISL1 appears first in the otic placode and it is then upregulated in the cells that will form the ccochleo-vestibular ganglion during placode invagination (Li et al., 2004). Subsequently, the expression of ISL1 in the neuronal lineage is maintained as the neuronal differentiation progresses in the terminally differentiated neurons. ISL1 is also one of the earliest markers of the developing sensory epithelia. ISL1 is expressed in all cells committed to form either hair cells or supporting cells, which suggests its role in the specification of the cell population committed to form these cell types (Li et al., 2004, Radde-Gallwitz et al., 2004, Huang et al., 2008). Upon initiation of hair cell differentiation, the expression of ISL1 is downregulated in cochlear epithelium in vertebrates (Radde-Gallwitz et al., 2004). It is not the case for chick inner ear that possess robust expression of Isl1 in adult auditory and vestibular supporting cells (Li et al., 2004) – cells that are able to re-enter cell cycle and by cost of which regeneration of hair cells occur in chick sensory epithelium (Edge and Chen, 2008). Based on the idea that expression of developmental genes in mature hair cells may

lead to reprogramming and rejuvenation of damaged hair cells, Huang et al. forced *Isl1* expression in mature outer and inner hair cells in mice, by this way protecting their hearing from age-related and noise-induced hearing loss (Huang et al., 2013).

1.2.2. Role of BDNF in development and regeneration

Neurotrophic factors are proteins responsible for the growth and surviving of developing neurons and maintenance of mature neurons in the central and peripheral nervous system under normal conditions and during injury (Maness et al., 1994, Terenghi, 1999). They can be produced and secreted by neurons, glial cells, sensory cells and muscle fibers. Neurotrophins' signaling is mediated via two major receptor types: low-affinity p75 receptor that is bound by all neutrotrophins and high affinity tyrosine kinase (Trk) receptor- own for each neurotrophin type (Lee et al., 2001). These receptors have opposed roles- while Trk receptors promote cell growth and survival, p75 have mostly proapoptotic effect (Casaccia-Bonnefil et al., 1996, Frade et al., 1996, Dechant and Barde, 2002). Neurotrophic factor family contains 4 proteins but only two of them have been shown to predominantly act in the cochlea: brain derived neurotrophic factor (BDNF) and neurotrophic factor 3 (NT3) (Pirvola et al., 1992, Staecker et al., 1996, Rubel and Fritzsch, 2002, Ramekers et al., 2012) and their receptors TrkB and TrkC respectively were found to be expressed in the developing (Schecterson and Bothwell, 1994) and mature (Ylikoski et al., 1993, Mou et al., 1997) cochlea.

During inner ear development BDNF is expressed in the otic vesicle (E11–E18) when the formation of the cochlear duct occurs and cochlear neurites reach presumptive sensory epithelium (Pirvola et al., 1992, Pirvola et al., 1994, Schecterson and Bothwell, 1994). *In vitro* BDNF induces neurite outgrowth in rat embryonic cochleovestibular ganglion, more effectively than NT3 (Pirvola et al., 1992, Avila et al., 1993). Treatment of El0.5 otocyst-CVG explants with BDNF antisense oligonucleotides results in extensive neuronal cell death that could be prevented by the simultaneous addition of BDNF (Staecker et al., 1996). This suggests the important role of BDNF during neuritic ingrowth of spiral ganglion neurons into the cochlear epithelium during embryonic development (Pirvola et al., 1992, Avila et al., 1993, Despres and Romand, 1994, Pirvola et al., 1994).

The role of BDNF in the mature cochlea is still elusive, because BDNF constitutive KO mice die before onset of hearing (Ernfors et al., 1994, Fritzsch et al., 2004). According to constitutive BDNF KO mouse models, BDNF is necessary for the recruitment of afferent

type II fibers to OHCs in the high frequency region of the cochlea during early postnatal development (Schimmang et al., 2003), and for the survival of vestibular neurons (Ernfors et al., 1994). After birth before onset of hearing BDNF is expressed in both IHCs and OHCs mostly in apical, low frequency part of the cochlea (Wiechers et al., 1999, Fritzsch et al., 2004). From postnatal day 4 (P4) onwards BDNF is downregulated in hair cells of the cochlea but remains expressed in the supporting inner border and phalangeal cells ensheathing inner hair cells (Wiechers et al., 1999, Sobkowicz et al., 2002) and is upregulated in SG where it is maintained throughout adult stages in a tonotopic gradient, increasing toward higher frequency cochlear turns (Adamson et al., 2002; Sobkowicz et al., 2002; Schimmang et al., 2003). BDNF receptor TrkB is shown to be expressed in adult human SGNs (Liu et al., 2011) and adult as well as developing mice inner ears (Bitsche et al., 2011).

While loss of BDNF in phalangeal cells does not affect hearing (Wan et al., 2014), the combined deletion of BDNF in the cochlea, the DCN, and the IC in BDNF^{Pax2} knock-out mice leads to reduced exocytosis of otherwise mature IHC synapses and to slightly diminished sound-induced auditory brainstem responses (Zuccotti et al., 2012).

Expression of BDNF and its Trk receptor in the auditory brainstem is correlated with the onset of hearing and sound evoked activity in the auditory system. Virtually no BDNF expression is found in auditory brainstem at birth but by P6 first signs of both BDNF and TrkB expression are detected in most brainstem auditory nuclei. Towards adulthood expression of BDNF and TrkB increase and by P15 it is widely expressed in the CN, the nuclei of the trapezoid body, superior olive, and IC (Hafidi et al., 1996, Hafidi, 1999). Upon sensory experience in the auditory (Xu et al., 2010, Kotak et al., 2012), visual (Gao et al., 2014), somatosensory (Jiao et al., 2011), and olfactory system (Berghuis et al., 2006), the dendritic complexity of parvalbumin (PV)-immunoreactive interneurons is particularly enhanced in response to increases in local cortical BDNF (Xu et al., 2010, Jiao et al., 2011, Bramham and Panja, 2014). This process is assumed to enhance sensory resolution and acuity, and requires an adequate and timely sensory input (Vogels et al., 2013, Griffen and Maffei, 2014, Singer et al., 2014). The selective role of cortical BDNF for improvement of sensory resolution was questioned in the retina where BDNF was proposed as a mediator of early environmental enrichment effects on visual acuity (Landi et al., 2007a). Accordingly, blocking retinal BDNF by means of antisense oligonucleotides prior to eye opening was shown to prevent the effects on dendritic segregation of retinal ganglion cells (Landi et al., 2007b) and development of retinal acuity (Landi et al., 2007a) upon exposure to environmental enrichment.

Positive effects of BDNF in supporting of neuronal surviving and synaptic plasticity made it a great candidate for drug development for the treatment of many neuodegenerative disesases (Levivier et al., 1995, Schabitz et al., 1997, Bemelmans et al., 1999, Kalra et al., 2003, Hoshaw et al., 2005, Makar et al., 2009, Nagahara et al., 2009). During the last two decades BDNF is being widely studied as a potential regenerative therapy for prevention of spiral ganglion degeneration after hair cell loss (Ramekers et al., 2012, Khalin et al., 2015). The studies employed different approaches to increase BDNF level or activity in the cochlea: prolonged application of BDNF using osmotic pump (Gillespie et al., 2003, Radeloff and Smolders, 2006b, Agterberg et al., 2008, Leake et al., 2011, Sly et al., 2012, Waaijer et al., 2013) or biodegradable materials (Endo et al., 2005, Ito et al., 2005, Havenith et al., 2011), intracochlear delivery of BDNF overexpressing cells (Rejali et al., 2007, Pettingill et al., 2011) or delivery of BDNF gene using viral vector (Staecker et al., 1998, Nakaizumi et al., 2004, Chikar et al., 2008, Shibata et al., 2010, Wise et al., 2010, Atkinson et al., 2012, Fukui et al., 2012). Most of the studies showed preservation of SG neurons (Ito et al., 2005, Chikar et al., 2008, Shibata et al., 2010, Wise et al., 2010, Havenith et al., 2011, Pettingill et al., 2011, Fukui et al., 2012) and some showed improvement of hearing thresholds (Chikar et al., 2008, Leake et al., 2011, Sly et al., 2012) during the BDNF treatment, while others showed no effect on hearing function (Radeloff and Smolders, 2006a, Agterberg et al., 2008, Havenith et al., 2011, Sly et al., 2012). Electroporation of plasmids encoding BDNF into cochlear tissues using cochear implant was shown to promote SGN neurite outgrowth and survival (Pinyon et al., 2014).

1.3. Regenerative therapy for the cochlea

Vulnerability of the vertebrate cochlea to insults such as acoustic overstimulation, ototoxic drugs, or aging is well known. Loss of hair cells or spiral ganglion neurons forms a morphological basis of the sensorineural hearing loss (SNHL) – the most common sensory disorder in humans. Until 1988 loss of cochlear sensory cells was considered irreversible in vertebrates and a concept of their regeneration was out the agenda. This changed after spontaneous regeneration in the bird's sensory epithelium had been reported (Corwin and Cotanche, 1988, Ryals and Rubel, 1988). Since mammals and birds evolve from a common ancestor it is possible that the mechanism for hair cell regeneration in mammals was evolutionary inhibited and can be potentially switched on. Since late 1980s regenerative process in birds has been extensively studied with the perspective to use obtained knowledge

for hair cell regeneration in mammals and, eventually, in human (for review see (Bermingham-McDonogh and Rubel, 2003). Substantial challenge in regeneration of fully functional cochlear epithelium in mammals possesses its unique and complex functional and spatial organization: after damage a correct number of cells should be generated in a correct position surrounded by a correct types of cells and innervated by correct afferent and efferent nerve fibers (Jahan et al., 2015).

1.3.1. Targets and strategies

The main targets for regenerative therapy are the cochlear hair cells and spiral ganglion neurons, loss of which causes SNHL. Until recently degeneration of the cochlear sensory epithelium was considered to be the primary mechanism of SNHL, making its cells the main target for development of regenerative therapy. Spiral ganglion neurons were thought to undergo retrograde degeneration secondarily to hair cells and main reason for spiral ganglion preservation was to provide best possible outcome for the cochlear implantation. Recently, though, it has been shown that exposure to environmental noise previously considered relatively safe can lead to a hidden hearing loss conditioned by primary degeneration of the IHC afferent synapses and consequent degeneration of spiral ganglion neurons with intact cochlear epithelium (Kujawa and Liberman, 2009, Makary et al., 2011). This brought regeneration of spiral ganglion into play along with hair cells.

At present no practical methods for cochlear regeneration have been developed, but major approaches are outlined. These include self-repair, direct trans-differentiation, mitotic proliferation (dedifferentiation) and cell transplantation (Nakagawa, 2014). These approaches in turn can employ a variety of methods such as gene therapy, molecular therapy and stem-cell therapy. Selection of the appropriate regenerative strategy would depend on the level of the inner ear damage.

Before hair cell or spiral ganglion neuron fully degenerate, stimulation of self-repair would be a preferred method. It includes promotion of cell survival and prevention of cell death or reconstruction of cellular components in damaged cells. To this type of regeneration we can ascribe support of spiral ganglion cell surviving by application of the neurotrophic factors (Shibata et al., 2010, Havenith et al., 2011, Pettingill et al., 2011, Fukui et al., 2012) or protection of cochlear hair cells and their afferent synapses from noise and ageing by overexpression of transcription factor Islet1 (Huang et al., 2013).

After cell death the main regenerative strategy could be its replacement with a new cell coming from the neighborhood or transplanted from outside. Hair and supporting cells share a common progenitor and manipulating the certain cell signaling pathways it is possible to induct trans-differentiation (phenotypic conversion) of supporting cell into hair cell. Ideal cell source for cochlear regeneration would be intrinsic stem cells that have been reported to be present in the postnatal mammalian vestibular epithelium (Li et al., 2003a) and spiral ganglion (Diensthuber et al., 2014), but not in the postnatal cochlear epithelium (Oshima et al., 2007). Both, spontaneous trans-differentiation and dedifferentiation (mitotic regeneration), when a cell re-enters the cell cycle and proliferate to increase the number of the cells with consequent differentiation of these cells into supporting and hair cells, have been reported during regeneration in chick epithelium (Ryals and Rubel, 1988, Adler and Raphael, 1996, Li and Forge, 1997, Roberson et al., 2004, Stone and Cotanche, 2007) and limited regeneration of vestibular epithelium in mammals (Forge et al., 1993, Rubel et al., 1995, Oesterle et al., 2003, Burns et al., 2012a). In experiment, trans-differentiation of supporting cells into hair cells *in vitro* and *in vivo* might be induced via inhibition of Notch signaling, which blocks differentiation in embryonic hair cells (Yamamoto et al., 2006, Hori et al., 2007, Lin et al., 2011, Mizutari et al., 2013) or introduction of Atoh1 gene into supporting cell (Zheng and Gao, 2000, Izumikawa et al., 2005). Dedifferentiation might be induced *in vitro* by introduction of transcription factors such as Oct3/4, Sox2, Klf4, and c-Myc (Burns et al., 2012b, Lou et al., 2013).

In case of cell transplantation, these cells might be activated toward desired fate prior to transplantation. Several *in vitro* studies proposed protocols employing principles of early embryonic development to generate population of otic progenitor cells capable of differentiating into mechanosensitive sensory hair cells (Li et al., 2003b, Oshima et al., 2010, Koehler et al., 2013). Numerous laboratories performed studies on cochlear epithelium regeneration using transplantation of different types of stem cells *in vivo* (for review see (Okano and Kelley, 2012) but the results vary: the fate of transplanted cells is not always clear and functional competence of acquired cells is low if any.

The functionality of the newly produced cells remains challenging in most cases of experimental regeneration. This is not surprising, since even after spontaneous regeneration of sensory epithelium in bird's inner ear sound perception may remain compromised in terms of frequency and temporal resolution (for review see (Ryals et al., 2013)). It is, however, assumed that complete understanding of the molecular development of the cellular mosaic of the OC and detailed knowledge about transcription factors that define the otic cell lineages

during inner ear development may lead to satisfying morphological and functional restoration of mammalian inner ear after damage (Brigande and Heller, 2009, Jahan et al., 2015).

1.3.2. Therapeutic approaches to the inner ear

Isolated anatomical position of the inner ear challenges the treatment of inner ear diseases for many years. The cochlea is separated by blood-labyrinth barrier from systemic circulation and by round window membrane and stapes from the middle ear cavity. Brief characteristics of the main therapeutic approaches to the cochlea are shown in the Figure 8.

Traditionally, drugs are delivered to the cochlea via systemic application that, however, is often associated with undesirable side effects or low therapeutic effect due to low perilymphatic concentration (Wilson et al., 1980, Moskowitz et al., 1984, Mccabe, 1989, Parnes et al., 1999, Zhou et al., 2009). Intracochlear delivery would dramatically increase drug availability and remove adverse effects, though, it possesses a substantial risk of permanent hearing alteration (Carvalho and Lalwani, 1999, Stover et al., 1999). This way of drug application into the inner ear is currently used in clinics only in addition to the cochlear implant insertion (De Ceulaer et al., 2003, Paasche et al., 2006). A less invasive strategy for drug delivery to the inner ear in man, including agents for the prevention, rescue, repair and regeneration, is the injection of an agent through the tympanic membrane into the middle ear space. Transfer of the agent, injected intratympanically into the cochlea is mostly mediated via the RWM. This way of drug administration, including gentamicin and steroids, has been used for the treatment of disorders including Ménière's disease, sudden hearing loss, tinnitus and autoimmune inner ear disease (Light et al., 2003, Light and Silverstein, 2004, Borkholder, 2008).

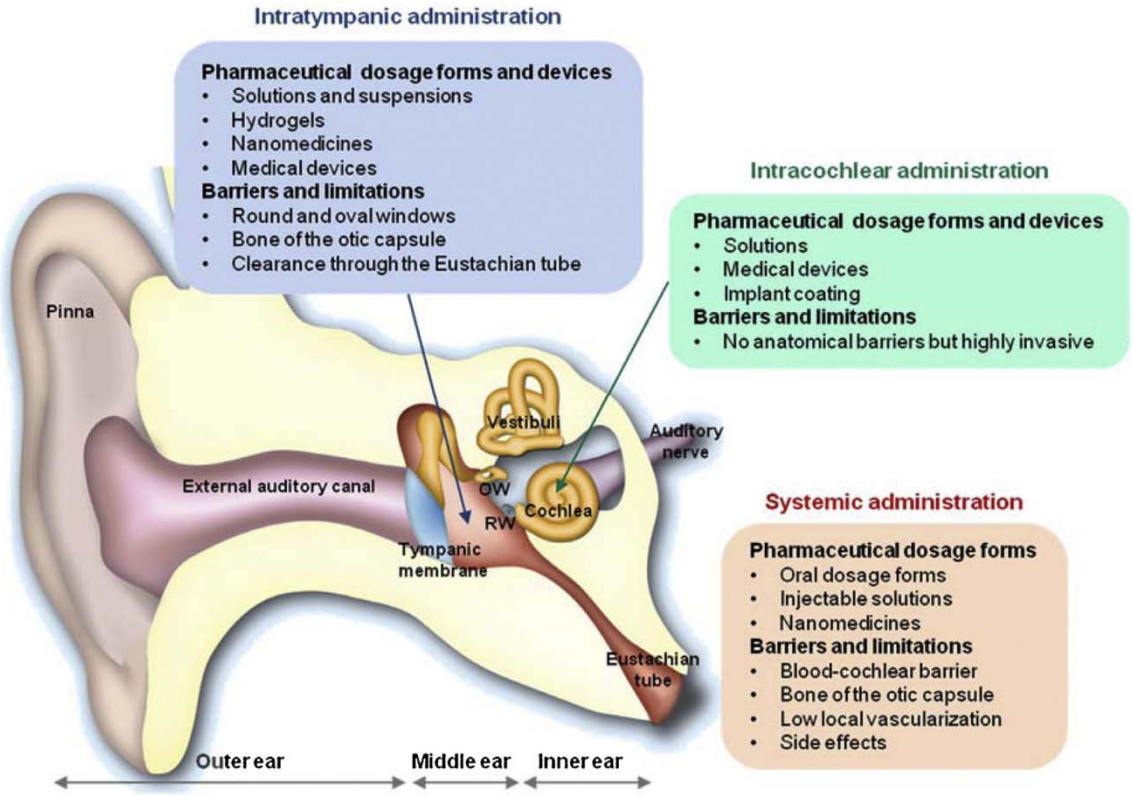

Figure 8. Therapeutic approaches to the inner ear

Modified from (El Kechai et al., 2015)

To facilitate intratympanic drug administration in humans several implantable devices were recently developed (MicroWick®, μCat®, for review see (El Kechai et al., 2015). Different biodegradable materials are being tested as means to overcome clearance of the drug solution from the tympanic cavity through the Eustachian tube and prolong the time of the contact between drug solution and RWM surface (gelfoam®, seprapack®, hydrogels, for review see (El Kechai et al., 2015).

1.3.3. Delivery of drugs to the inner ear using nanoparticles

Another tool to improve drug delivery to the cochlea is nanoparticle based delivery systems. Nanoparticles are defined as solid particles with diameter under 500 nm that may be assembled from organic or inorganic material and aimed for carrying drug either in a hollow core or incorporated into the matrix of a particle (Poe and Pyykko, 2011). Nanoparticles may compensate drug weaknesses such as low solubility, toxicity and short half-life. Direct contact of some therapeutic agents with middle ear structures (e.g., hydrocortisone) can elicit

morphological changes in the RWM (Spandow et al., 1990, Nordang et al., 2003) another substances have low permeation ability through the RWM. This may be preventable by using nanoparticles (NPs) as delivery vehicles for the transport of therapeutic agents to the cochlea. Ideal multifunctional nanonanoparticle would contain specific ligands on its surface for targeted delivery to particular cells; it would be coated with polyethylene glycol to minimize fouling of nanoparticles by host opsinizing proteins and as a payload it would be able to carry drugs and plasmid, for *in vivo* vizualization it would contain MRI contrast agent (Figure 9, (Poe and Pyykko, 2011).

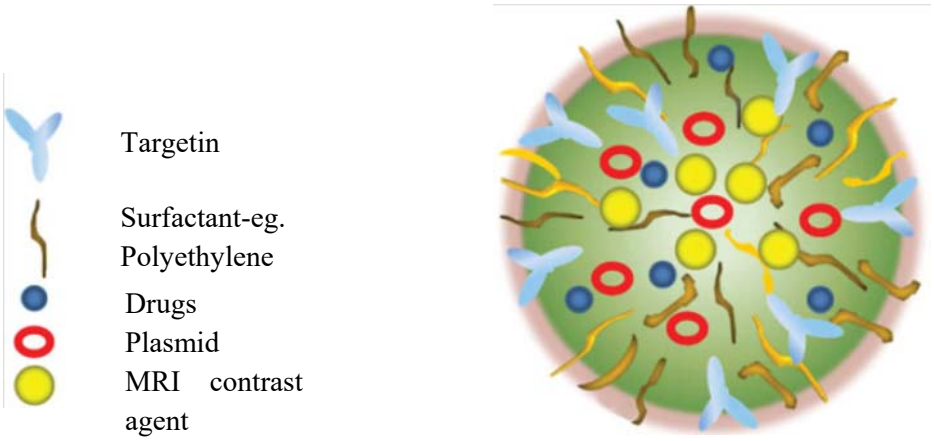

Figure 9. Schematic of a multifunctional nanoparticle.
Modified from (Poe and Pyykko, 2011)

It has been previously shown that poly(lactic acid-co-glycolic acid) NPs (Tamura et al., 2005, Ge et al., 2007), lipid core nanocapsules (Zou et al., 2008), silica NPs (Praetorius et al., 2007), liposomes (Jero et al., 2001, Maeda et al., 2007) and polymersomes (Zhang et al., 2010b) can permeate through the RWM from the middle ear to the cochlea. Relative nanoparticle targeting is conditioned by their size and surface chemistry leading to their accumulation in certain cell types (Zhang et al., 2012, Glueckert et al., 2015). However, *in vitro* studies are in progress developing ways of nanoparticle surface labeling with specific ligands that are supposed to interact with specific receptors expressed on the target cell population facilitating targeted attachment and internalization of the NP by the certain type of cells (Roy et al., 2010, Glueckert et al., 2015).

Three types of nanoparticles were tested *in vivo* in this study: liposomes, polymersomes and hyperbranched polylysine (Figure 16). Liposomes and polymersomes have similar vesicular structure with hollow space inside. In liposomes the vesicle wall is

made of phospholipid bilayer, while polymersomes are formed by the self-assembling amphiphilic block copolymers. Both can encapsulate either hydrophobic molecules in the hydrophobic membrane, or hydrophilic molecules in the aqueous core. Polylysine is a dendrimer represented by a randomly branched polymer. It has a potential to be used for non-viral gene delivery.

2. Aims of work and hypotheses

To develop regenerative therapy for inner ear it is particularly important to understand the whole network of genes and transcription factors sequentially activated during the inner ear development and factors, important for normal function of the auditory system. Besides that the ways of safe and targeted delivery of active agents, such as transcription factors and genes, able to induce and control the regenerative process are currently in great demand. Islet1 transcription factor and brain derived neurotrophic factor (BDNF) have a great potential to play a role in regenerative inner ear therapy. In the present study we aimed to gain an insight into their role in development and function of the auditory system using two transgenic mice models. Besides that we aimed to test three types of nanoparticles for their ability to safely penetrate inside the cochlea and deliver there sufficient amount of an active agent.

2.1. Role of ISL1 in development and function of the auditory system

Hypothesis: ISL1-expressing cells are the common precursors for both sensory epithelia and neurons suggesting its potential role for regeneration of these types of inner ear cells. By modulating the expression of Isl1, we expected to change the fate specification of cells in the inner ear.

Specific aims:

- To test whether overexpression of Pax2Isl1 affects embryonic development of the inner ear and increases the sensory and neural domains in developed cochlea.
- To test whether Pax2Isl1 overexpression leads to functional and/or morphological changes in hearing in adult mutant mice compared to wild type animals.
- To analyze the process of aging in the auditory system in mutant and wild type animals.

2.2. Role of "peripheral" BDNF in the auditory system

Hypothesis: BDNF in the lower parts of the auditory pathway or within the cochlea is necessary for the maturation of auditory nerve activity after onset of hearing.

Specific aims:

- To study a role of BDNF in the lower part of the mature auditory pathway in mouse using extracellular recording of neuronal activity in the inferior colliculus of BDNF^{Pax2} knock-out mice.
- To understand the physiology behind the reduced range of suprathreshold ABR responses generated at the level of the IC in BDNF^{Pax2} knock-out mice.

2.3. Use of nanoparticles as a potential drug delivery tool

Hypothesis: Nanoparticles are a suitable tool for delivery of active agents to the cochlea during regenerative therapy.

Specific aims:

- To study the ability of nanoparticles to penetrate the round window membrane and their distribution inside cochlea.
- To compare the pattern of cochlear distribution of different types of nanoparticles.
- To determine whether an active agent can be delivered to the inner ear using nanoparticles in sufficient amount and condition to produce a detectable effect.

3. Materials and methods

3.1. Animals

The studies were conducted in accordance with the Guide for the Care and Use of Laboratory Animals (NIH Publication No. 85-23, revised 1996). The experimental protocols were approved by the Expert Commission of the Academy of Sciences and followed the guidelines of the EU directive 2010/63/EU. Mice were kept under standard laboratory conditions in a constant environment (12/12 h light/dark cycle), with food and water available ad libitum. All experimental procedures were conducted during the light phase of the cycle.

To study the role of transcription factor Isl1 in the auditory system wild-type (WT, n = 38) or heterozygous Pax2-Isl1 transgenic mice ($Tg^{+/-}$, n = 50) generated on an FVB background (strain code 207, Charles River) were used.

Wild type (WT, n = 4) and $BDNF^{Pax2}$-KO mice (KO, n = 4), obtained by mating Pax2-Cre (Ohyama and Groves, 2004) with BDNFlox/lox mice (Rios et al., 2001) were used to study the role of BDNF in the lower auditory brain regions.

Nanoparticle transport in the inner ear and their ability to deliver there an active agent was tested using 40 2–3 months old C3H mice. In individual animals, either polylysine (n = 5), polylysine-plasmid complex (n = 5), liposomes (n = 8), disulfiram-loaded liposomes (n = 5), polymersomes (n = 7) or disulfiram-loaded polymersomes (n = 6) were applied unilaterally to the middle ear. In controls, saline (n = 2), or disulfiram solution (n = 2) was applied instead of nanoparticles.

3.2. Anesthesia

For the hearing measurements, surgical procedures and extracellular measurements of neuronal activity mice were anaesthetized by intraperitoneal injection of 35 mg/kg of ketamine (Calypsol 5%, Gedeon Richter Ltd., Budapest, Hungary or Narkamon 5%;

Spofa, Prague, Czech Republic) and 6 mg/kg of xylazine (Xylapan 2%, Vetoquinol, Gorzów Wielkopolski, Poland or Sedazine 2%; Fort Dodge, Animal Health, Fort Dodge, Iowa) in saline via intraperitoneal injection.

Supplemental doses of anesthetic were injected subcutaneously when needed.

3.3. Hearing measurements

The hearing function of mice was studied using recording of Auditory Brainstem Responses (ABR) and Distortion Product Otoacoustic Emission (DPOAE). Both measurements were performed in a sound-attenuating and anechoic chamber in anesthetized mice maintained on a temperature - regulated blanket.

3.3.1. Recording of ABRs

ABR recording gives information about the integrity of the hearing system from the cochlear level up through the lower brainstem and is used routinely to evaluate auditory function in human or in laboratory animals. In animals ABR is measured using subcutaneous electrodes, which pick up the electric potentials generated by the synchronous activity of the population of neurons in different parts of the auditory brainstem evoked by acoustic stimulus. ABR is a short latency response, occurring within 1.5-15 ms after the stimulus onset and represented by series of waves with amplitude not exceeding 10 μV. In mouse ABR five waves (I–V, Figure 10) are distinguished, and they are accounted to the certain structure, where they are predominantly generated: I – auditory nerve, II – cochlear nucleus, III – superior olivary complex, IV and V correspond to lateral lemniscus and inferior colliculus (Melcher and Kiang, 1996, Land, 2016). Most often ABR measurement is used for evaluation of hearing thresholds (determination of the lowest intensity of the sound still audible for the subject) or for analysis of ABR wave amplitudes (to indirectly evaluate the function of particular auditory centers-wave generators).

In the present study frequency-specific ABRs were employed to evaluate animals' hearing thresholds. For this, three needle electrodes were placed in mice subcutaneously: an active electrode on the vertex and two electrodes- ground and reference- in the neck muscles (Figure 10A). ABRs were evoked using short tone bursts (3 ms duration, 1 ms rise/fall times, frequencies of 2, 4, 8, 16, 32 and 40 kHz) presented with decreasing stimulus level (from 100 to 0 dB SPL) by 5dB with each step. Acoustic stimuli were generated with a TDT (Tucker Davis Technologies, FL, USA) System III using Enhanced Real-Time Processor RP 2.1. Acoustic stimuli were delivered in free-field conditions via a two-way loudspeaker system (Jamo® woofer [Denmark] and SEAS® T25CF 002 tweeter [Norway]) placed 70 cm in front of the animal’s head. The acoustic system was calibrated with a B&K® 4939 microphone (Denmark), a ZC0020 preamplifier and a B&K 2231 Sound Level Meter. For calibration, the

microphone placement relative to the position and orientation of the animal's head was replicated throughout the experiments. The frequency-response curve was relatively flat and varied by less than ±9 dB between 0.15 and 40 kHz.

The signal from an electrode was amplified 10000-times and band-pass filtered over the range of 300 Hz to 3 kHz. The signal was processed with a TDT System III Pentusa Base Station and analyzed using BioSig™ (TX, USA) software. The response threshold to each frequency was determined as the minimal tone intensity that still evoked a noticeable potential peak in the expected time window of the recorded signal (Figure 10B). Thresholds were then plotted in audiograms (Figure 10C).

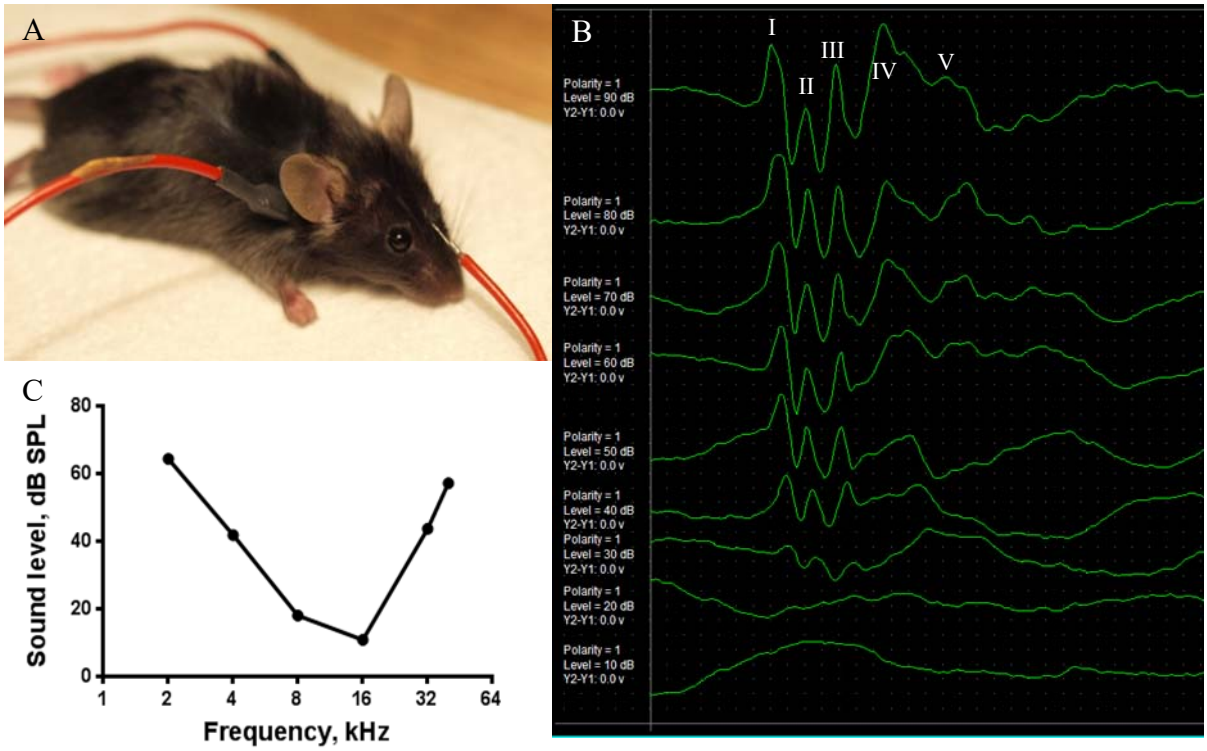

Figure 10. Auditory brainstem responses.

A. Position of the subcutaneous electrodes for ABRs recording in mice: active electrode is on the vertex, ground and reference are in the neck muscles. B. ABR worksheet created during the experiment and used to determine hearing threshold. Amplitude of ABR waves decline with decrease of sound level of the stimulus. Single ABR waves are highlighted by the order number. C. Example of the resulting audiogram showing hearing thresholds at frequencies from 2 to 40 kHz.

Hearing thresholds were measured in all experimental animals either in different ages or before and after experimental manipulations. When needed, monaural ABRs were

recorded in free-field conditions with one outer ear canal closed by Vaseline® (Unilever, Rotterdam, The Netherlands). Measurements of sound attenuation demonstrated that the vaseline attenuated the sound pressure level in the occluded ear canal by 20 dB at a frequency of 4 kHz and by 30–45 dB at frequencies above 8 kHz.

3.3.2. Recording of DPOAEs

Otoacoustic emissions (OAE) are tiny sounds generated by the outer hair cells (OHCs) in the inner ear and related to amplification function of cochlea. They can be generated spontaneously or evoked by sound stimulation, which is often used in clinics or in laboratory to evaluate the function of the OHCs of a subject. OAEs cannot be used to fully describe auditory thresholds, but they can validate other threshold measures or specify the possible site of the lesion.

Distortion product otoacoustic emissions (DPOAEs), used in this study, were evoked using a pair of tones of slightly different frequency and intensity. The most prominent distortion product is the cubic difference tone at 2F1−F2. Cubic (2F1−F2) distortion product otoacoustic emissions (DPOAEs) over a F2 frequency range from 4 to 38 kHz were recorded with a low-noise microphone system (Etymotic probe ER-10B+, Etymotic Research, IL, USA). Acoustic stimuli (ratio F2/F1=1.21, F1 and F2 primary tone levels of L1/L2=70/60 dB) were presented to the ear canal with two custom-made piezoelectric stimulators connected to the probe with 10-cm-long silastic tubes (Figure 11 A, B). The signal from the microphone was analyzed by the TDT System III (RP2 processor, sampling rate 100 kHz) using custom-made Matlab software.

DPOAEs were recorded in both ears of the animals at individual frequencies over the frequency range 4–38 kHz with a resolution of four points per octave (Figure 11C). Average for all animals in the group audiograms and DPOAE-grams were produced to compare results between experimental and control groups.

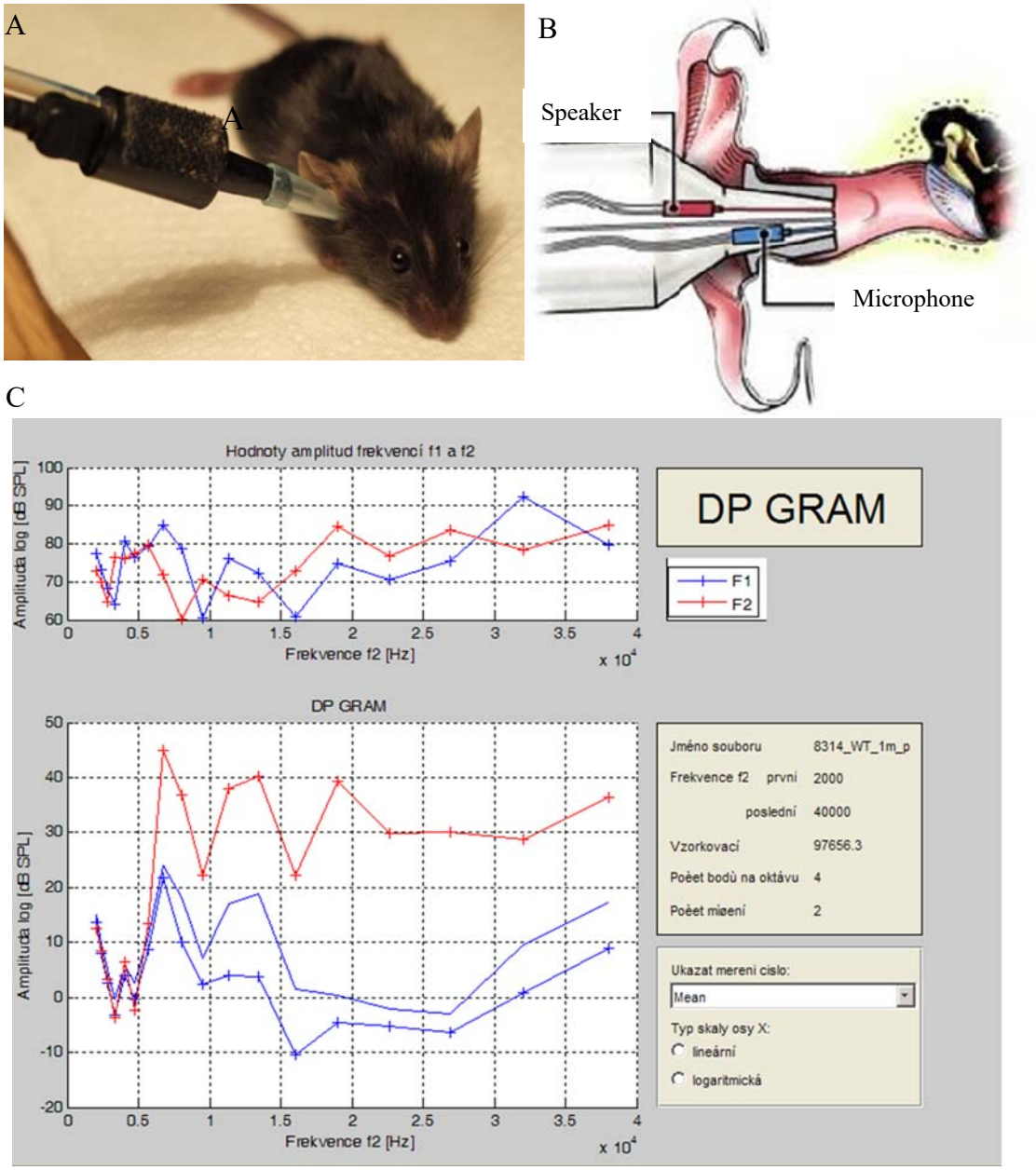

Figure 11. Distortion product otoacoustic emissions.

A. Position of the probe in the outer ear canal of the animal. B. The probe contains the loudspeaker and a microphone that are placed close to the eardrum. C. Example of the resulting DPOAE-gram showing amplitudes of two sounds, presented to the ear (upper graph) and DP-gram itself (lower graph) showing cochlear response (red) above the background noise (blue) covering frequency range from 4 to 38 kHz.

3.4. Extracellular Recording of the Neuronal Activity in the IC

3.4.1. Surgical Procedures

The surgery and extracellular recording in the IC were performed in mice anesthetized with 35 mg/kg ketamine (Narkamon 5%; Spofa, Prague, Czech Republic) and 6 mg/kg xylazine (Sedazine 2 %; Fort Dodge, Animal Health, Fort Dodge, Iowa) in saline via intraperitoneal injection.

For access to the IC, an incision was made through the skin of the skull and underlying muscles were retracted to expose the dorsal cranium. A head holder was glued to the skull. Small holes were drilled over both IC of the mouse; the animal was transported to the soundproof anechoic room and placed on a heating pad, which maintained a 37–38 °C body temperature for recording of the extracellular neuronal activity in the IC.

3.4.2. Procedure of neuronal activity recording

We performed acute *in vivo* extracellular measurement of the neuronal activity in the IC of BDNF^{Pax2}-KO and BDNF^{Pax2}-WT mice. This type of measurement implies random placing of an electrode into the brain tissue of interest (in case of this study inferior colliculus) and acquirement of action potentials from neurons located nearby the electrode.

Acoustic stimuli were generated with a TDT (Tucker Davis Technologies, FL, USA) System III using Enhanced Real-Time Processor RP 2.1. and delivered in free-field conditions via a two-way loudspeaker system (Jamo® woofer [Denmark] and SEAS® T25CF 002 tweeter [Norway]) placed 70 cm in front of the animal's head. The acoustic system was calibrated with a B&K® 4939 microphone (Denmark), a ZC0020 preamplifier and a B&K 2231 Sound Level Meter.

Two types of electrodes were used: 16-channel, single shank probe (NeuroNexus Technologies) with the electrode spots located 100 μm from each other and single parylene-coated tungsten electrode (Bionic Technologies Inc). Microelectrode probe was connected to motorized micromanipulator enabling its smooth moves in 3 axes. The signal obtained from the electrode was amplified 10000 times, band-pass filtered over the range of 300 Hz to 10 kHz, and processed by a TDT System III (Tucker Davis Technologies, Alachua, FL, USA) using an RX5-2 Pentusa Base Station. Extracellular recording of neuronal activity let us acquire electrical signals of neurons located in the proximity of the electrode inserted in the

gray matter of the brain. Each channel on the multichannel probe yield a group of action potentials from the group of neurons located close to it.

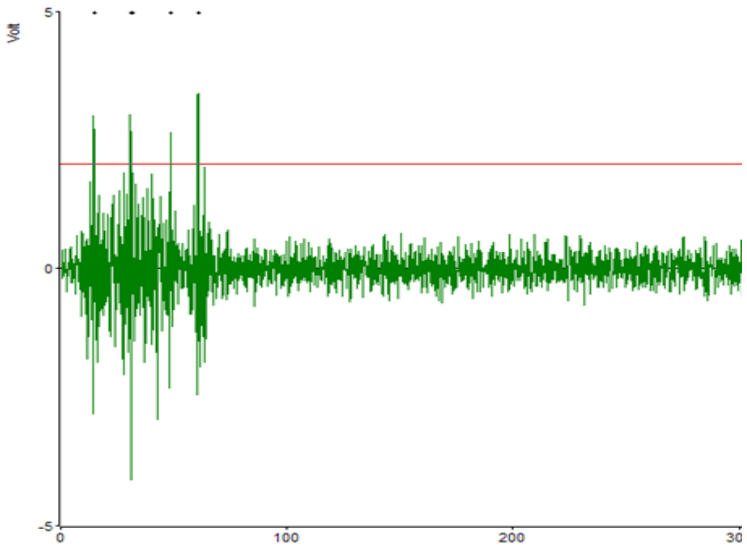

Figure 12. Raw data obtained from a single electrode channel of the 16-channel electrode, placed in the mouse IC.

Spikes of the highest amplitude were separated from the background noise by thresholding line (red).

The recorded data were processed and analyzed with custom software based on MATLAB.

Spontaneous activity of neurons and properties of their responses to different stimulation types (pure tones, broad band noise and two-tone stimulation) were analyzed.

3.4.3. Frequency-Intensity Mapping

The tuning properties of individual IC neurons were evaluated using frequency-intensity mapping.

To determine the excitatory response area, pure tone bursts (100 ms in duration, 5 ms rise/fall times) with variable frequency (1/8 octave step) and intensity (5 dB step) were presented in random order. A two-dimensional matrix was thereby obtained, with elements corresponding to the response magnitudes in the respective frequency-intensity points. The discrete point matrix was then converted to a smooth function of two variables, frequency and intensity, a process involving cubic smoothing spline interpolation. This averaging method allowed us to overcome the limited resolution of the frequency-intensity map (Figure

13A). The resulting smooth function thereafter served as a basis for the extraction of all the parameters of interest: (i) the excitatory response threshold, the lowest stimulus intensity that excited the neuron, measured in dB SPL; (ii) the characteristic frequency (CF), the frequency with the minimal response threshold, measured in kHz; and (iii) the bandwidth of the excitatory area 10 dB above the excitatory threshold, measured by quality factor Q10 (Figure 13B). Quality factor Q10 is a common measure of frequency selectivity that is reciprocally related to the excitatory area bandwidth (the higher the Q10, the sharper the response), defined as

Q10=CF/bandwidth.

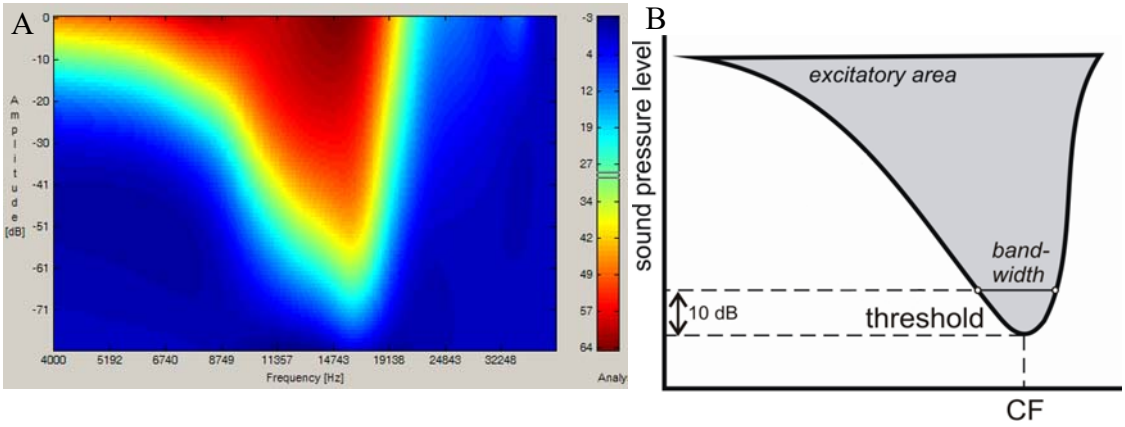

Figure 13. Frequency-Intensity Mapping.

A. heat map of one neuronal response to pure tone stimulation, created using Matlab software on the basis of measured data. B. A schematic plot showing the excitatory area of a frequency–intensity response area. The evaluated parameters are outlined: the excitatory response threshold, characteristic frequency (CF), bandwidth of the excitatory area 10 dB above the threshold.

3.4.4. Two-Tone Stimulation

To detect inhibitory areas, a two-tone stimulation was employed. The two-tone stimulation paradigm is commonly used to evaluate the local inhibition on the level of the cochlear nucleus (CN) (Konrad-Martin et al., 1998, Spirou et al., 1999, Kopp-Scheinpflug et al., 2002), the IC (Egorova et al., 2001, Lu and Jen, 2001), and the auditory cortex (AC) (Sugimoto et al., 2002). During recording neurons are stimulated with two tones simultaneously. One tone has fixed parameters and excites the neuron at its CF 10 dB above threshold, second tone varies in frequency and intensity analogously to excitatory area

mapping. Second tone can increase excitation evoked by constant tone (summation of excitation), decrease the response to the CF tone (inhibition) or it can have no visible effect.

Similarly to frequency-intensity mapping, a two-dimensional matrix was obtained (Figure 14A) as the result of the measurement. Spike rates of responses in non-inhibited areas (outside the excitatory area) and inhibited areas were determined. Inhibitory strength was calculated as the ratio of spike numbers per stimulus in inhibitory areas to those in non-inhibitory areas. Low- and high-frequency inhibition bands were analyzed separately. Neurons displaying inhibition with a strength of 20% and higher were considered to be neurons displaying inhibition, and their numbers were compared between groups.

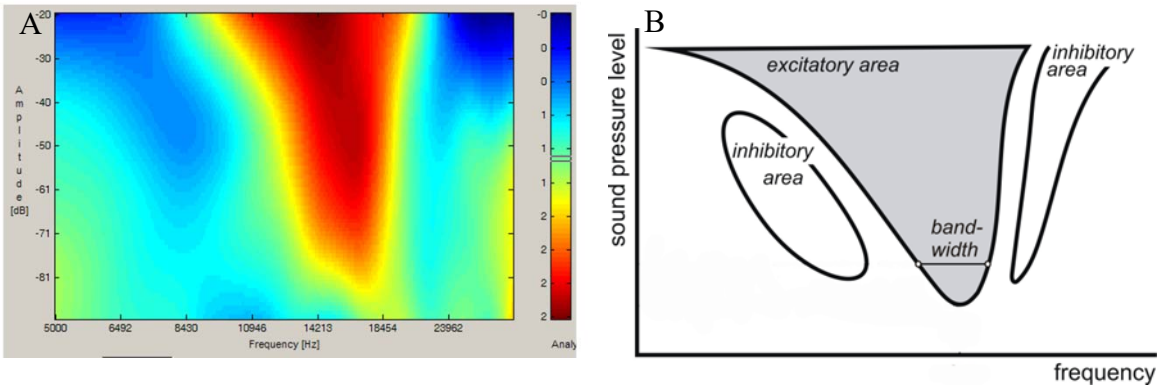

Figure 14. Two-Tone Stimulation.

A. heat map of one neuronal response to two-tone stimulation, created using Matlab software on the basis of measured data. B. A schematic plot showing the excitatory and inhibitory areas of a frequency–intensity response area.

3.4.5. Intensity Coding in the IC

Neuronal responses to broadband noise (BBN) bursts of variable intensity (from 0 to 90 dB SPL, 10 dB steps, 50 repetitions) were used to construct the rate-intensity function (RIF) (Bures et al., 2010). On each RIF, two points of interest were defined: R10, describing the starting point of the RIF's rise, and R90, describing the RIF's transition to the saturated region (0). A 100% scale was assigned to the neuron's total range of response amplitudes, 0% corresponding to spontaneous activity and 100% corresponding to its maximum response magnitude. The two points of interest, R10 and R90, correspond to 10 and 90% of this scale, respectively.

The following parameters of the RIFs were evaluated: (i) the response threshold; (ii) the sound pressure level (S10) corresponding to point R10; (iii) the sound pressure level (S90) corresponding to point R90; (iv) the dynamic range (DR) of the RIF (DR = S90 − S10);

(v) the relative initial slope of the RIF – taken from the normalized RIF, calculated from the first 20 dB above threshold, expressed as a percentage of change per dB; and (vi) the maximum response magnitude.

Minimum first-spike latency (mFSL) was evaluated from the poststimulus time histograms to BBN stimuli at 80 dB SPL, as the amount of time between the onset of sound presentation and the appearance of first spikes of neuronal responses.

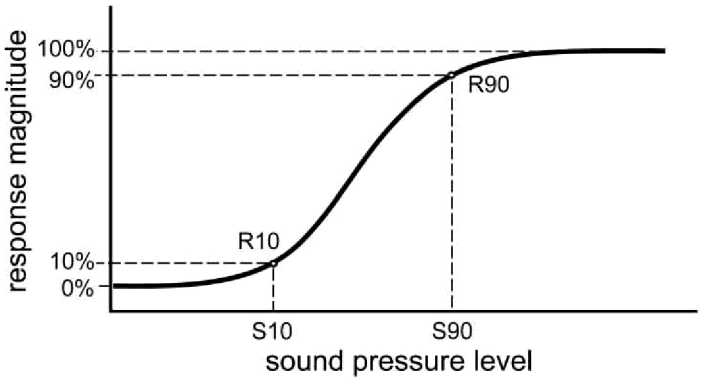

Figure 15. Schematic plot of a general rate–intensity function.

The relative response scale and two points of interest, used for the quantification of the RIF shape, are defined: 0% corresponds to spontaneous activity, and 100% to the maximum response magnitude; the two points of interest, R10 and R90 correspond to 10 and 90% of this scale, respectively.

3.5. Round window membrane application

3.5.1. Nanoparticles

Penetration of three types of nanoparticles: liposomes (average size: 82 ± 5 nm polydispersity index: 0.05), polymersomes (hydrodynamic diameter 89.5 ± 19.5 nm) and hyperbranched polylysine (Mn: 24600 g/mol, polydispersity index: 12.5, hydrodynamic radius: 10 nm) from the middle ear to the cochlea was investigated using C3H mice (Figure 16). Nanoparticles were labeled with fluorescent dye to enable their detection in the cochlear structures (rhodamine for liposomes, 1,1′-dioctadecyl-3,3,3′3′ tetramethylindocarbocyanine perchlorate [DiI] for polymersomes and fluorescein for polylysine). The ability of nanoparticles to deliver active agent into the inner ear after middle ear application was also tested. To deliver DNA using polylysine two model plasmids were used: polylysine-plFL, containing plasmid, tagged with fluorescent marker (fluorescein) and polylysine- eGFP, containing plasmid, coding GFP (green fluorescent protein), detectable as green fluorescence.

As a model for drug delivery by liposomes and polymersomes neurotoxic drug disulfiram was used.

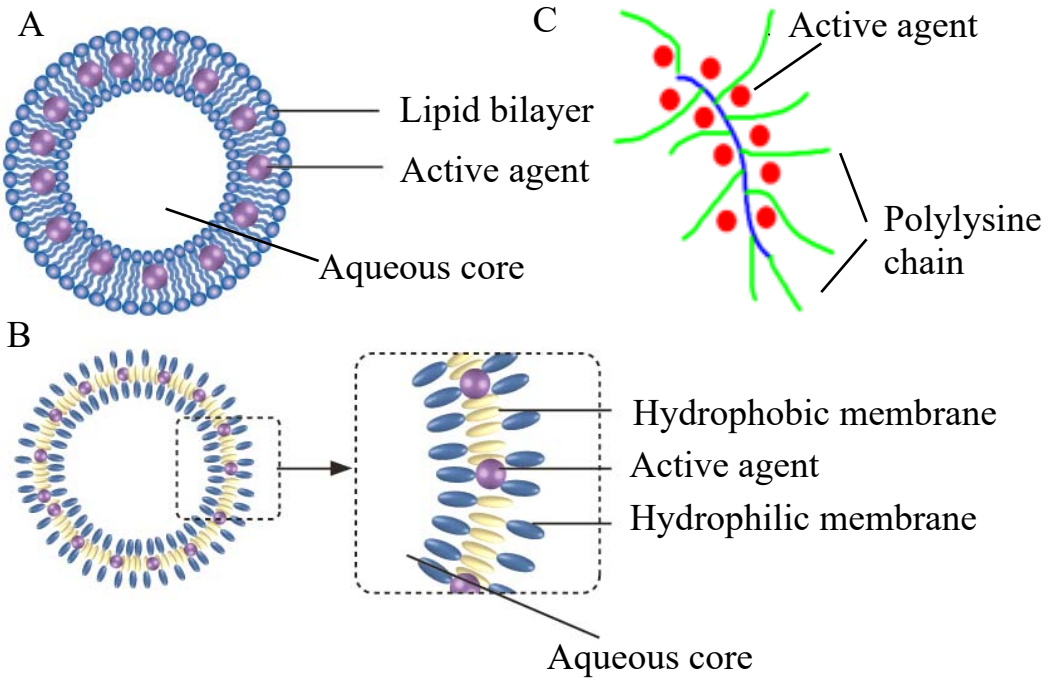

Figure 16. Structure of different types of nanoparticles.

(A) Liposomes and (B) polymersomes have a hydrophobic membrane that encapsulates an aqueous core. Membranes are formed from molecules made up of a hydrophilic and a hydrophobic domain (lipids in liposomes and block copolymers consisting of two different polymer chain units joined together in polymersomes) that self-assemble in water into vesicle-like structures. Hydrophobic compounds such as disulfiram can be encapsulated in the hydrophobic membrane. (C) Hyperbranched polylysine is represented by randomly branched chains of polymer that permits DNA complexation due to its high cationic charge.

NPs and plasmids were shipped from the producing laboratory (liposomes from University of Helsinki, polymersomes from University of Southampton, polylysine and plasmids from The École polytechnique fédérale de Lausanne), stored at 4 °C and used within 2 weeks after production. Polylysine-plasmid complex was prepared according to manufacturer instructions: polylysine and DNA were mixed together and incubated for 10 minutes before application.

3.5.2. Surgical procedure

C3H mice were anesthetized with 35 mg/kg of ketamine (Calypsol 5%, Gedeon Richter Ltd., Budapest, Hungary) and 6 mg/kg of xylazine (Xylapan 2%, Vetoquinol, Gorzów Wielkopolski, Poland). Middle ear (acoustic bulla) of the mouse was accessed from the postauricular approach (Figure 17A). An incision was made in the skin to expose the acoustic bulla and enable visualization of the cochlear RW niche (Figure 17B).

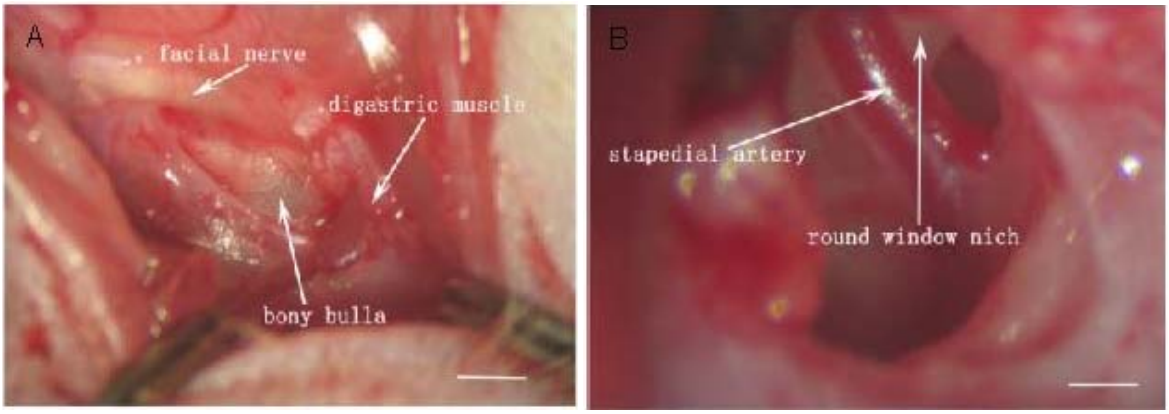

Figure 17. Surgical exposure of the mouse round window niche.

A. Acoustic bulla is exposed through the wound in the neck muscles. B. A hole is made in the bulla to expose the cochlea, stapedial artery and round window niche. The white bar indicates 1 mm. Modified from (Reif et al., 2013)

A small piece of gelfoam (Gelaspon, Chauvin Ankerpharm GmbH, Berlin, Germany) was placed in the RW niche (Figure 18), and 2–3 μl of the NP suspension, saline or disulfiram in saline (controls), was injected into the gelfoam using a Hamilton syringe (Figure 18).

The opening in the acoustic bulla was closed using acrylic resin, antibiotics were applied to the wound and the skin was sutured.

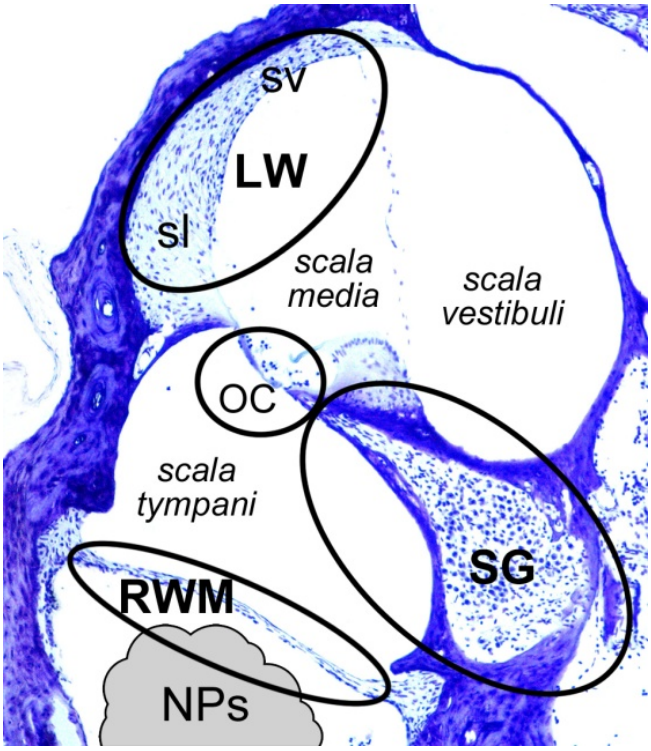

Figure 18. Delineation of gel foam location and analyzed cochlear structures.

Section through the basal turn showing the location of gel foam, where the nanoparticle (NP) suspension was injected and cochlear structures where the nanoparticle distribution was analyzed: round window membrane (RWM), spiral ganglion (SG), organ of Corti (OC) and the stria vascularis (SV) and spiral ligament (sl) of the lateral wall (LW). Scale bar = 100 µm.

3.6. Evaluation of gene expression

3.6.1. Gene Expression Analysis by RT-qPCR (performed by collaborators)

Total RNA was isolated from one or two cochleae per one mouse sample by TRIzol® Reagent (Thermo Fisher Scientific Inc., Waltham, MA, USA). After DNase I treatment (Thermo Fisher Scientific Inc., Waltham, MA, USA), RNA concentration and purity were determined by NanoDrop ND-1000 (Thermo Fisher Scientific Inc., Waltham, MA, USA). cDNA was obtained from RNA samples (0.25 or 0.5 µg) by reverse transcription using the RevertAid H Minus First Strand cDNA Synthesis Kit (Thermo Fisher Scientific Inc., Waltham, MA, USA). cDNA samples were diluted 10× or 20×, respectively. Each reaction for qPCR contained 4 µl diluted cDNA, 5 µl SYBR Green JumpStart Taq ReadyMix for qPCR (Sigma-Aldrich, St. Louis, MO, USA), 0.5 µl water, and 0.25 µl 10 mM forward primer and 0.25 µl 10 mM reverse primer. qPCR was performed with the initial activation at 94 °C for 120 s, followed by 39 cycles at 94 °C for 15 s, 59 °C for 30 s, and 72 °C for 30 s

using CFX384™ Real-Time PCR Detection System (Bio-Rad Laboratories, Hercules, CA, USA). The Hprt1 gene was selected as the best reference gene for our analyses from a panel of 12 control genes (TATAA Biocenter AB, Sweden). The relative expression of prestin, Myo7a, and IsI1 with Hprt1 as a reference gene was calculated using −ΔΔCq method, based on qPCR efficiencies (E) and the quantification cycle (Cq) difference (Δ) of Tg sample (Tg) versus WT (ratio= (Etarget)ΔCq(Mean WT−Mean Tg)/(EHprt1)ΔCq Hprt1(Mean WT−Mean Tg) (Pfaffl, 2001). Quantitative reverse transcription PCR (RT-qPCR) data were analyzed using the GenEX5 program (http://www.multid.se/genex/). Primer sets for Myo7a and prestin used are from Xia et al. (Xia et al., 2013), and Hprt1 primers are from Bohuslavova et al. (Bohuslavova et al., 2010).

3.6.2. Transgene Copy Number Estimation by qPCR (performed by collaborators)

The copy number of transgene was estimated using qPCR. qPCR reactions were first performed on serial dilutions of genomic DNA from tail biopsies to identify an appropriate amount of DNA template for experimental reactions and primer efficiencies. Primers were designed to amplify sequences from Isl1 exon 3 and a reference gene, Hprt1. Primer sets were designed using Primer 3 software (http://frodo.wi.mit.edu/primer3/). Primers were selected according to the following parameters: length between 18 and 24 bases, melting temperature (Tm) 60 °C, and G+C content between 40 and 60% (optimal 50%). Genomic DNA from six mice of each genotype was diluted to use 20 ng/20-µl reactions. qPCR was performed as described above. Reactions were run on gels to confirm that primers amplified only a single product. Threshold cycles (Cp) were normalized to Hprt1, of which two copies are present in both WT and Tg DNA. ΔCq was calculated for each sample (CqHprt1−CqIsl1). Fold change of a target transgene was calculated using ΔΔCq method as described (Pfaffl, 2001, Schoen et al., 2013).

3.6.3. Western Blot (performed by collaborators)

Proteins were extracted using the NucleoSpin RNA/protein kit (Macherey-Nagel, Germany) following the manufacturer's instructions. SDS-PAGE and Western blotting were carried out using the "XCell II SureLock™ Mini-Cell and XCell II Blot Module" (Invitrogen, Germany). The blotted proteins were incubated with either rabbit polyclonal or mouse

monoclonal antibodies for parvalbumin (Merck Millipore, Darmstadt, Germany), GAD67 (Merck Millipore, Darmstadt, Germany), or GAPDH (Abcam, Cambridge, UK) and subsequently secondary antibodies (HRP labeled anti-mouse from sheep and anti- rabbit from donkey, respectively, GE Healthcare) signals were visualized (Enhanced Chemiluminescence Plus Western Blotting Detection Reagent, GE Healthcare, AGFA X-ray film).

3.7. Morphological analysis

In the end of the experiment animals were sacrificed and tissues were taken for histological analysis.

3.7.1. Analyses of Embryos (performed by collaborators)

The noon of the day on which the vaginal plug was found was designated as E0.5. The developmental stage was classified for each embryo by morphological criteria. The embryonic morphology was assessed using a Nikon SMZ dissection microscope. Frozen 8-μm-thick sections of E10.5 embryos were fixed in 4% paraformaldehyde (PFA) for 15 min, incubated with 0.6% H2O2 (to block endogenous peroxidase), blocked with serum, and followed by incubation with the primary mouse anti-ISL1 monoclonal antibody (#39.4D5, Developmental Hybridoma Bank, Iowa City, IA, USA). The sections were labeled with secondary anti-mouse IgG-peroxidase (#A9044, Sigma) and developed in diaminobenzidine substrate (DAB; #D3939, Sigma). Semiquantitative analyses were performed to determine the relative number of cells expressing ISL1 per each field, using the threshold tool in the NIH ImageJ program (http://imagej.nih. gov/ij/download.html), as described (Turgeon and Meloche, 2009). The slides (n=3 − 4 × 3 embryos/each group) were analyzed under a Nikon Eclipse 50i microscope with a ×20 magnification objective using the NIS-elements program. For the dye-tracing experiment, the heads of E12.5 embryos were removed and fixed for a minimum of 24 h in 4% paraformaldehyde (PFA). NeuroVue® dye-coated filter microstrips were cut to appropriately sized pieces using microscissors and inserted into the brainstem and saccule nerve tracts and incubated at 60 °C for 4 days. A two-colour tracing system using NeuroVue® Maroon and Red, which have 647- and 568-nm excitation, respectively, was applied (Kersigo et al., 2011). Progression of dye diffusion was monitored using epifluorescent microscopy. On completion of dye diffusion, wet mounts of inner ear and brain stem were prepared using glycerol and coverslips as spacers. Images were taken using a

Leica SP5 confocal laser scanning system to generate stack of images. These stacks were subsequentially collapsed to generate single images.

3.7.2. Analyses of adult tissues

3.7.2.1. Brain sections (performed by collaborators)

To study Islet1 expression in the brain, it was cut into two hemispheres and sectioned serially into 50-µm-thick slices using a vibratome following overnight postfixation in 4% PFA. The brain sections were stained with primary anti-ISL1 (#39.4D5, Developmental Hybridoma Bank, Iowa City, IA, USA) and anti-PAX2 (#PRB-276P, Covance) overnight.

To study the consequencies of BDNF deletion in the inferior colliculus and auditory cortex, brains were fixed in 100 mM phosphate-buffered saline (PBS) containing 2% PFA and 125 mM sucrose, pH 7.4, for 48 h. Brains were embedded after fixation in 4% agarose, cut at 60 µm thickness with a Vibratome (Leica VT 1000S, Wetzlar, Germany), and stored in PBS at 4 °C. Brain regions were identified in accordance with the mouse atlas of Franklin and Paxinos (Franklin and Paxinos, 2008). Serial sections derived from coronal brain slices between 1.8 and 2.3 mm posterior to bregma were analyzed. Tissue sections were washed with PBS, permeabilized and incubated overnight with primary antibody at 4 °C. For double labeling studies, specimens were simultaneously incubated with both antibodies. Primary antibodies were detected with Cy3-conjugated (Jackson ImmunoResearch) and AlexaFluor 488-conjugated secondary antibodies (Life Technologies GmbH, Darmstadt, Germany). Slices were mounted with Vectashield mounting medium containing DAPI (Vector laboratories, Burlingame, CA, USA). Sections were viewed using an Olympus BX61 microscope equipped with epifluorescence illumination. Mouse anti-parvalbumin (Sigma-Aldrich, Munich, Germany) rabbit and mouse anti-GAD67 (Merck Millipore, Darmstadt, Germany) antibodies were used.

3.7.2.2. Cochlear whole mount preparation

A cochlear surface specimen preparation was performed for visualization and quantitative analysis of organ of Corti and its innervation. Acoustic bullas were removed

from the skull of a sacrificed animal. Bone of the bullas was removed, oval and round windows in the basal turn of the cochlea were opened, hole was made on the apical turn and the cochlea was left in 4% PFA for 2 h for fixation. After that the cochlear bone capsule was removed using tweezers sequentially from apex to base, and the basal membrane with the organ of Corti was dissected into 3–4 pieces per cochlea. Cochlear pieces aimed for nerve fiber visualization were decalcified 0.12 M ethylendiaminotetraacetic acid for 10 min prior to staining. Specimens were treated with 0.1% trypsin for 20 min and, depending on aim, stained using the following primary antibodies: anti-prestin (# sc-30163, Santa Cruz Biotechnology Inc., Dallas, TX, USA), anti-200-kDa neurofilament protein (NF200, # N4142, Sigma-Aldrich Co., St. Louis, MO, USA), anti-choline acetyltransferase (ChAT, # AB144P Millipore Corporation, MA, USA) and anti-myosin 7a (Myo7a, # 028918, Sigma-Aldrich Co., St. Louis, MO, USA). Phalloidin (# 59033, Dyomics) was used for F-actin and DAPI (# D9542, Sigma-Aldrich Co., MO, USA) for nuclei visualization. Preparations were examined under Zeiss 510 DUO laser confocal scanning microscope with ×40 Plan-Apochromat oil immersion objectives (numerical aperture 1.4). To determine the region of interest (part of the cochlea, corresponding to particular frequency), the ImageJ plugin was used
(http://www.masseyeandear.org/research/otolaryngology/investigators/laboratories/eatonpeabody-laboratories/epl-histology-resources/imagej-pluginfor-cochlear-frequency-mapping-in-whole-mounts/). Z stacks through the thickness of the cochlea with step sizes from 0.2 to 1 μm depending on the aim were obtained from the cochlear parts representing particular hearing frequencies (region of interest).

3.7.2.3. Cochlear paraffin sections

Paraffin embedded cochlear sections were used for visualization of cochlear parts to study nanoparticle distribution, quantification of spiral ganglion neuron number and detection of spiral ganglion cell death.

After overnight fixation in 4% PFA cochleas were decalcified in 0.12 M ethylendiaminotetraacetic acid for 1 week, dehydrated through a graded alcohol series, cleared in xylene, and embedded in paraffin. Horizontal serial sections (10 μm) were mounted on 3-triethoxysilylpropylamine-coated glass slides. Antifading medium (Polyscience, IL, USA) was used for mounting the sections.

Sections were used for detection of fluorescent signal from nanoparticles, or further staining to analyze cochlear morphology using light (Olympus BX40) or confocal microscope (Zeiss 510 DUO).

Part of cochlear sections was stained using cresyl violet (Sigma) solution for 30 min and examined under a light microscope. A cell that exhibited either a small, round dark blue nucleus with space surrounding it due to shrinkage of the cell, or 2–3 small dark dots in a cluster was classified as a dying cell (Willingham, 1999).

A series of sections for active caspase-3 immunostaining were briefly trypsinized, then incubated with anti- active caspase-3 antibody (Promega, WI, USA). After PBS washes, secondary antibodies (goat Fab anti-rabbit IgG) labeled with Alexa Fluor 594 (Millipore) were used for visualization.

3.7.3. Quantitative analysis

Cochlear hair cell number counting

To plot cochleograms, photographs were taken consecutively from the whole length of the cochlea starting from the apical turn. The images were then manually superimposed using Corel Draw software to create a picture of the whole cochlea from apex to base. Cells were counted in each 7% of the cochlear length using ImageJ software, and the loss of outer hair cells (OHCs) was calculated using Excel.

Analysis of cholinergic terminal size.

For quantitative analysis of ChAT positive (ChAT+) staining, the 3D stacks from the 16–20 kHz cochlear region were analyzed. Three cochleae from each group were examined. To minimize the possibility of biased results, the analysis was carried out blindly. The volumes of ChAT+ MOC terminals and volumes of ChAT+ particles in the region of Deiters' cells (DCs) were calculated using the 3D object counter ImageJ plugin (Bolte and Cordelieres, 2006). ChAT+ particles in the DC area are shown as a volume per 1 OHC.

Analysis of the number of the spiral ganglion neurons containing NPs or survived after the treatment or with age.

The number of SG neurons either containing NPs (cells containing at least one fluorescent dot) or survived after the application of disulfiram-loaded NPs in C3H mice or during ageing in Pax2Isl1 transgenic mice was assessed. Cochlear slices were stained with

diluted cresyl violet solution (Alvarez-Buylla et al., 1990) and Z stacks through the spiral ganglion were acquired using the Zeiss confocal microscope 510 DUO. For quantitative analysis the optical dissector software Ellipse® (India) was used (Sterio, 1984, Cizkova et al., 2009). The dissector probe is represented by a 'virtual box' (counting frame) that is placed inside the physical section. The size of the counting frame was 76.5 × 74.8 µm and 9.24 µm high for detection of cells, containing NPs or 99 × 88 µm, dissector height 8.4 µm, for SGN counting. Each cell of interest was manually marked in the first optical section of the virtual box; the software then showed this marker in deeper optical sections, allowing the experimenter to define the last optical section where the neuron is still visible and unmark the cell in that level (with the information about the cell stored). This procedure was repeated for all neurons in the slice thickness excluding impaired cells on the sheares. SGNs were counted in the basal, middle, and apical regions of the cochlea from one animal; minimum of three ears per group and five slices from each cochlea were analyzed. The numerical density was defined as the number of objects per cubic millimeter.

Analysis of the expression of parvalbumin and GAD67 (performed by collaborators)

The acquired images were analyzed using the free software ImageJ (NIH, Bethesda, MD, SA) to evaluate the expression of parvalbumin and GAD67. In every picture, the background was reduced with the rolling ball algorithm, and therefore, the red, green, and blue channels have been separated. In the green channel (parvalbumin or GAD67), a threshold (with ImageJ standard parameters) has been applied and therefore the ImageJ built-in plugin, Analyze Particles, has been used to count the numbers of parvalbumin or GAD67 puncta.

3.8. Statistical Analysis

Data are presented either as the mean ± standard deviation (SD) or standard error of the mean (SEM) for values with normal distributions or the median (Mdn) for values with non-normal distributions. For statistical analysis, the GraphPad Prism software (San Diego, USA) was used. To assess differences in mean or median values between groups Student's t tests, one-way or two-way analysis of variance (ANOVA) with Bonferroni's multiple comparison test, Kruskal-Wallis tests with Dunn's multiple comparison test, or chi-square tests were employed. Significance was assigned at the $P<0.05$ level.

4. Results

4.1. Role of ISL1 in development and function of the auditory system

4.1.1. Pax2-Isl1 transgenic mice

The Pax2-Isl1 transgenic mice [Tg(Pax2-Isl1)] were generated using a transgenic construct, containing Isl1 gene insert and the 8.5-kb Pax2 regulatory sequences with regulatory activities in the midbrain–hindbrain region and otic vesicle, which closely mimic the activities of the endogenous Pax2 gene at E9.5.

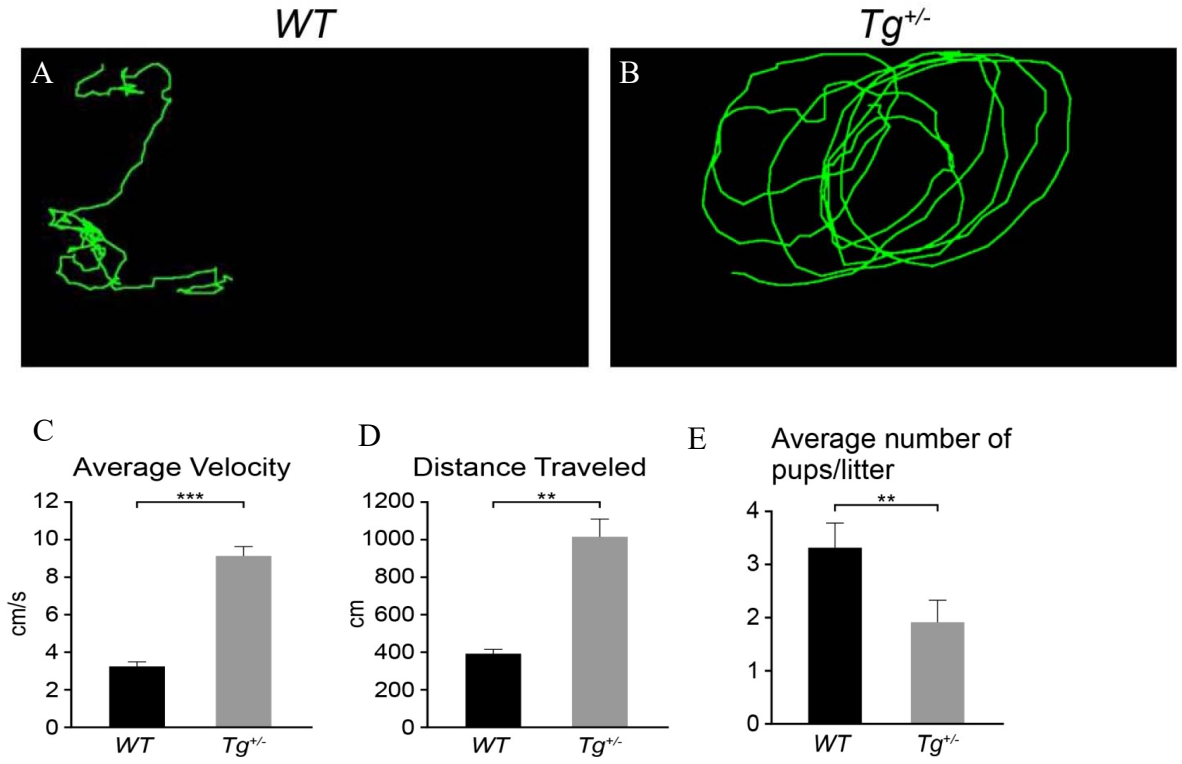

Figure 19. Pax2-Isl1 transgenic mice.

*A, B Traces and C, D quantification of mouse locomotion in an open field showing circling and hyperactivity of $Tg^{+/-}$ mice (n=3) in comparison to WT littermates (n=3). E. Average number of surviving $Tg^{+/-}$ offspring per litter is significantly decreased compared to their WT littermates (n=27 litters). The values represent means ± SEM. **p<0.01; ***p<0.001, t test*

$Tg^{+/-}$ mice exhibited increased levels of motor hyperactivity, including augmented locomotion and circling behavior compared to WT littermates (Figure 19A, B). The average velocity of $Tg^{+/-}$ mice was 2.8 folds higher compared to WT ($P < 0.001$; Figure 19 C). The average distance travelled in 2 minutes was 10 ± 0.9 m and 3.9 ± 0.2 m for $Tg^{+/-}$ and WT, respectively ($P < 0.01$; Figure 19 D).

Mating produced a lower number of transgenic offspring at weaning than the expected Mendelian frequencies. The number of surviving offspring at weaning from WT and $Tg^{+/-}$ intercrosses was 89 WT and 52 $Tg^{+/-}$ pups in 27 litters. The average number of surviving transgenic heterozygous offspring per litter (1.926 ± 0.2871, n = 27) was significantly lower compared to their WT littermates (3.296 ± 0.3988; Figure 19E). We noticed a decreased survival rate of the $Tg^{+/-}$ pups in the first two days of life compared to their WT littermates. We did not notice any abnormal gross appearance in the pups; however, these pups were found outside their nest, rejected by the mother and unable to feed, which could be associated with neuromuscular defects or/and absence or diminished vocalization of newborns.

4.1.2. Gain in embryonic development of Pax2-Isl1 transgenic mice

To establish the Isl1 expression pattern in the otocyst of $Tg^{+/-}$ compared to WT mice, we analyzed the expression of ISL1 at E10.5 embryos.

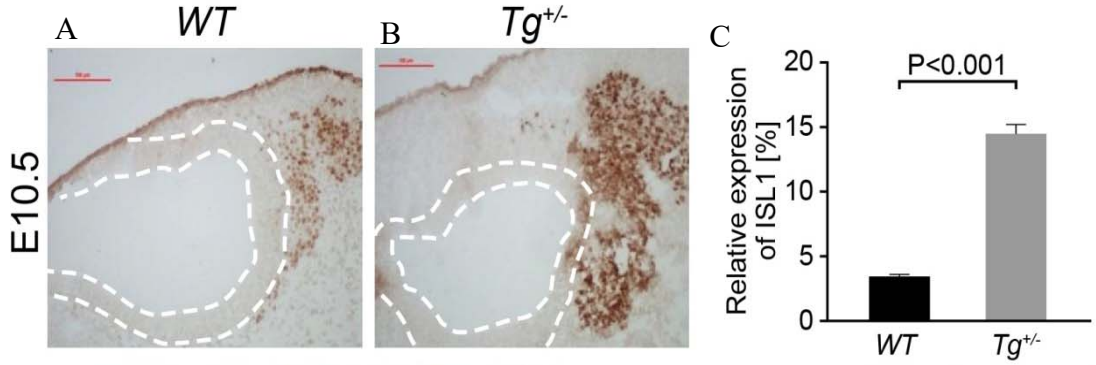

Figure 20. ISL1 expression in the otocyst at E10.5.

A, B. Transverse sections of embryos stained with anti-ISL1 antibody. Mutant embryos show increased ISL1 expression compared to WT at E10.5. The dashed lines indicate the borders of the otic epithelium. C. $ISL1^{+}$ area quantified as a percentage of total tissue area in the field using the ImageJ software. Scale bar 0.1 mm. The values are means ± SEM (n=5 for WT, n=3 for $Tg^{+/-}$, t test).

The ISL1+ expression domain was enlarged in the $Tg^{+/-}$ otocysts. The size of the cochleo-vestibular ganglion delaminating from the otic epithelium and differentiating into ganglion neurons was increased in $Tg^{+/-}$ embryos compared to WT littermates (Figure 20A, B). Likewise, the size of ISL1+ domain was significantly enlarged in $Tg^{+/-}$ compared to WT littermates, likely reflecting the effects of transgenic Isl1 expression (Figure 20C).

We injected lipophilic dyes into the cerebellum (Figure 21A, B) or the ear (Figure 21C, D) in order to analyze the nerve fiber extension and branching in E12.5 embryos.

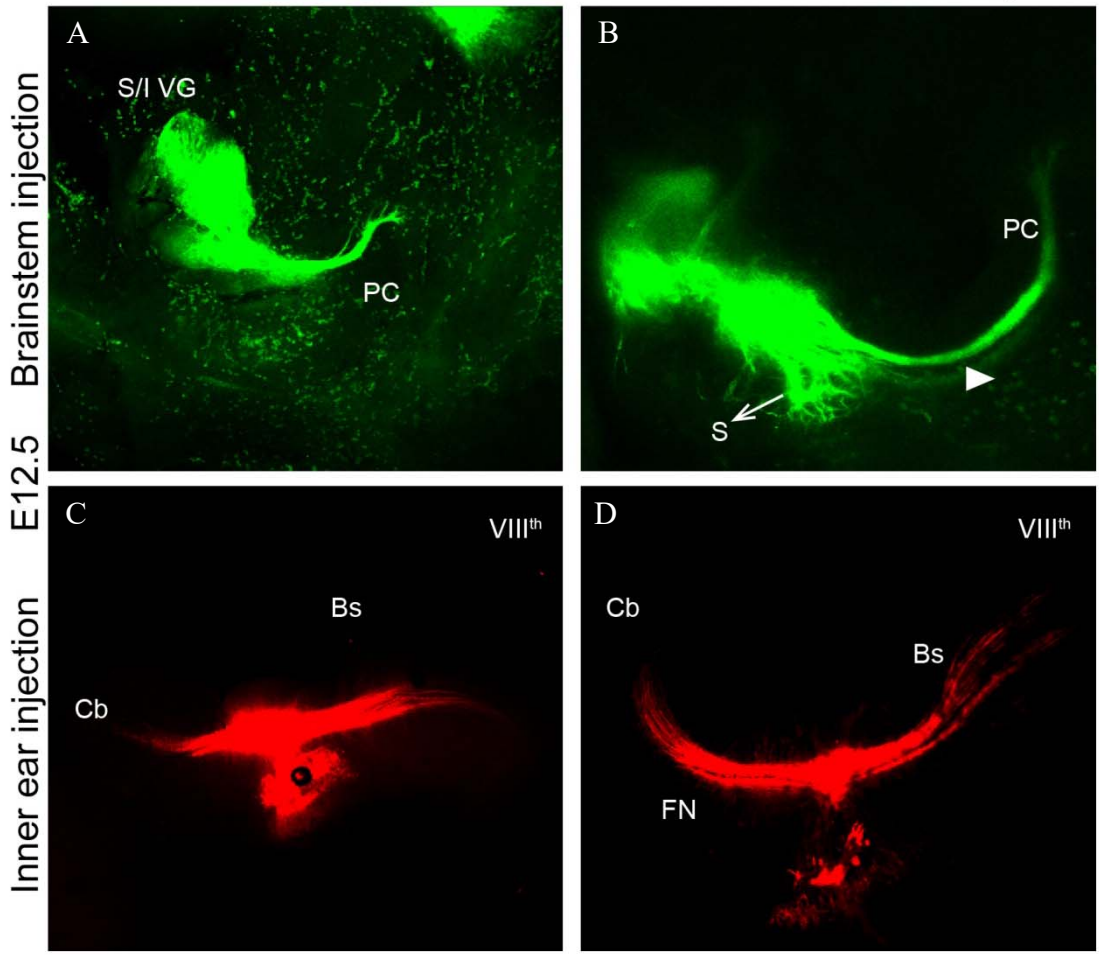

Figure 21. Affected nerve fiber development

Transgenic expression of Pax2-Isl1 causes faster nerve fiber extension and branching in E12.5 embryos. The lipophilic dye tracing of fiber extension and branching in E12.5 embryos (green, brainstem injection) shows more branching in the saccule and more fibers going through the posterior canal in $Tg^{+/-}$ (B) compared to WT embryos (A). The inner ear injection (red) shows more fibers going to the cerebellum in the $Tg^{+/-}$ (D) than in WT embryos (C). S saccule, VG vestibular ganglion, Cb cerebellum, Pc posterior canal, Bs brain stem

The saccule is the first to differentiate and extends to the brainstem and cerebellum. More branching is seen in the saccule and more fibers going to the posterior canal can be observed in $Tg^{+/-}$ compared to WT mice (Figure 21A, B). Ear injections revealed more fibers extending earlier already into the cerebellum in the transgenic embryos (Figure 21C, D). Cochlea projections were not investigated as they just reach the brainstem at this stage (Li et al., 2004). Thus, increased expression levels of Isl1 in mutant embryos were associated with more rapid differentiation of afferents.

4.1.3. Impairement in cochlear innervation in Pax2-Isl1 transgenic mice

Because we detected an increased branching of nerve fibers in E12.5 transgenic embryos, we examined the state of the cochlear innervation after birth.

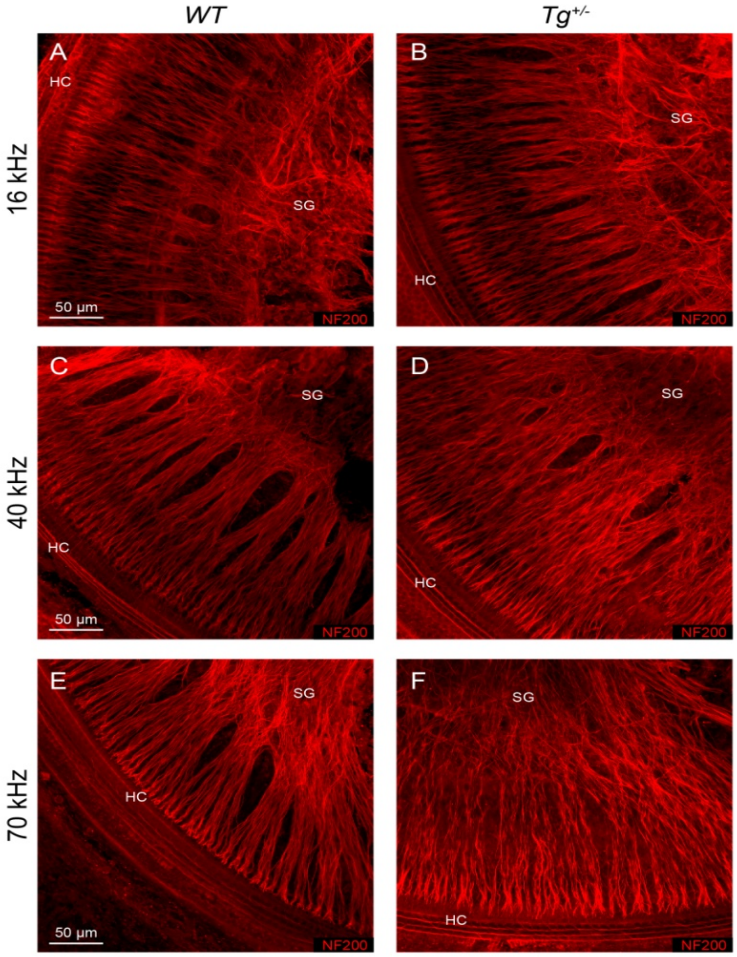

Figure 22. Affected cochlear radial innervation in mutant mice.

Spatial organization of radial fibers (NF200) is not affected in the middle cochlear turn (16 kHz, B) but is altered in the basal part of the cochlea (40 kHz and above, D and F) in $Tg^{+/-}$ mice at P3 compared to WT littermates (A, C, E).

Compared to WT animals at P3, radial afferent fibers of $Tg^{+/-}$ mice at 40-70 kHz were not properly organized in tight bundles (Figure 22). To check whether spiral ganglion enlargement, found in $Tg^{+/-}$ during embryonic development persisted in adult animals, we counted spiral ganglion neuron number in young WT and $Tg^{+/-}$ animals. We found that, in contrast to embryonic period, in young adult animals the total number of SGNs in all cochlear turns was significantly smaller in $Tg^{+/-}$ animals than in WT mice (Figure 23C, D). Because

spiral ganglion neuron (SGN) degeneration is known to increase with age in mice (Radde-Gallwitz et al., 2004) and also in humans (Huang et al., 2008) we analyzed also the number of SGNs in different age groups in WT and $Tg^{+/-}$ mice.

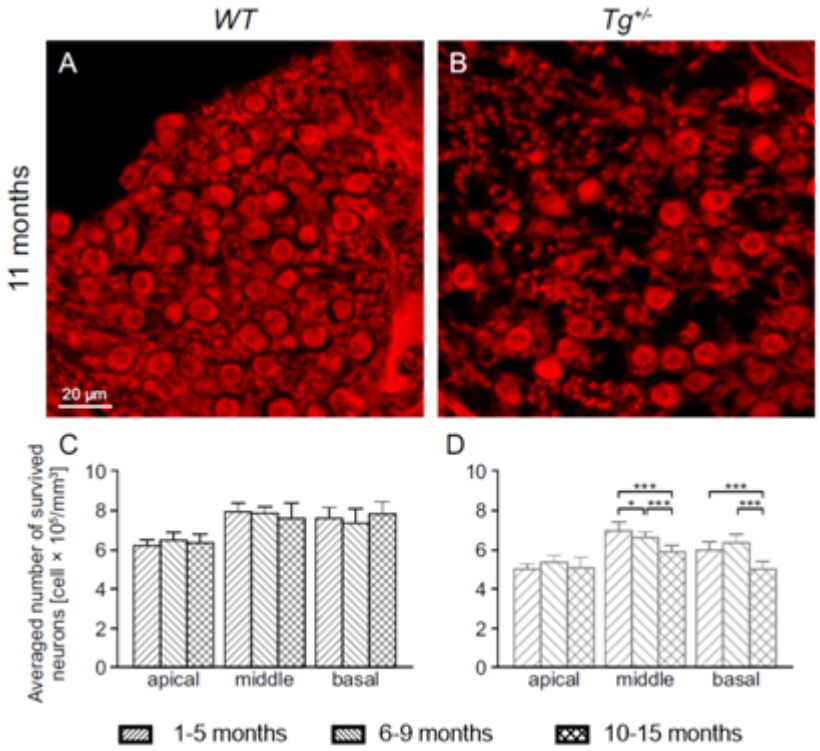

Figure 23. Loss of spiral ganglion neurons in transgenic cochleae.

*The number of spiral ganglion neurons (SGNs) is preserved in all cochlear turns in WT mice in all ages (A, C). In contrast, a progressive age-related loss of SGNs is found in the middle cochlear turn of $Tg^{+/-}$ mice (D). A significant loss of SGNs is also noticeable in the oldest tested group of $Tg^{+/-}$ mice (B, D). Values are presented as means ± SD; *p<0.05, ***p<0.001, one-way ANOVA with the Bonferroni correction test.*

No significant reduction in the number of SGNs was observed in WT animals in any analyzed age group (Figure 23A, C). In contrast, $Tg^{+/-}$ mice showed an age-related reduction in the number of SGNs in the middle turn (from 6.932 × 105 / mm^3 in young to 5.872 × 105 / mm^3 in old mice, $P \leq 0.001$) and the basal turn (from 5.945 × 105 / mm^3 in young to 4.765 × 105 / mm^3 in old mice, $P \leq 0.001$) (Figure 23B, D).

4.1.4. Hearing loss in adult Pax2-Isl1 transgenic mice

To test whether impaired development of the spiral ganglion affected hearing in transgenic mice we measured ABR and DPOAE responses.

Young mutant mice (1–5 months) had significantly higher ABR thresholds than WT mice only at 32 kHz (Figure 24B). However, the ABR thresholds of 6 to 9-month-old $Tg^{+/-}$ mice were significantly higher in overall frequency range with the smallest difference of 10 dB at 40 kHz and the highest of 35 dB at 16 kHz (Figure 24D). The hearing thresholds of mutant mice at this age underwent the largest shift detected during the experiment. The ABR thresholds of $Tg^{+/-}$ animals at 8 and 16 kHz were the most affected by aging and they shifted by 35 dB and 45 dB, respectively, when the youngest and the oldest tested groups were compared. In contrast, the shift in hearing thresholds during the aging of WT animals was more uniform over the whole frequency range. It did not differ by more than 22 dB between the youngest and oldest tested groups at any of the tested frequencies.

DPOAE analysis is used to assess the function of OHCs in the cochlea, which is known to decline with age in mice (Parham, 1997, Jimenez et al., 1999, Guimaraes et al., 2004) and humans (Lonsbury-Martin et al., 1991, Uchida et al., 2008, Abdala and Dhar, 2012). The age-related decline of DPOAE amplitudes started from the high frequency region in both WT and $Tg^{+/-}$ groups. However, the loss of DPOAEs was much more rapid in $Tg^{+/-}$ animals. The DPOAE amplitudes at 32–40 kHz were reduced already in one-month-old $Tg^{+/-}$ compared to WT animals. DPOAE deterioration progressed with age and 5-month- old $Tg^{+/-}$ animals had significantly smaller DPOAE amplitudes at the majority of tested frequencies (8–25 kHz) and a complete loss of DPOAEs at 32–40 kHz compared to WT mice (Figure 24A). $Tg^{+/-}$ mice completely lost DPOAEs by the age of 6–9 months (Figure 24C), while DPOAEs of WT mice were only slightly decreased at high frequencies at this age and were still present at the middle frequencies in 15- month-old animals (Figure 24E).

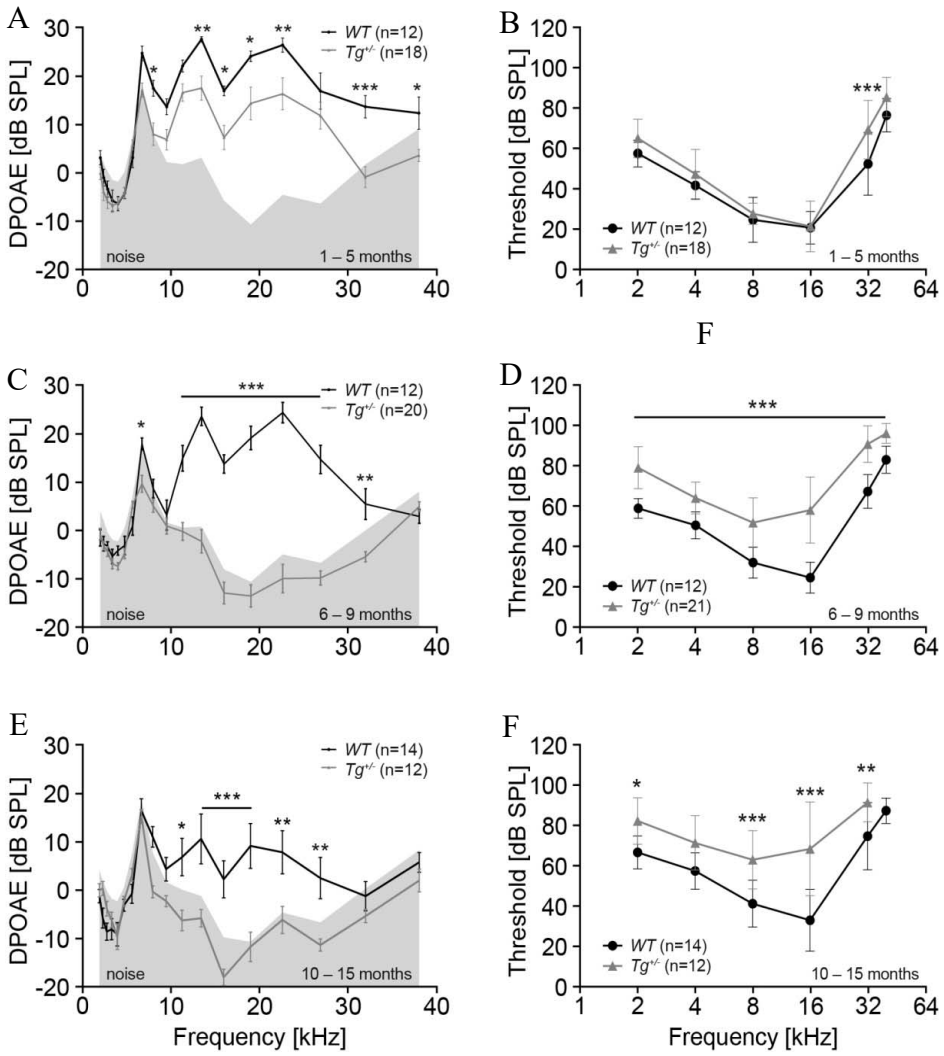

Figure 24. Deteriorated hearing in transgenic mice

*Results of hearing tests presented as DPOAE-grams (A, C, E) and audiograms (B, D, F) demonstrate significantly lower DPOAE levels in 1- to 5-month-old $Tg^{+/-}$ animals (A) and complete loss of DPOAEs in 6- to 9-month-old $Tg^{+/-}$ mice (C). In contrast in WT mice, DPOAE levels only decrease in older animals and are still present in 10- to 15-month old mice (E). Changes in ABR thresholds confirm changes in DPOAEs being significantly increased in 6- to 15-month-old $Tg^{+/-}$ compared to the WT mice of the same age (D, F). Results are means ± SEM for DPOAEs and means ± SD for hearing threshold. *p<0.05, **p<0.01, ***p<0.001, two-way ANOVA with the Bonferroni correction test.*

4.1.5. Cellular and molecular changes in auditory hair cells in Pax2-Isl1 transgenic mice

The nature and dynamics of functional changes (DPOAEs, hearing thresholds) in mutant mice suggest primary abnormalities in OHC function. To characterize the OHC state,

we analyzed the OHC number, spatial organization, and expression of prestin, F-actin, and myosin 7a (Myo7a) using cochlear whole mount preparation. The spatial organization of hair cells was unaltered in transgenic mice. Hair cells were arranged in three OHC rows and one row of inner hair cells (IHCs) in both experimental groups of animals. We did not notice any visible differences between the young $Tg^{+/-}$ and WT animals in the hair cell stereocilia visualized by phalloidin staining (Figure 25A, B). In the oldest group of animals (11 months and older), $Tg^{+/-}$ mice demonstrated a greater degree of disorganization and loss of OHC stereocilia in the high frequency cochlear region than WT animals (Figure 25D, E). The hair cell marker, Myo7a, did not reveal any visible differences between the hair cells of WT and $Tg^{+/-}$ animals in all age groups (Figure 25G, H). The number of present and missing cells in each 7% of cochlear length was counted and the loss of OHCs was plotted as a cochleogram (Figure 25C, F, I). Missing OHCs were rare in cochleae of both experimental groups at P3 and P15. However, we detected OHCs loss in 1 to 5-month-old animals averaging 24% in WT and 37% in $Tg^{+/-}$ animals (Figure 25C, insert). The distribution of OHC loss was similar in both experimental groups (Figure 25C–F). The predominant OHC loss was detected in high frequency regions, and was lower in low frequency regions. OHCs were the most preserved in the middle part of the cochlea in animals of all age groups. However, we detected a significantly higher loss of OHCs in the high frequency region of the cochlea (above 30 kHz) in young transgenic mice compared to WT (Figure 25C). While OHC loss extended from the high frequency region to the direction of lower frequency regions in older $Tg^{+/-}$ and WT animals (6–9, 10–15 months; Figure 25F, I), OHC loss was significantly higher in $Tg^{+/-}$ animals. Regardless of the tonotopic position, the total OHC loss was significantly higher in 6 to 9 and 10 to 15-month-old $Tg^{+/-}$ mice compared to WT ($P < 0.05$, Figure 25F, I, inserts). However, the progression of OHC loss with age was the same for both groups with the difference of 13–14% between WT and $Tg^{+/-}$ mice. The number of IHCs did not change along the whole cochlear length in most animals from both groups across age. However, we observed some IHC degeneration in the high frequency region of the cochlea (30 kHz and above) in 11-month-old $Tg^{+/-}$ animals when the OHCs were completely lost.

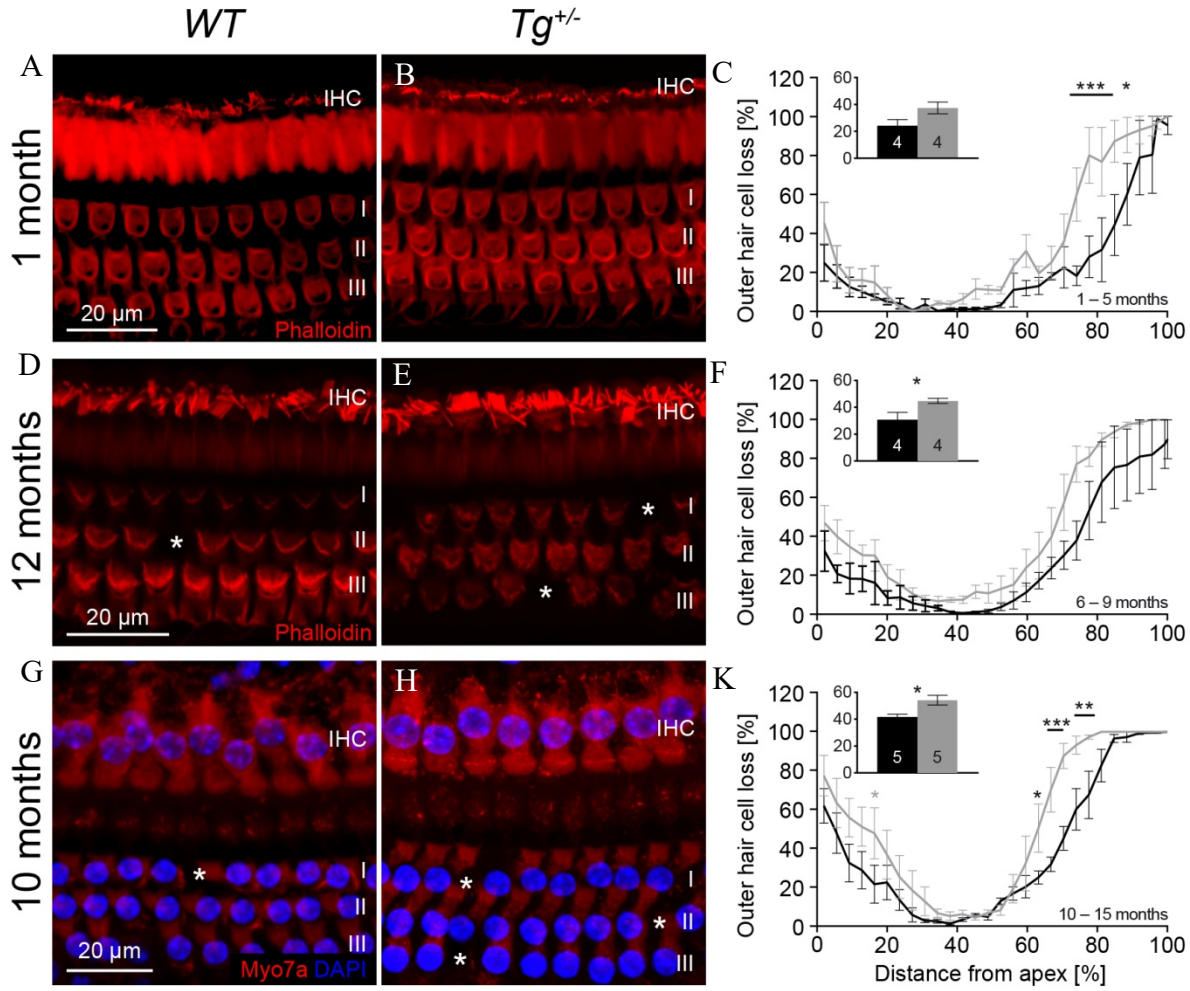

Figure 25. Loss of high-frequency OHCs in Tg+/− mice with no evident alteration of HC morphology.

*HCs appear to be normal when visualized using phalloidin and anti-Myo7a antibodies (A, B, D, E, G, H). Moderate disorganization of OHC cilia is noticeable in 12-month-old $Tg^{+/-}$ mice (E). A decreased number of OHCs is already detected in 1- to 5-month-old animals, mainly in the high-frequency region of the cochlea (C), and the same trend continues in older animals (F, I). However, the progression of OHC loss with age is the same with the difference of 13–14 % between WT and $Tg^{+/-}$ mice for all ages (C, F, I, inserts), suggesting a similar level of OHC loss progression with age for both groups. Stars indicate missing OHCs. Values are presented as means ± SEM; *p<0.05, **p<0.01, ***p<0.001, one-way ANOVA with the Bonferroni correction test. IHC inner hair cells; OHC outer hair cells; I, II, III 3 rows of OHCs.*

Although mutant mice had a significantly higher loss of OHCs compared to WT animals, it does not fully explain the complete loss of DPOAEs by the age of 6–9 months.

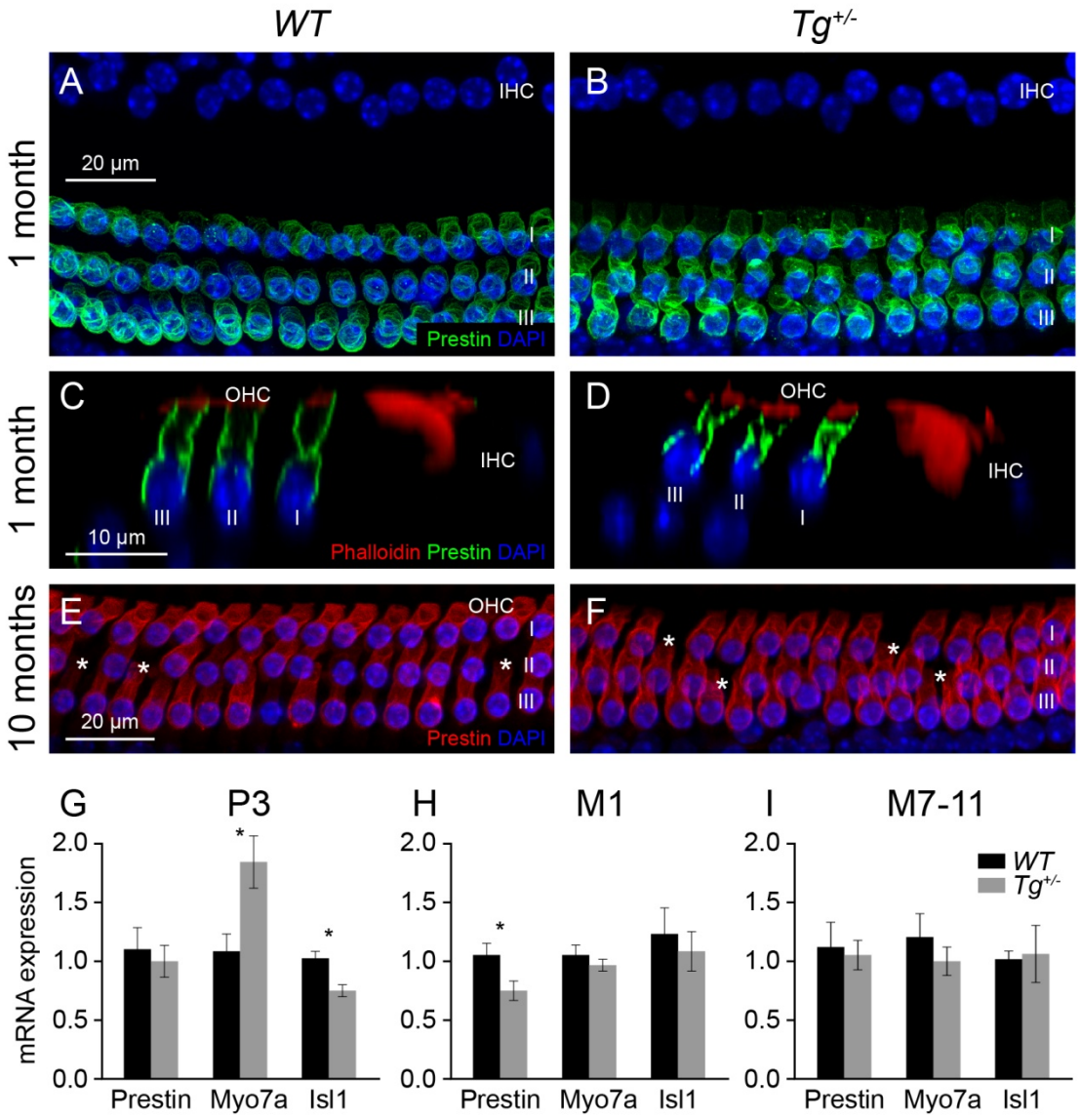

Figure 26. Preserved prestin distribution and decreased levels of prestin mRNA in OHCs.

*Prestin location and distribution inside OHCs is not different between WT and $Tg^{+/-}$ mice and is not affected by aging (A–F). RT-qPCR analysis shows lower prestin levels of mRNA in 1- month-old $Tg^{+/-}$ mice compared to WT (H; n=6 mice/genotype). No significant differences in prestin expression are detected in P3 (G; n=5 $Tg^{+/-}$ and 7 WT) or M7-11-month-old cochlea (I; n=5 mice/genotype). Stars indicate missing OHCs. Values are presented as means ± SEM; *p<0.05, t test. IHC inner hair cells; OHC outer hair cells; I, II, III 3 rows of OHCs*

This suggests a loss of OHC function despite the continuing presence of the vast majority of OHCs in the cochleas of $Tg^{+/-}$ 6 to 9-month-old mice. In order to better understand this loss of function, we analyzed the expression and distribution of motor protein prestin in the OHCs of WT and transgenic mice (Figure 26). The distribution of prestin did

not differ between experimental groups. Prestin was localized in the cell wall from approximately the mid-nuclear level to the level of the cuticular plate on top of the cell (Figure 26C, D) and corresponded to other published reports. The mRNA levels of prestin quantified by RT-qPCR were significantly lower in $Tg^{+/-}$ cochlea than in WT at one month of age (Figure 26H), whereas the expression of prestin did not differ between WT and $Tg^{+/-}$ cochlea in P3 and in older mice (7 to 11-month-old mice; Figure 26G, I).

4.1.6. Impaired medial olivocochlear innervation of outer hair cells in Pax2-Isl1 transgenic mice

Medial olivocochlear (MOC) endings, contacting basal part of OHCs, might influence their function. To analyze the state of MOC terminals we performed choline acetyl transferase staining of cochleas from both groups of animals. The volume of MOC terminals was significantly reduced in $Tg^{+/-}$ compared to WT in all age groups (by 20% in young group Figure 27A, C, G, I, and M). $Tg^{+/-}$ animals showed progressive age-related deterioration of the MOC terminals with a 30% volume reduction in 10 to 15-month-olds compared to the younger $Tg^{+/-}$group (Figure 27C and I). In both $Tg^{+/-}$ and WT animals, the loss of OHCs was accompanied by the degeneration of the efferent terminals related to the missing cells (Figure 27G, I, stars). The volume of $ChAT^{+}$ particles in the DC region was also decreased in $Tg^{+/-}$ (Figure 27B and D, H and J, N). However, no progressive age-related decrease was detected in the $ChAT^{+}$ area in DCs of both WT and $Tg^{+/-}$ groups (Figure 27N).

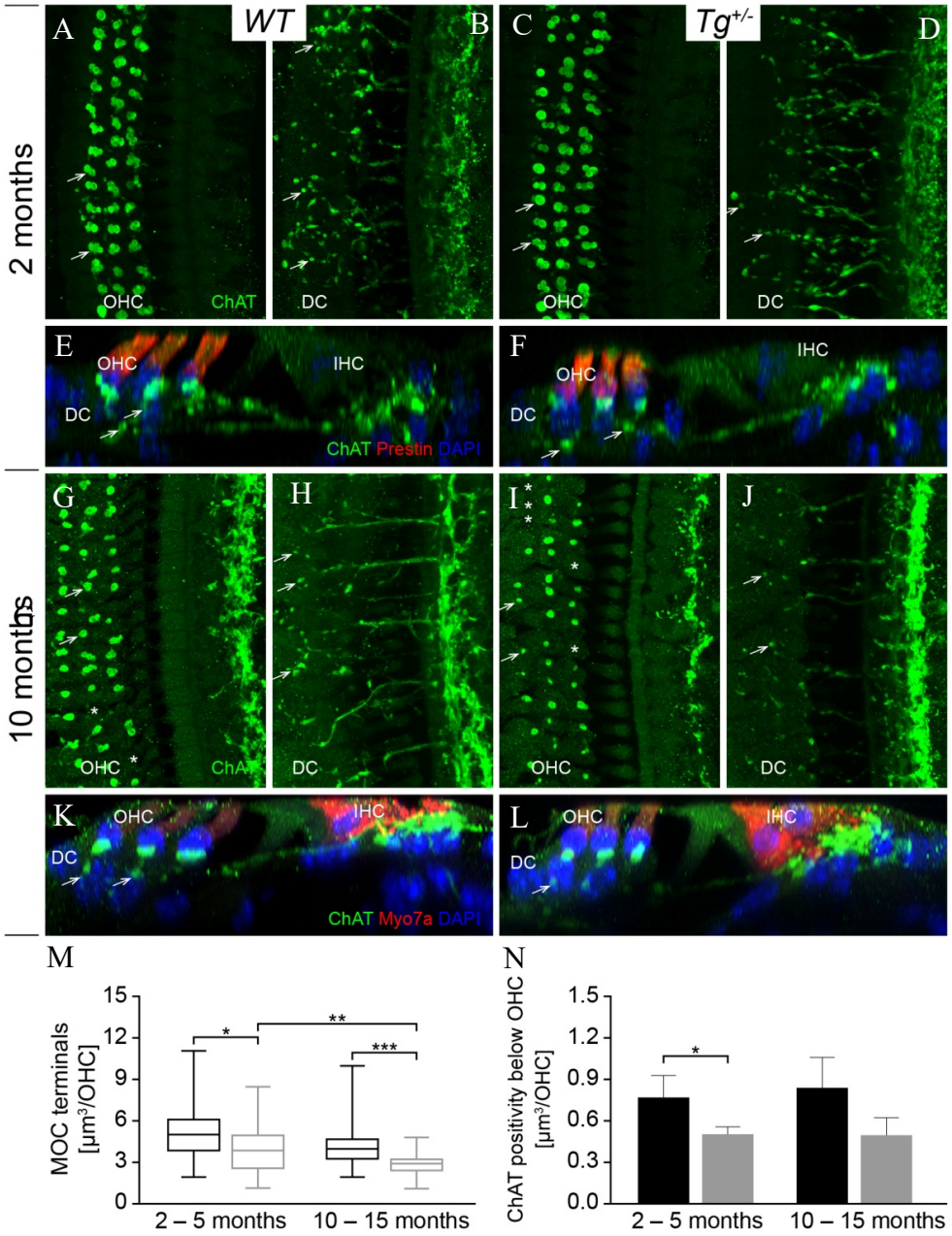

Figure 27. Altered efferent innervation.

*Despite visible similarities, the quantitative analysis shows a decrease in the volume of MOC terminals of OHCs (A, C, arrows; quantified in M) and efferent vesiculated fibers in the region of Deiters' cells (B, D, arrows; quantified in N) in young $Tg^{+/-}$ mice (I, M) than in WT animals (G, M). The progressive loss of efferent fibers is visible in older $Tg^{+/-}$ (J) compared to WT (H). In both WT and $Tg^{+/-}$ groups, efferent endings are missing if the OHC is lost (G, I; stars). Side view (E, F, K, L) represents the maximum projection of a focal series through the thickness of one OHC, arrows here and in b, d, h, j point out ChAT positive particles in the region of Deiters' cells. Values are median with 25% and 75% percentiles (M) and means ± SEM; *p<0.05, **p<0.01, ****p<0.0001, t test. IHC inner hair cells, OHC outer hair cells, DC Deiters' cells*

The MOC efferents originate in the medial portion of the superior olivary complex and project to outer hair cells.

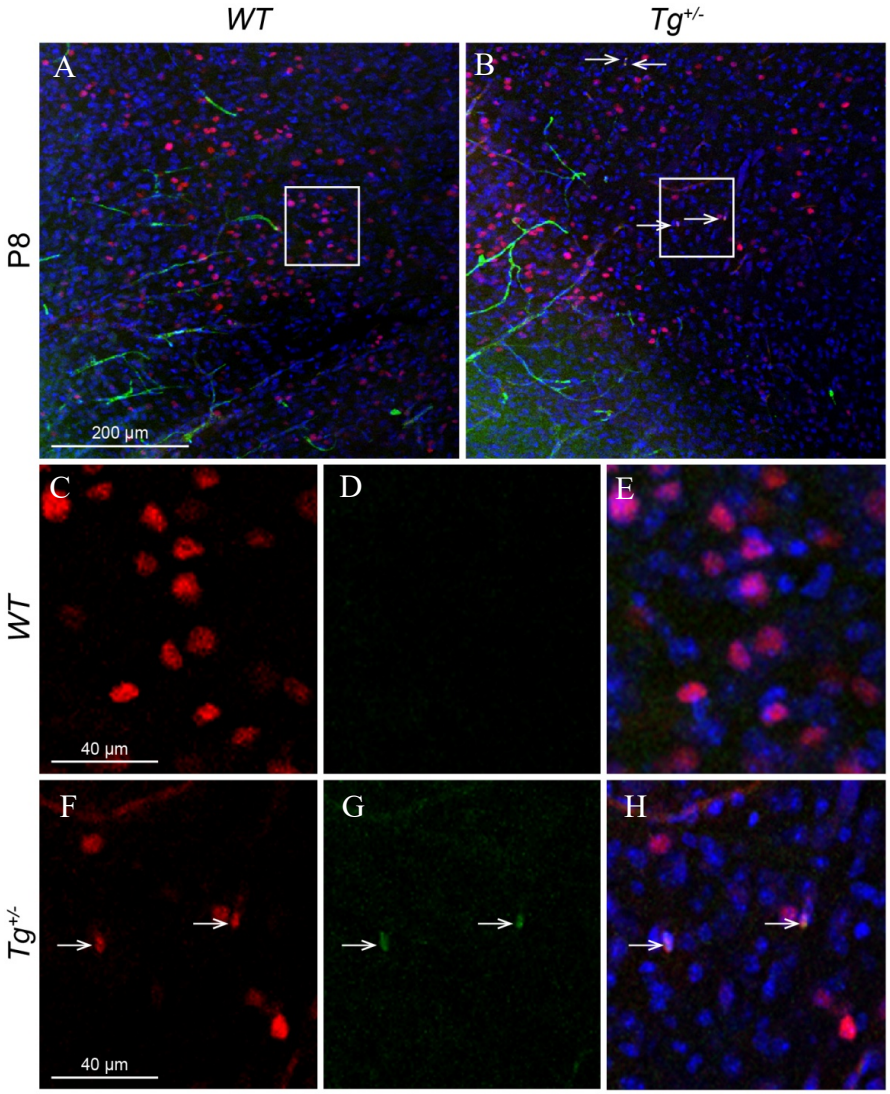

Figure 28. ISL1 expression in the transgenic brainstem at P8.

The immunostaining of neurons in the area of superior olivary complex in the brainstem with antibodies for PAX2 (red) and ISL1 (green) shows PAX2 and ISL1 co-expression in neurons in $Tg^{+/-}$ (B; arrows) but not in WT (A). Boxed areas are shown at a higher magnification, WT (C–E) and $Tg^{+/-}$ (F–H). Hoechst 33342 (blue) was used as a nuclear counterstain.

Since we detected degenerative changes in the MOC terminals at the base of OHCs, we additionally analyzed the postnatal expression of the Isl1 transgene in these olivary neurons prior to hearing. We found ISL1 expressed in Pax2+ cells in the area of the superior olivary complex in the brain of P8 $Tg^{+/-}$ (Figure 28B, F–H). There was no ISL1 expression in the WT littermates (Figure 28A, C–E). Thus, the misexpression of ISL1 might negatively affect the development and function of MOC neurons.

4.2. Role of "peripheral" BDNF in the auditory system

4.2.1. BDNF KO mice

Knock-out mice with deletion of BDNF under Pax2 promoter (BDNF^{Pax2}KO) used in this study were generated by mating Pax2-Cre mice (Ohyama and Groves, 2004) with BDNFlox/lox mice (Rios et al., 2001). Zuccotti et al. (2012) showed that in obtained knock-out mice BDNF is deleted in the cochlear epithelium and spiral ganglion, DCN, and IC. Lack of BDNF in these mice is accompanied by slight elevated ABR thresholds to click and to most pure tone frequencies and decreased amplitude of the first ABR wave, corresponding to cochlear nerve activity. These functional changes were shown to be caused by altered IHC exocytosis resulting from loss of ribbon synapses, particularly in high frequency cochlear region. Interestingly, this deficit shows up upon hearing onset at P12. Another finding worth paying attention is decreased amplitude of reflecting IC activity ABR waves IV-V compared to previous waves corresponding to lower brain structures (Zuccotti et al., 2012).

To obtain more insight the role of peripheral BDNF on basic sound processing and understand the physiology behind the reduced range of suprathreshold ABR responses generated at the level of the IC in knock-out mice electrophysiological response behavior of IC neurons in BDNF^{Pax2} knock-out (KO) and wild type (WT) mice was assessed in the present work.

4.2.2. Deletion of BDNF in KO Constricts Thresholds and Dynamic Range of IC Neurons

Extracellular recording of neuronal activity in the IC in 3–4 -month-old WT and KO mice was performed. The responses to BBN and pure tones of a total of 469 IC units were recorded, comprising 264 units from WT (n=4) and 232 from KO (n=4). The whole sample of units was divided into three main non-overlapping frequency bands according to their characteristic frequency (CF): 4–9 kHz (low), 10–15 kHz (middle), and 16–30 kHz (high).

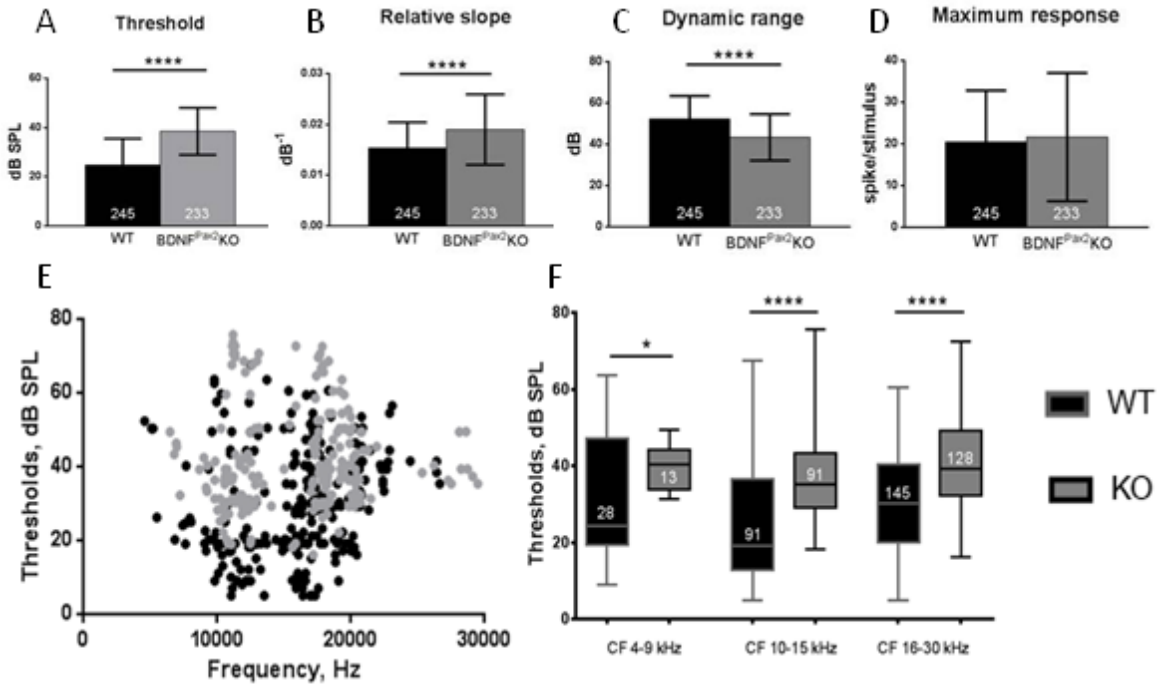

Figure 29. Response thresholds of IC neurons to broadband noise (BBN) and tone stimulation for WT and KO animals.

*A. Averaged thresholds of responses to BBN stimulation. B, C, D. Parameters of the rate-intensity function (RIF) of responses to BBN stimulation: average dynamic range, relative slope, and maximum response for all groups of mice. E. Scatter plots of pure tone thresholds as a function of neuronal CF, shown separately for WT (n=4) and KO (n=4) animals. F. Box and whisker plot for thresholds of tone-evoked responses for neurons of individual CF frequency ranges (4–9, 10–15, 16–30 kHz). One-way ANOVA with Bonferroni's post hoc test and Kruskal-Wallis test with Dunn's multiple comparison test, n.s. p>0.05, *p<0.05, ****p<0.0001. Data are presented as mean ± SD or median with interquartile range and extremes. The numbers in the graphs indicate the numbers of neurons.*

The thresholds of IC neurons to BBN stimulation were significantly higher in KO than in WT mice (Figure 29A, KO, 38.62 ± 9.6 dB SPL; WT, 24.78 ± 10.76 dB SPL; ****p<0.0001). Same trend was valid for response thresholds to tone stimulation in all frequency bands (Figure 29F, low CF WT: Mdn = 24.11; KO: Mdn = 40.39, *p<0.1, middle CF, WT: Mdn = 19.18; KO: Mdn = 35.14, ****p<0.0001; high CF, WT: Mdn = 30.28; KO: Mdn = 39.38, ****p<0.0001). Thresholds of individual IC neurons as a function of CF are presented in scatter plots for WT and KO animals (Figure 29E). Finally, the parameters of the RIFs such as dynamic range (WT 52.37 ± 11; KO 43.23 ± 11, ****p<0.0001) and slope (WT 0.01424 ± 0.006; KO 0.01919 ± 0.007, ****p<0.0001), but not maximum response magnitude (WT 20.52 ± 12.48; KO 21.83 ± 15.56, n.s. p>0.05) of IC neurons, were significantly reduced in KO mice (Figure 29B, C, D). These findings reveal that after the

onset of hearing, BDNF in lower auditory pathway improves hearing sensitivity and the threshold of IC neurons.

4.2.3. Deletion of BDNF in KO Mice Alters Latency and Tuning Characteristic of IC Neurons

CF detection thresholds have been hypothesized to be influenced by onset stimuli (Heil et al., 2008). Differences in onset stimuli should be reflected by differences in mFSL, which can be evaluated from poststimulus time histograms. mFSLs for 80 dB SPL stimuli were similar in WT and KO animals for the low- and middle-frequency bands (Figure 30A; low CF, 4–9 kHz, WT: Mdn = 7.28; KO: Mdn = 7.4, n.s. $p>0.05$; middle CF, 10–15 kHz, WT: Mdn = 6.8; KO: Mdn = 6.9, n.s. $p>0.05$), but were significantly longer for neurons with high CF (16–30 kHz) (Figure 30A; WT: Mdn = 6.8; KO: Mdn = 7.5, ****$p<0.0001$). This indicates that after the onset of hearing, BDNF improves the short latency responses of IC neurons to sound. The quality factor Q10 of sound responses of IC neurons, which is reciprocally related to the excitatory area bandwidth 10 dB above threshold (the higher the Q10, the sharper the tuning), may help to identify the type of neuron which responds to BDNF in the IC. Q10 did not significantly differ between WT and KO mice over all CF ranges (Figure 30 B, C). Differences in peak Q10 values in scatter plots categorized for frequency bands in WT and KO animals (Figure 30 B, C) prompted us to investigate individual Q10 values. Interestingly, in CF regions >10 kHz, the number of IC neurons with Q10 values >4 was significantly lower in KO than in WT animals (Figure 30D, *$p<0.05$, **$p<0.01$). This indicates that after the onset of hearing, BDNF in lower brain parts sharpens a very narrow tuning characteristic of IC neurons.

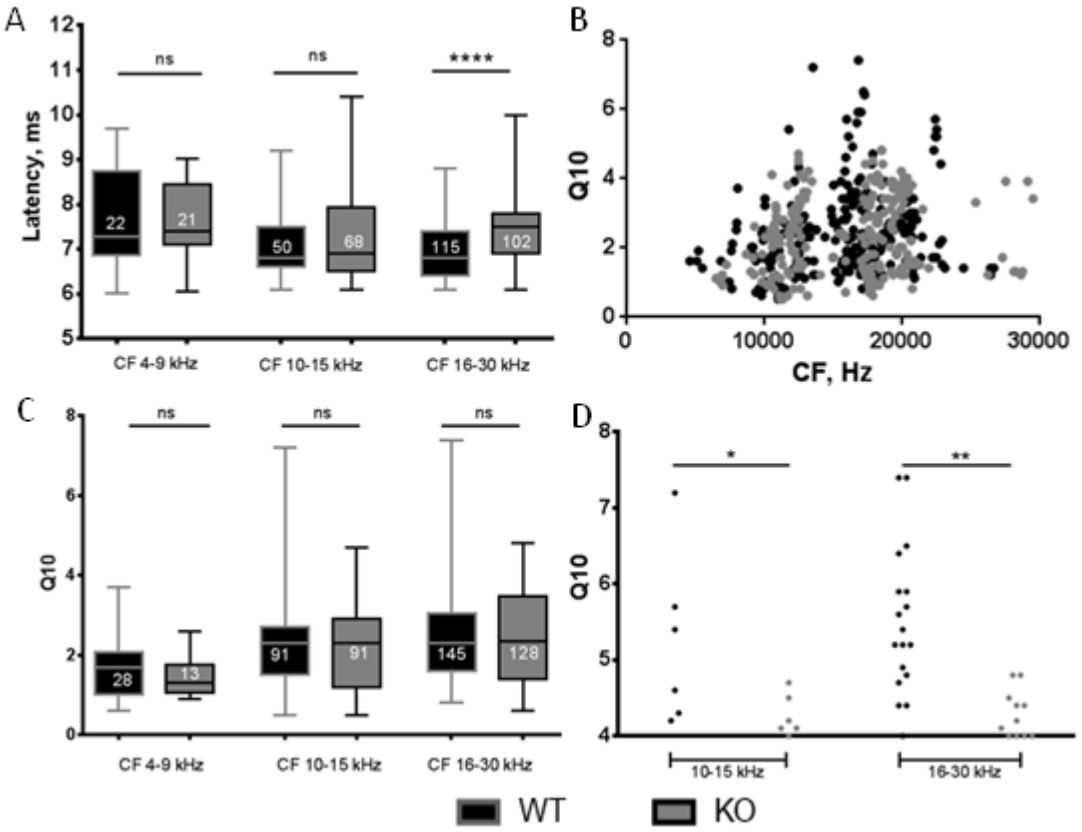

Figure 30. Minimum first spike latency (mFSL) and quality factor (Q10) of IC neurons.

*A. mFSL of responses to 80 dB SPL BBN bursts for WT (n=4) and KO (n=4) animals. Box and whisker plot for mFSL for neurons of individual CF frequency ranges (4–9, 10–15, 16–30 kHz). Kruskal-Wallis test with Dunn's post hoc test: n.s. p>0.05, *p<0.05, ****p<0.0001. Data are presented as medians with interquartile ranges and extremes. B–D Q10 of IC neuron responses to pure tone stimulation for WT (n=4) and KO (n=4) animals. B. Scatter plots illustrating the Q10 as a function of neuronal CF. C. Box and whisker plot for Q10 for neurons of individual CF frequency ranges (4–9, 10–15, 16–30 kHz). D. Scatter plots for Q10 with y scale 4–8 for the neurons of individual frequency ranges (10– 15 and 16–30 kHz). Note that IC neurons >10 kHz with Q10 >5 are absent in KO mice (D). Kruskal-Wallis test with Dunn's multiple comparison test: n.s. p>0.05, *p<0.1, **p<0.01. Data are presented as medians with interquartile ranges and extremes. The numbers in the graphs indicate the numbers of neurons.*

4.2.4. Deletion of BDNF in KO Mice Affects the Inhibitory Strength of IC Neurons

To investigate the difference in tuning characteristics of IC neurons in more detail, inhibitory, excitatory, and non-inhibitory (Figure 31A) response characteristics of IC neurons

of WT and KO mice were investigated using two-tone inhibition. In both groups of mice almost 80 % of neurons displayed low-frequency and/or high-frequency lateral inhibition. The strength of firing rate suppression by lateral inhibition was calculated as a percentage of rate suppression separately for low- and high-frequency sideband inhibition for neurons with a CF <10 kHz and CF >10 kHz. Low CF neurons did not exhibit altered low- or high-frequency sideband inhibitory strengths in the absence of BDNF (Figure 31B). Likewise, in the neurons with a CF of 11–30 kHz, the low-frequency sideband was similar in WT and KO animals (Figure 31B). However, high-frequency sideband inhibition strength was significantly reduced in KO mice (Figure 31B, *p<0.05). This indicates that after the onset of hearing, BDNF in lower brain parts increases the inhibitory strength of IC neurons.

This finding strengthens the conclusion that BDNF may improve signal-to-noise ratio by increasing the inhibitory strength of neurons.

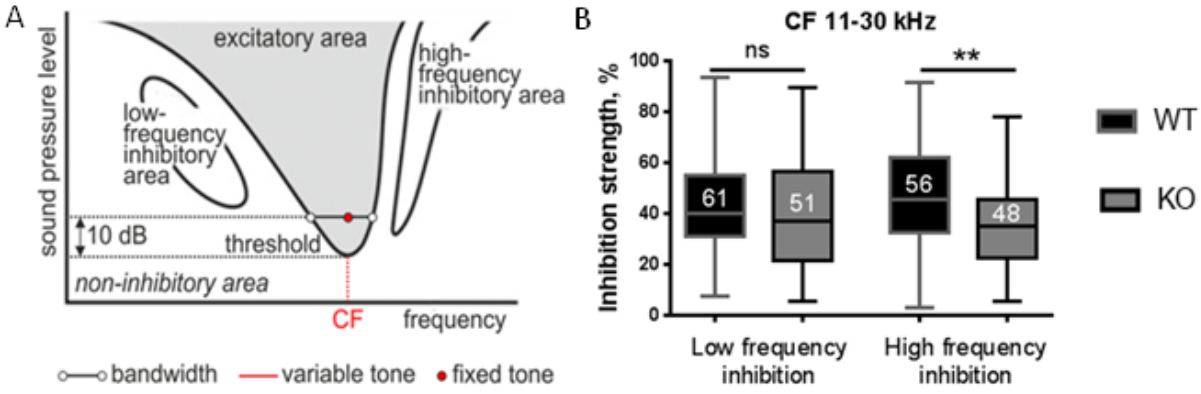

Figure 31. Inhibition characteristics in WT (n=4) and KO (n=4) animals.

A. *Schematic of response map to two-tone stimulation showing excitatory, inhibitory, and non-inhibitory areas.* ***B.*** *Comparison of low- and high-frequency sideband inhibition strength in middle and high CF (11–30 kHz) IC neurons with inhibitory strength of 1% and higher. One-way ANOVA with Bonferroni's post hoc test: n.s. p>0.05, **p<0.01. Data are presented as median with interquartile range and extremes. The numbers in the graphs indicate the numbers of neurons.*

4.2.5. Deletion of BDNF in KO Reduces the Density of PV-Immunopositive Puncta in IC and AC Projecting Neurons

In many projection neurons, changes in inhibitory conductances are assumed to require specialized GABA (γ- aminobutyric acid) A receptors. Particularly, the differentiation

of PV basket cells, a subpopulation of GABAergic neurons that regulate a critical period of plasticity in the cortex which depends on BDNF (for review, see (Hu et al., 2014), may play a role during the alteration of inhibitory strength in KOs. Likewise, elevated auditory startle amplitude and latencies in $PV^{-/-}$ mice suggested a specific role of PV basket cells for inhibitory circuits in auditory processing (Popelar et al., 2013). To investigate a role of PV for the observed changes in inhibitory strength in KO mice, we used antibodies for PV (Sale et al., 2010, Le Magueresse and Monyer, 2013) and antibodies for the 67-kDa isoform of GABAergic interneurons. We found that the intensity and number of PV immuno-positive puncta, but not the number of PV immuno-positive somata or GAD67-immuno-positive puncta (not shown), are decreased in the IC and AC of $BDNF^{Pax2}$- KO (Figure 32A, C) mice. Reduced levels of PV expression was also confirmed by Western blots (Figure 32B, inset). Quantification of the intensity of labeling revealed a significantly reduced number and intensity of PV-positive puncta (Figure 32B, D, 10–20 slices of 3–6 independent experiments of n=3 animals) in KO mice.

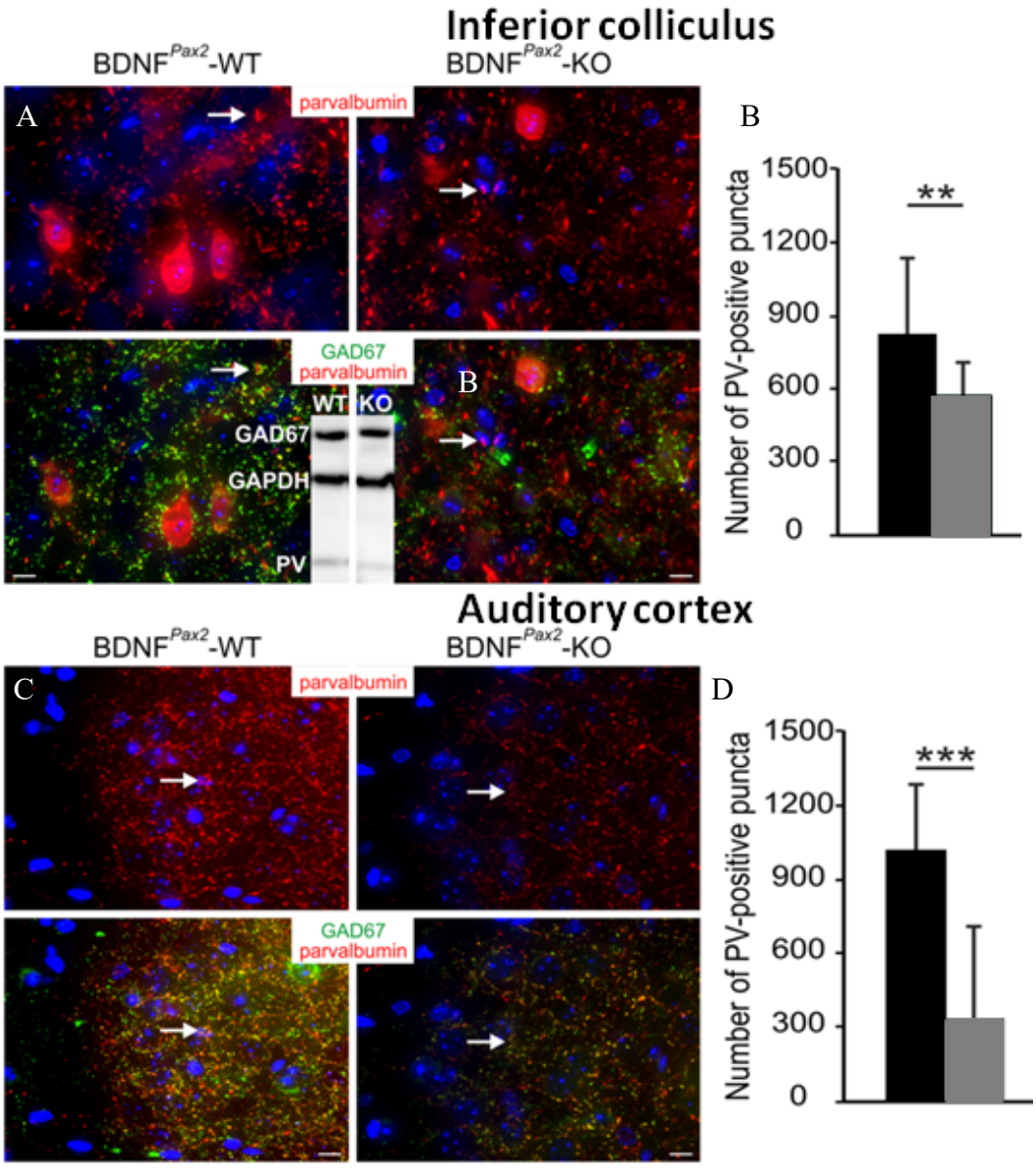

Figure 32. Immunohistochemistry of the inferior colliculus and auditory cortex.

*A, C. Immunohistochemistry of the IC and AC immunolabeled with anti-parvalbumin (red) and anti-GAD67 (green). A reduction of PV- and GAD67- immunoreactive puncta in both IC (A) and AC (D) in KO mice compared to WT mice is observed. Arrows point to PV-immunoreactive puncta. Reduced PV levels in KO in the IC are confirmed by Western blot (A, insets). B, D Quantification of PV-immunoreactive puncta in the IC (B) of WT and BDNF^{Pax2}- KO, (10–20 slices of 3–6 independent experiments of n=3 animals) and in the AC (D) of WT and KO, mice (10–20 slices of 3–6 independent experiments of n=3 animals). Two-way ANOVA with Bonferroni's post hoc test (**p<0.01, ***p< 0.001). Data are presented as mean ± SD.*

4.3. Nanoparticles as a potential drug carrier for regenerative inner ear therapy

4.3.1. Distribution of nanoparticles in the inner ear after middle ear application

NP distribution in the inner ear after RWM application was evaluated in the RWM- the site of most probable NP entrance into the cochlea, and cochlear tissues disposed to irreversible damage and cell loss in SNHL (Wong and Ryan, 2015): SG, organ of Corti and the lateral wall. Analyzed targets are shown in the histological section through the basal turn in Figure 33.

RWM

All three types of nanoparticles penetrated through the RWM as shown in Figure 33. A specific fluorescent signal from the NPs is represented by green color (fluorescein, Figure 33C, D) for polylysine or in red color for liposomes (rhodamine, Figure 33E, F) and polymersomes (DiI, Figure 33G, H), the slight red or green nonspecific fluorescence was used as a background to outline the tissue structure, also in control cochlea (Figure 33A, B).

Specific fluorescence was detected in cells in all layers of the RWM one day after NP application (Figure 33C, E, G). In case of polylysine strong affinity of NPs to cochlear bone was noticed. This let NP penetration also into the scala vestibuli through the bone surrounding round window and through the oval window (stapes and annular ligament).

After passing the RWM, the NPs spreaded into the perilymph of the ST and penetrated individual cochlear structures. In the low-magnification image of the basilar cochlear turn the polylysine (Figure 33D), liposomes (Figure 33F) and polymersomes (Figure 33H) can be identified in the SG, organ of Corti, lateral wall, spiral ligament and spiral limb.

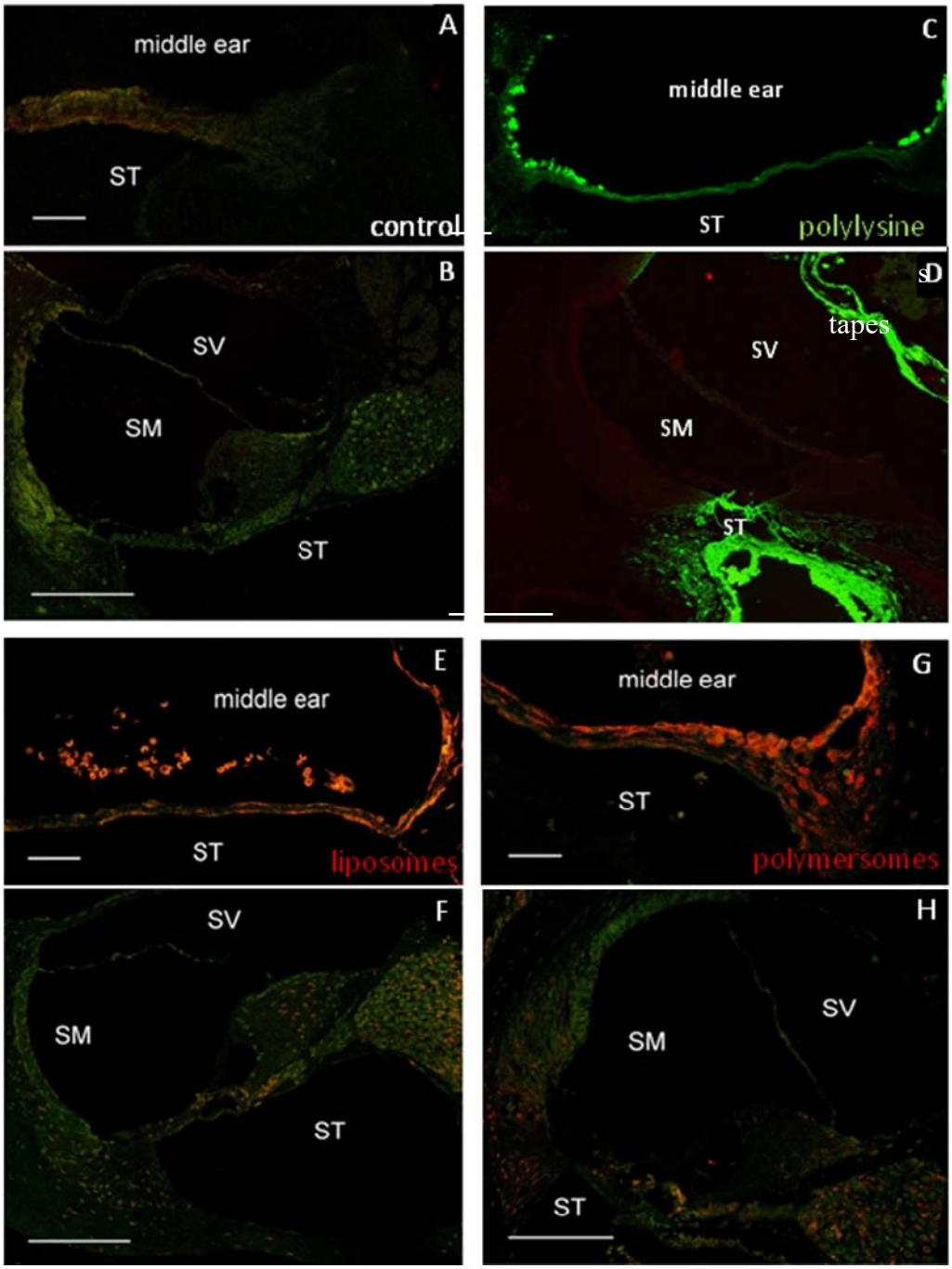

Figure 33. Nanoparticle distribution in the basal turn of the cochlea.

Localization of nanoparticles in all layers of the round window membrane (C, E, G), but not in control cochlea (A). Sections through the basal turns from untreated ear (B), and the cochleas treated with polylysine (D), liposomes (F) and polymersomes (H) demonstrating localization of nanoparticles in individual cochlear structures. Nanoparticles are represented by green fluorescent signal in C, D and red signal in E–H, nonspecific fluorescence used to outline the tissue structure. Scale bar in A, C, E, G = 25 µm, scale bar in B, D, F, H = 100 µm. SM: Scala media; ST: Scala tympani; SV: Stria vascularis.

SG

The cochlear SG is located in the bony modiolus and consists of neurons with their fibers and glial cells. One day after application NPs were found in SG of all cochlear turns. Nanoparticles of all types were found in the cytoplasm of spiral ganglion cells (Figure 34D, G, J), polylysine was detected also extracellularly (Figure 34J). When visualized using confocal microscopy, the NPs are visible as red or green fluorescent dots, that in case of intracellular localization are thought to be an accumulations of NPs in endosomes and lysosomes (Chithrani et al., 2009). Nanoparticles of neither type were detected in the nuclei of the SG cells.

Organ of Corti

A small amount of NPs were found in the organ of Corti in all cochlear turns. Examples of sections through the organ of Corti in Figure 34E, H, K demonstrate that liposomes and polymersomes were diffusely distributed in the cytoplasm of hair cells (inner and outer hair cell), between hair cells and in supporting cells (Figure 34E, H), while polylysines created rather small clusters between and inside cells (Figure 34K), often near cell nucleus. Strong specific fluorescent signal suggested high polylysine saturation of basilar membrane of the organ of Corti and bonny wall of the modiolus (Figure 34K). No specific fluorescence was detected in the organ of Corti in the control cochlea (Figure 34C).

Lateral wall

Cochlear lateral wall is formed by stria vascularis and spiral ligament. Liposomes and polymersomes were mainly detected between or within the fibroblasts of the spiral ligament and sparsely in all three layers of the stria vascularis in the basal and middle turns of the cochlea (Figure 34F, I). In contrast, polylysine was found more often dispersed or forming small clusters in the extracellular matrix of the lower part of the spiral ligament and less often as intracellular clusters (Figure 34L). When specific polylysine fluorescence was found in the stria vascularis it was usually related to capillary walls. No specific fluorescence was detected in the lateral wall in the control cochlea (Figure 34C).

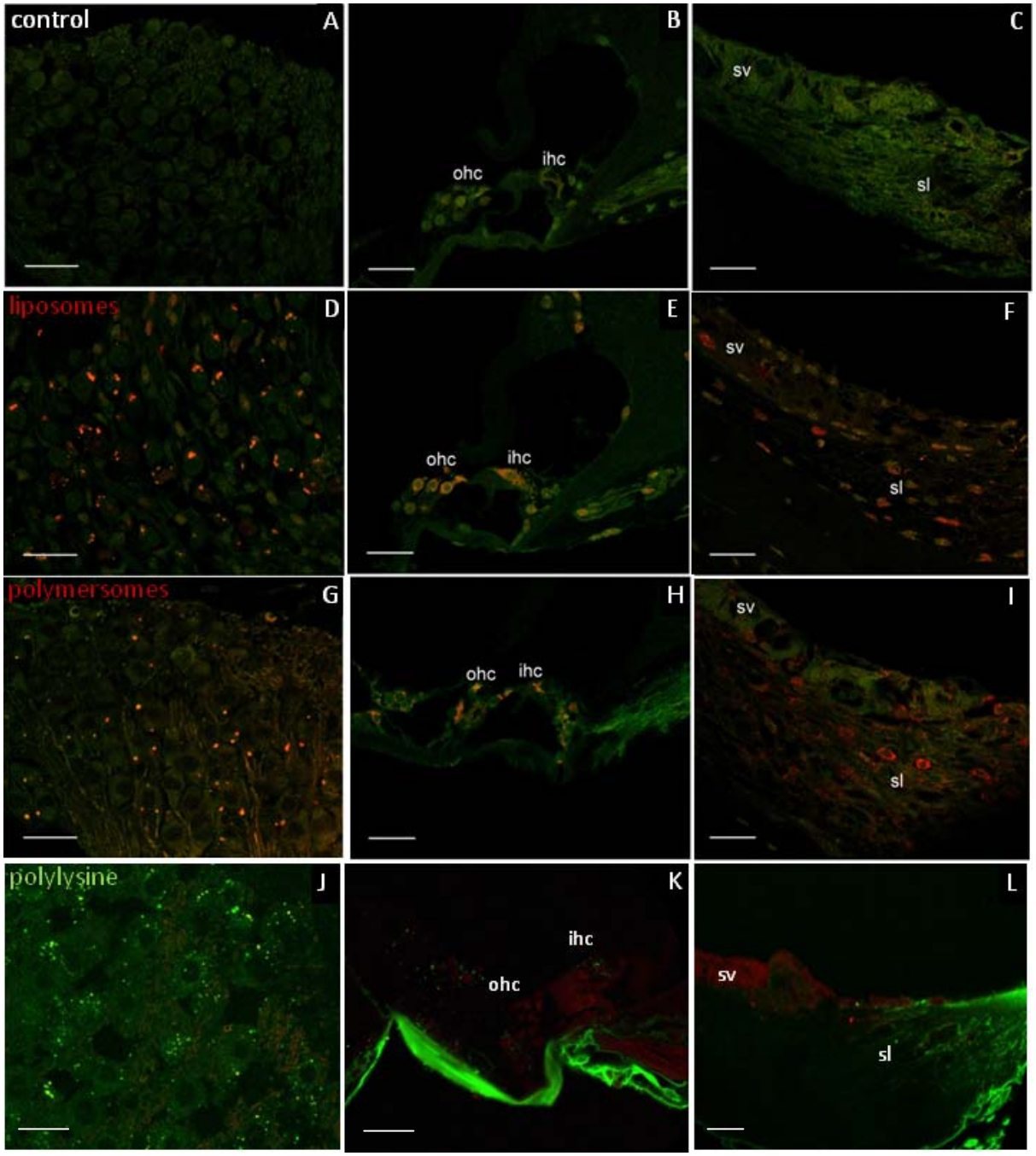

Figure 34. Nanoparticle distribution in individual cochlear structures.

Sections through the spiral ganglion (A, D, G, J), organ of Corti (B, E, H, K) and the lateral wall(C, F, I, L), showing the localization of liposomes (D–F), polymersomes (G–I) and polylysine (J–L) in cochlear structures. (A–C) represent control sections without any nanoparticle application. Depending on nanoparticle type red (liposomes, polymersomes) or green (polylysine) color represents nanoparticle fluorescent signal, respectively, green or red background color represents nonspecific fluorescence of the cochlear tissue. Scale bar = 20 µm. IHC: Inner hair cell; OHC: Outer hair cell; SL: Spiral ligament; SV: Stria vascularis.

4.3.2. Nontoxicity of NPs confirmed by monitoring of hearing threshold

Hearing thresholds were assessed in animals before and 2 weeks after the administration of nanoparticles. Neither type of NPs had any overt impact on the hearing thresholds (Figure 35) (one-way analysis of variance with multiple comparison Bonferroni test).

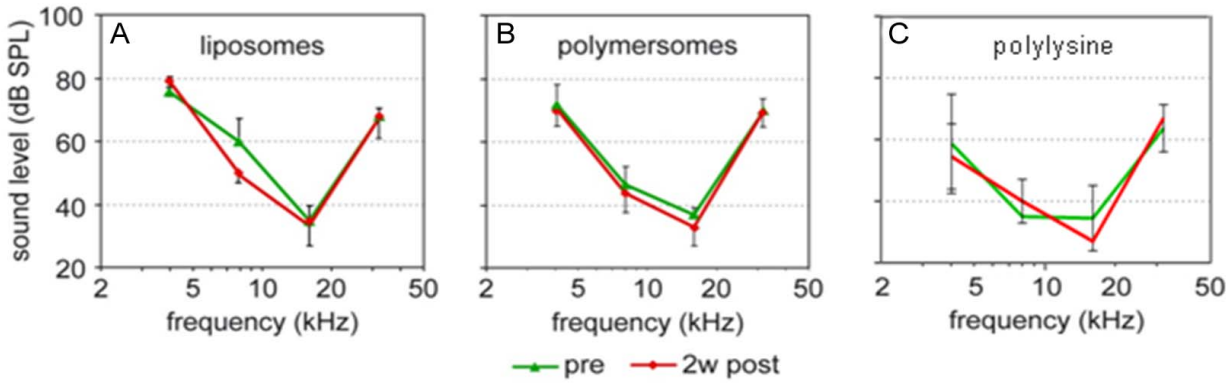

Figure 35. Nontoxicity of nanoparticles.

Average hearing thresholds evaluated in mice before and 2 weeks after the round window membrane application of liposomes (A, n = 4) polymersomes (B, n = 3) or polylysine (C, n = 3). Data are presented as means ± SD. SPL: Sound pressure level.

4.3.3. Use of nanoparticles as drug delivery tool

4.3.3.1. Delivery of plasmid using hyperbranched polylysine

Polylysine belongs to the most studied and promising polymeric carriers for gene delivery (Zauner et al., 1998, Vanderkerken et al., 2000, Putnam et al., 2001, Zhang et al., 2010a, Kim, 2012, Zhao et al., 2016). For transfection experiment we used complex of polylysine with either of two types of plasmids: i) polylysine – plFL, containing plasmid, tagged with fluorescent marker (fluorescein) with no expected expression activity and supposed to be used only as a positive control of polylysine – plFL intracochlear permeation, and ii) polylysine – eGFP, containing plasmid, coding GFP (green fluorescent protein) that in case of its intracellular delivery would lead to synthesis of GFP, detectable as green fluorescence.

No specific fluorescence was found inside the cochlea after RWM application of either polylysine-plasmid complex 1 and 3 days after injection (Figure 36).

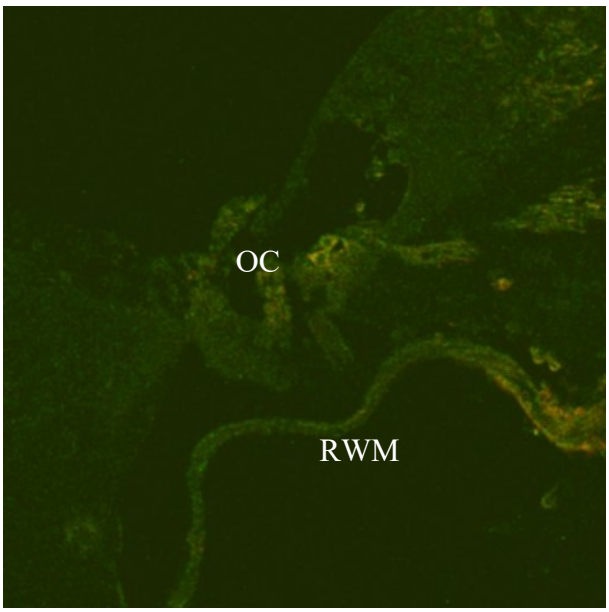

Figure 36. Basal turn of the cochlea, treated with polylysine-eGFP complex.

No specific fluorescence was detected in any cochlear structure 1 day after treatment with polylysine-eGFP complex.

4.3.3.2. Delivery of drug using liposomes and polymersomes

To determine whether liposomes and polymersomes are able to deliver to the cochlea drug in condition and amount, sufficient to elicit a functional effect, disulfiram-loaded liposomes and polymersomes were applied to the RWM.

4.3.3.3. Effects of disulfiram-loaded NPs on hearing of treated mice

Hearing of animals was tested using ABR and DPOAE recording before and two weeks after the surgery. ABRs were measured monaurally to enable evaluation of function of treated and non-treated ears separately.

Average hearing thresholds measured in animals before and 2 weeks after disulfiram-loaded NP administration are shown in Figure 37A. Significant threshold shifts (20–35 dB) were present at 8 and 16 kHz using liposomes and at 8–25 kHz after polymersome application. Threshold shifts were also present at 4 kHz after liposome application; however, they were not significant. No hearing loss was found in contralateral untreated controls (Figure 37A).

The function of outer hair cells was not altered significantly according to results of DPOAE measurement showing no significant differences between DPOAE amplitudes recorded before the treatment, 2 weeks after the disulfiram-loaded NPs application and in non-treated ears (Figure 37B).

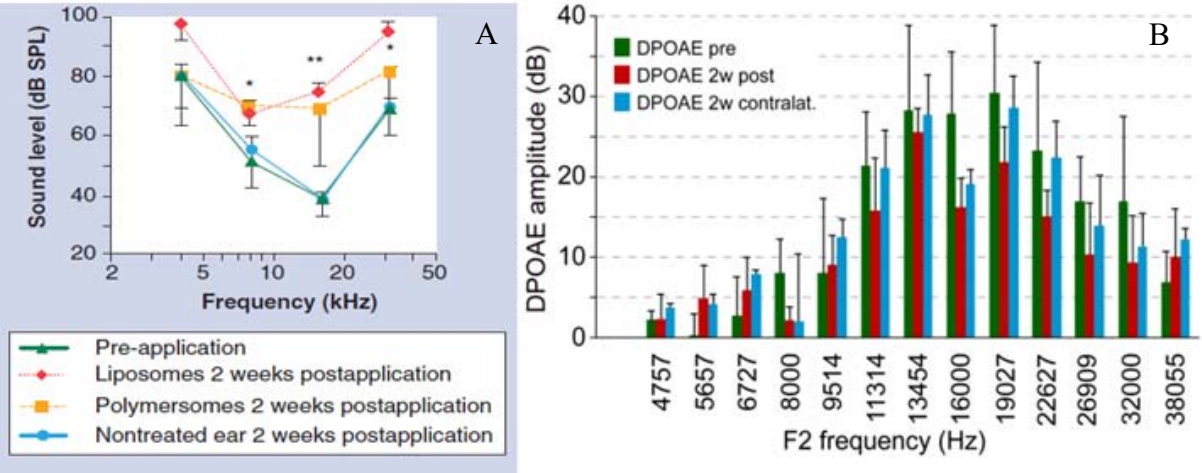

Figure 37. Hearing function after disulfiram-loaded nanoparticle application.

*A. The average hearing thresholds evaluated before the disulfiram-loaded nanoparticle application (green full line with triangles, n = 7), in contralateral untreated ears (blue full line with circles, n = 7), 2 weeks after liposome (red dotted line with diamonds, n = 3) and polymersome (orange dashed line with squares, n = 4) application. Error bars represent ± SD. *p < 0.05, **p < 0.01, one-way analysis of variance with Bonferroni's multiple comparison test. B. DPOAE amplitudes evaluated in mice before (green columns, n = 7), 2 weeks after the disulfiram-loaded nanoparticles treatment (red columns, n = 7) and in contralateral non-treated ears (blue columns, n = 7). Data are presented as means ± SD. DPOAE: Distortion product otoacoustic emission.*

4.3.3.4. Effects of disulfiram-loaded NPs on the cochlear morphology

A significant increase of the hearing thresholds was accompanied by the pronounced damage to spiral ganglion.

In the SG sections stained with cresyl violet, signs of morphological damage were evident in the SG cells of the basal, middle and apical cochlear turns as early as 2 days after NP application. Sections from the basal turn of four cochleas, harvested at intervals after NP application and stained with cresyl violet, are shown in Figure 38A–D. In contrast to controls (Figure 38A), shrunken nuclei or the presence of two to three small dark dots in a cluster (a characteristic marker of cells undergoing apoptosis) were observed in some neurons in SG sections fixed and stained 2 days and later after disulfiram-loaded NP application (red arrows

seen in Figure 38B, C). A pronounced loss of SG neurons was first evident 2 days following disulfiram-loaded NP application (Figure 38B) and was still present up to 2 weeks postapplication (Figure 38C, D).

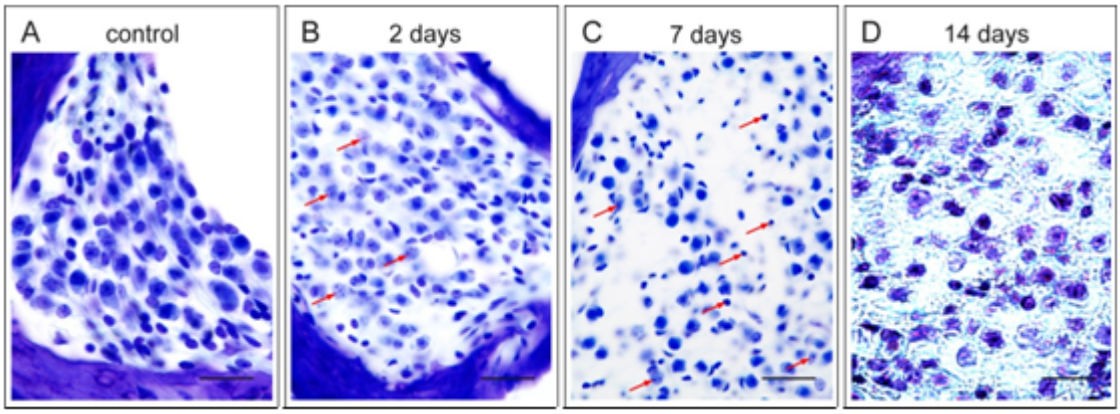

Figure 38. Detection of apoptosis in the spiral ganglion cells with Nissl staining.

Cresyl violet staining of the spiral ganglion in a control mouse (A), in mice 2 days (liposomes, B), 7 days (liposomes, C) and 14 days (polymersomes, D) following the administration of disulfiram-loaded nanoparticles on the round window membrane. Red arrows in (B and C) point out examples of apoptotic cells with shrunken nuclei or the presence of two to three small dark dots in a cluster. Scale bar = 20 µm.

Evidence of apoptosis was confirmed by the presence of activated caspase-3 in SG cells. Figure 39A demonstrates cytoplasmic localization of caspase-3 immunoreactivity in SG neurons detected 7 days after disulfiram-loaded NP administration. No signs of caspase-3 activity were found in the SG of the control cochlea (Figure 39B). No differences were found between the signs of apoptosis induced by disulfiram delivered by liposomes or polymersomes.

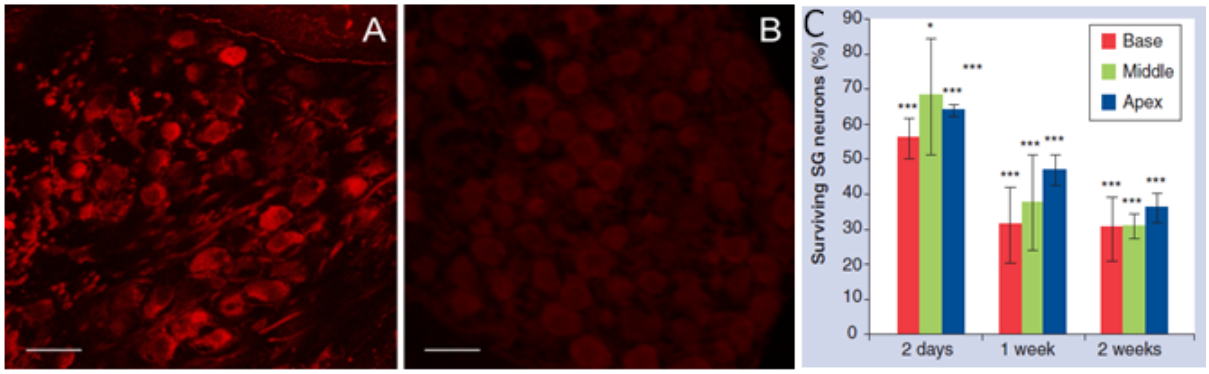

Figure 39. Active caspase-3 immunoreactivity and loss of spiral ganglion neurons.

(A) An example of active caspase-3 immunoreactivity (red fluorescence) in the spiral ganglion cells 7 days after the application of disufiram-loaded nanoparticles (liposomes). (B) Weak nonspecific fluorescence in a control cochlea. (C) The percentage of surviving spiral ganglion neurons in individual cochlear parts evaluated over 2 weeks after disulfiram-loaded nanoparticle application. Each column represents the amount of surviving cells averaged from six samples (two cochleas). Scale bar = 20 μm.

The numbers of intact SG neurons in individual cochlear turns evaluated at intervals after disulfiram-loaded NP application are illustrated in Figure 39C. Only neurons without any signs of apoptosis were considered intact. Due to the small number of histological slices available from individual time points, the data for both types of NPs was pooled.

The evident loss of SG neurons was observed as early as 2 days after NP application. The percentage of surviving neurons without signs of apoptosis in individual cochlear turns amounted to average values of 56–68% ($p < 0.001–0.05$, one sample t-test against 100%). The neuronal damage continued, reaching average values of 31–47% of surviving neurons at 1 week postapplication. However, the decrease in the number of surviving neurons observed in the second week postapplication was minimal. The results indicate that RWM application was sufficient to produce a toxic effect within 1 week after the NP application.

Histological evaluation of the organ of Corti and the lateral wall cells 2 weeks after the application of disulfiram-loaded NPs to the RWM did not reveal any morphological alterations.

4.3.3.5. Effects of free disulfiram in saline on the hearing thresholds

To exclude the possibility that the toxic effect was produced by free disulfiram that had diffused out of the NPs into the medium prior to the application, two control mice received a solution of disulfiram in saline. No threshold shift was observed in any of the animals when tested up to 2 weeks postapplication (Figure 40). Owing to this negative result, no further investigations were carried out into the toxicity of disulfiram on the RWM. The results demonstrated that the morphological alterations and the pronounced hearing loss observed in the mice treated with disulfiram-loaded NPs must be produced by the disulfiram released from NPs once within the cochlea.

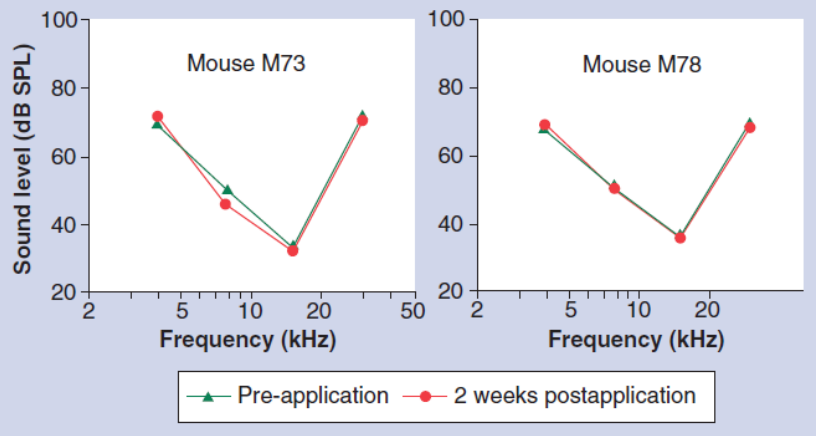

Figure 40. Nontoxicity of free disulfiram application on the round window membrane.

Hearing thresholds evaluated in two mice before and 2 weeks after the round window membrane application of free disulfiram. SPL: Sound pressure level.

5. Discussion

5.1. Role of ISL1 in development and function of the auditory system

In this study we overexpressed *Isl1* under Pax2 regulatory sequence. Pax2 is expressed in the developing inner ear. It is one of the earliest genes to be expressed in the pre-otic region (Hans et al., 2004) but slightly after Foxg1 (Copley et al., 2013). PAX2 is a key regulator of otic cell identity and shape in chick (Christophorou et al., 2010) and PAX2 combined with PAX8 is needed for mouse ear development (Bouchard et al., 2010a). Pax2 is required for the expression of otic transcription factors and for cell adhesion molecules, which in turn are necessary for epithelial integrity and subsequent placode invagination. In the mouse, PAX2 is expressed in all sensory and some non-sensory epithelia, but within sensory epithelia at E16.5 it is restricted to hair cells (Lawoko-Kerali et al., 2004). Although PAX2 is expressed in differentiating hair cells, mature murine hair cells do not express PAX2 protein. In Pax2 null mouse, ear cochlear outgrowth is delayed and pattern of the cochlear sack and its innervation is heavily impaired (Bouchard et al., 2010a). A rudimentary cochlea sack of Pax2 knockout inner ears lacks the spiral ganglion and contains a few scattered neuron-like cells. Thus, Pax2 affects the regional patterning of the early otocyst and cellular patterning within the sensory epithelia of the inner ear.

At E7.5 Pax2 expression is initiated also in the neural plate, particularly in the midbrain-hindbrain boundary (Puschel et al., 1992, Rowitch and Mcmahon, 1995). This crucial developmental signaling center is responsible for patterning mesencephalic and metencephalic regions of the vertebrate brain. (Dworkin et al., 2012, Fritzsch et al., 2015). Pax2 expression in these regions is extensive at E8.0, becomes limited to isthmus area by E9 (Rowitch and Mcmahon, 1995) and completely ceases after E11 (Puschel et al., 1992).

5.1.1. Role of ISL1 during embryonic development

In this study, we examined the functional role of ISL1 in the development and maintenance of auditory sensory cells and neurons in the inner ear. We hypothesized that modulating ISL1 expression will change the fate specification of cells in the inner ear.

In compliance with our hypothesis Pax2-regulated Isl1 overexpression increases the embryonic ISL1+ domain and the size of the cochleo-vestibular ganglion in the inner ear at E10.5. Isl1 overexpression is also accompanied by premature afferent fibers differentiation-

rapid extension and branching of afferent fibers in the inner ear and connecting the ear and the developing brainstem in E12.5 embryos. Our findings confirm that Isl1 as a developmental gene plays an important role in the inner ear cell fate specification in early stages of the inner ear development. These stages have been recently shown to be crucial in production of a sufficient amount of functional mechanosensory cells from the pluripotent stem cells *in vitro* (Koehler et al., 2013). More than that, a protective role of Isl1 in adult hair cells against noise induced and age-related hearing loss has been recently reported (Huang et al., 2013). All together this makes Isl1 a promising candidate for use in gene or stem cell therapy to regenerate damaged inner ear epithelium.

5.1.2. Detrimental effect of ISL1 brain misexpression in adult animals

Pax2-Isl1 transgenic mice were created on the basis of FVB strain, which is a mouse strain with a normal pattern of age related hearing deterioration. Our results of hearing evaluation in the FVB strain are comparable to previous reports (Jones et al., 2006, Martin et al., 2007) that show completely preserved DPOAEs up to at least 5 months of age and the minor ABR threshold shift of 20 dB in 14-month-old animals compared to 1-month-old mice. In contrast, $Tg^{+/-}$ mice displayed a significant functional hearing deficit already at the youngest analyzed group (1–5 months). The first signs of age related sensory hearing loss are associated with the decrease of DPOAE amplitudes at the high frequency cochlear region (Schuknecht, 1964). Although the initial changes in DPOAE amplitudes in this region were detected in 6 to 9-month-old *WT* mice, the premature decline in DPOAEs in the high frequency region was already found in the youngest $Tg^{+/-}$ group. $Tg^{+/-}$ mice completely lost DPOAEs by the age of 6–9 months, whereas 10–15-month-old *WT* animals still had apparent otoacoustic emissions in the middle frequency region.

DPOAEs reflect the cochlear amplification facilitated by OHCs (Trautwein et al., 1996, Hofstetter et al., 1997). Usually, a decrease of DPOAE amplitudes relates to the loss of OHCs (Trautwein et al., 1996, Hofstetter et al., 1997) or the decline in their function (Li et al., 1999, Popelar et al., 2006). Accordingly, we detected a higher OHC loss in the high frequency region of the cochlea in 1 to 5-month-old $Tg^{+/-}$ mice compared to *WT*. Interestingly, we also found disorganized radial fibers that did not form regular bundles in the high frequency basal cochlear region of P3 $Tg^{+/-}$ animals. The higher loss of OHCs in $Tg^{+/-}$ animals could be associated only with the loss of DPOAEs at high frequencies (32–40 kHz), whilst the number of OHCs in the middle frequency region of $Tg^{+/-}$ cochleae did not differ

significantly from that in *WT* animals. Since the complete absence of DPOAEs could not be explained by the loss of OHCs, another possibility for the loss of cochlear amplification in $Tg^{+/-}$ might be an impaired function of OHCs.

Cochlear amplification is thought to be of two main sources: somatic, caused by prestin motility (Liberman et al., 2002, Dallos et al., 2008) and streocilia-based (Chan and Hudspeth, 2005, Kennedy et al., 2005). Prestin is a motor protein located in the OHC lateral wall and it is responsible for the OHC motility. Homozygous mice with partial deletion of prestin gene showed a 40 to 60 dB loss of cochlear sensitivity across all frequencies (Liberman et al., 2002), which represents a standard threshold shift in the case of the absent OHC motility. Although we found a moderate reduction in prestin mRNA expression in $Tg^{+/-}$ cochlea in 1-month-old mice compared to *WT* littermates, no significant changes in prestin mRNA levels were detected in older animals (7–11 months). We noticed no obvious difference in the prestin distribution in the OHCs between *WT* and $Tg^{+/-}$ animals. The analysis of stereocilia of the OHCs revealed that the stereocilia in 1 to 9-month-old $Tg^{+/-}$ and *WT* animals did not differ. We found more profound disorganized OHC stereocilia in 11-month-old and older $Tg^{+/-}$ animals than in *WT*, which points to the accelerated age-related degeneration of transgenic OHCs (Adams and Schulte, 1997). Thus, the premature and severe DPOAE loss in $Tg^{+/-}$ animals was unlikely due to prestin abnormalities or the deterioration of stereocilia.

The maintenance and function of OHCs is influenced by the MOC efferent innervation. The activation of the MOC system enhances auditory processing of distracting noise (Winslow and Sachs, 1987, Kawase and Liberman, 1993, May and McQuone, 1995) and it may thus protect the inner ear from acoustic trauma (Liberman, 1991, Maison et al., 2002a, Lauer and May, 2011). MOC terminals are the endings of the efferent fibers, which make OHCs hyperpolarized when activated. The MOC efferents originate in the superior olivary complex and enable modulation of the auditory periphery by higher auditory centers in the brain. We detected ISL1 misexpression in the neurons in the region of the superior olivary complex of $Tg^{+/-}$ mice, which may affect the formation of MOC efferent neurons. The reduced or altered MOC $Tg^{+/-}$ efferents may contribute to the reduction of MOC terminals and accelerate the deterioration of OHC function in mutant mice. Similarly, a surgical de-efferentation accelerates the age-related deterioration of DPOAEs without an extensive loss of OHCs (Liberman et al., 2014a). The reduction in the MOC-negative-feedback-gain-control may also explain the particular deterioration in the hearing thresholds

of $Tg^{+/-}$ animals at 16 kHz since this region has the maximal density of MOC terminals (Maison et al., 2003).

Isl1 is highly expressed in developing motoneurons (Pfaff et al., 1996) and efferents are derived from facial branchial motoneurons (Simmons D, 2011). It is possible that Pax2, known to be expressed in the hindbrain where efferents form, can affect the normal development of efferents and, as a side effect, the long term viability of hair cells and overall hearing performance. Likewise *Pax2*-driven ISL1 overexpression alters the development of efferents and, consequently, the maintenance of OHCs and hearing functions. Because neuronal degeneration is the common predisposing factor for the pathology of age-related neurodegenerative diseases, this possibility is worth exploring. Our data provide the first evidence that the alternation of MOC efferent system accelerates the age-related functional decline of hearing without the loss of OHCs.

5.2. Role of "peripheral" BDNF in the auditory system

We show here that BDNF present in the lower parts of the auditory CNS or the peripheral end organ improves the dynamic range of sound responses.

$BDNF^{Pax2}$ deletion was shown to result in altered IHC exocytosis and decreased sensitivity of the auditory nerve, particularly in the high frequency region (Zuccotti et al., 2012). These changes become apparent upon hearing onset at P12. It has been shown more than once in previous studies that peripheral deafferentation and decreased peripheral input showns up as decreased amplitude of ABR wave I. More centrally located auditory nuclei tend to compensate the decreased input by hyperactivity expressed in normal or less decreased amplitude of later ABR waves especially corresponding to the IC waves IV–V (Salvi et al., 1990, Schaette and McAlpine, 2011, Konrad-Martin et al., 2012, Sergeyenko et al., 2013). This is called "central gain" and has been implicated in the generation of tinnitus (Lockwood et al., 2002, Knipper et al., 2013). This is, however, not the case for $BDNF^{Pax2}$KO (Zuccotti et al., 2012, Chumak et al., 2015) in which suprathreshold amplitude of waves IV–V decrease compared to the previous waves suggesting a role of “peripheral” BDNF in activity of the inferior colliculus.

When auditory phenotypes of two BDNF knock-out mice – one with peripheral, another with central BDNF deletion are compared, it becomes evident that lack of BDNF in the lower brain structures but not in the auditory cortex affects hearing (Chumak et al., 2015). In both knock-out models: $BDNF^{Pax2}$KO (Zuccotti et al., 2012), showing hearing

deterioration compared to wild type animals and BDNF^{TrkC}KO animals, having normal hearing (Chumak et al., 2015), BDNF is deleted in SGNs and in the IC, suggesting that alterations of BDNF activities in these compartments are unlikely to be responsible for the differences between sound induced ABR wave I and IV in these mice. As BDNF^{Pax2}KO mice do not have a BDNF deletion in neither the AC, VCN, or olivary complex (Zuccotti et al., 2012, Chumak et al., 2015), descending central feedback loops are also unlikely to be involved. The observed hearing phenotype in BDNF^{Pax2}KO mice may therefore be linked to a Pax2-driven BDNF deletion in the lower parts of the auditory CNS or the cochlea. In the cochlea, BDNF is expressed postnatally in phalangeal, SGN, or satellite cells (Sobkowicz et al., 2002, Schimmang et al., 2003, Zuccotti et al., 2012, Singer et al., 2014). Given that (i) BDNF deletion in phalangeal cells does not affect hearing thresholds (Wan et al., 2014), (ii) BDNF deletion in SGNs and in a minor number of supporting cells as observed in BDNF^{TrkC}KO mice does not lead to an auditory phenotype (Chumak et al., 2015), and (iii) BDNF expression in inhibitory interneurons has been excluded (Heimel et al., 2011, Leto et al., 2012), the loss of BDNF expression in glial cells may be considered as being responsible for the observed phenotype in BDNF^{Pax2}KO animals.

In the previous study, reduced exocytosis in otherwise mature IHCs in high-frequency cochlear turns of 2–3 -week-old BDNF^{Pax2}KO mice (Zuccotti et al., 2012) pointed out a critical role of BDNF for pre- and postsynaptic maturation of IHCs. The alterations in ABR waves I and IV found in BDNF^{Pax2}KO (Zuccotti et al., 2012) but not BDNF^{TrkC}-KO mice (Chumak et al., 2015) indicate that BDNF activities that are carried out independently of higher auditory brain regions improve sound sensitivity at least up to the level of the IC. No difference in DPOAEs within the range of the stimulus levels in which ABR functions were quantified as it has been reported previously (Zuccotti et al., 2012), suggesting that electromechanical properties of OHCs are not affected in BDNF^{Pax2}KO. BDNF is therefore more likely to improve ABR amplitudes through its influence on IHC exocytosis and/or auditory fiber sensitivity for low intensity sounds. Elevated thresholds that are independent of changes in cochlear amplification are expected to be seen only when high-SR, low-threshold fibers are affected that comprise 60% of all afferent fibers (Yates, 1991) and trigger thresholds due to their high sensitivity to sound together with their shorter latencies (Heil et al., 2008, Buran et al., 2010). When low-SR afferent fibers are lost after moderate trauma, no elevated hearing thresholds are seen(Furman et al., 2013). As at any given CF in the auditory system, high-SR neurons have the shorter and low-SR the longer latencies (Rhode and Smith, 1986), BDNF-dependent afferent fibers have to be considered to correspond to low-threshold,

high-SR fiber types. The loss of low-threshold, high-SR afferent fibers would best explain the highly-significant loss of short latency responses in IC neurons of BDNF^{Pax2}KO mice in middle and high CF regions, covering the frequency region (15–20 kHz) where behavioral auditory thresholds are lowest in mice (Hage and Ehret, 2003a). In this context, it is important to consider that characteristics of high spontaneous rate, low threshold auditory nerve fibers develop only after hearing onset (Grant et al., 2010, Knipper et al., 2015). Also in the visual system, a role of retinal BDNF for improved retinal and visual acuity has been suggested (Landi et al., 2009). Accordingly, an antisense-based inhibition of BDNF in the retina prevented an improvement of retinal stripe segregation induced by environmental enrichment as well as cortical acuity, even prior to eye opening (Landi et al., 2007a, Landi et al., 2007b, Landi et al., 2009). To date, conditional deletion of retinal BDNF has not been performed, and it is therefore elusive if it improves the baseline of visual sensitivity independently of environmental enrichment, similar to the present findings.

The current findings suggest that BDNF-dependent effects on auditory nerve activity are responsible not only for improving the ABR amplitude size of high-frequency sound responses spreading along the ascending pathway, but also for expanding the range of CF thresholds in these high frequency CF regions. The affected CF regions >10 kHz span areas (15–20 kHz) where murine behavioral auditory thresholds are at their lowest level (Hage and Ehret, 2003b). We thus have to consider the improved CF thresholds, short latencies, and the increased strength of inhibitory sidebands of sharply tuned IC neurons in WT versus BDNF^{Pax2}KO animals in the context of an enhanced auditory fidelity in behaviorally relevant frequency regions. The IC neurons that show altered tuning characteristics depending on the presence of BDNF are reminiscent of type II (Hage and Ehret, 2003b) and type I (Hernandez et al., 2005) class IC neurons. Both IC cell types predominate in high-frequency regions and are characterized by their short latency, narrow and sharp tuning, low-frequency border with a shallow slope, and high frequency border with a steep slope (Hage and Ehret, 2003b, Hernandez et al., 2005). It thus may be considered that these neurons are shaped under the control of BDNF activities at hearing onset.

PV expressing interneurons play a crucial role for hippocampal microcircuit formation and plasticity changes (Jonas P, 2007). The significant loss of density of PV-immunopositive puncta in the IC and AC may suggest that a BDNF-modified driving force for auditory processing improves the baseline for mature circuit formation and plasticity changes along the entire ascending auditory network. This finding, moreover, suggests that the altered brain network activity shaped under the influence of BDNF in the lower parts of

the auditory CNS or within the cochlea is a prerequisite for cortical maturation processes that occur with sensory experience (Kilgard et al., 2002, Han et al., 2007, Carcea and Froemke, 2013).

5.3. Nanoparticles as a potential drug carrier for regenerative inner ear therapy

5.3.1. Distribution in the inner ear and non-toxicity of nanoparticles after middle ear application

The results of this study show that all three types of NPs, although composed of different materials and have different structure, can penetrate inside the cochlea and enter identical cochlear structures (i.e., the SG, the organ of Corti and the lateral wall). Besides RWM polylysine was able to permeate inside cochlea through the cochlear and stapedial bone and annular ligament surrounding footplate of the stapes (oval window). It increased permeation of polylysine into the scala vestibuli and, possibly into the tissues of interest such as SG, OC and lateral wall. Inner ear entry of substances through the oval window (Salt et al., 2012, King et al., 2013) and cohlear bone (Mikulec et al., 2009) has been previously shown, but considered less effective compared to RWM permeation (Salt et al., 2012, Zou et al., 2012a, Zou et al., 2012b).

Within the cochlear tissues liposomes and polymersomes were localized mainly intracellularly and only rarely in the intercellular space (organ of Corti), while polylysines were detected both, intra- and extracellularly in all analysed structures. The cochlear distribution of different types of NPs applied on the RWM has been previously demonstrated for poly(lactic/glycolic acid) NPs (Tamura et al., 2005, Ge et al., 2007), lipid nanocapsules (Zou et al., 2008), hyperbranched polylysines (Zhang et al., 2011) and silica NPs (Praetorius et al., 2007). Maeda *et al.* (Maeda et al., 2007) and Jero *et al.* (Jero et al., 2001) used RWM application of liposomes with plasmid for a successful transfection of the mouse cochlea.

The distribution of individual types of NPs in various cochlear partitions differs. After RWM application, nanoparticles were most abundantly found in the SG, while lesser amounts of NPs were found in the organ of Corti, the spiral ligament and the stria vascularis. A similar distribution of polymersomes was observed by Zhang *et al.* after middle ear application in rats (Zhang et al., 2010b). Scheper *et al.* (2009) found large amounts of lipid nanocapsules or hyperbranched polylysines in both outer and inner hair cells in the organ of Corti after

intracochlear application in guinea pigs (Scheper et al., 2009) that correlate with our results for polylysine. Similarly to distribution after intracochlear administration, polylysine created small clusters inside the cells and between them and often localized near the cochlear nucleus. Although Zhang *et al.* (2011) reported nuclear localization of polylysine *in vitro* and *in vivo* (Zhang et al., 2011), we were not able to detect it during our experiments similarly to Scheper *et al.* (Scheper et al., 2009). However, perinuclear polylysine localization is speculated to be enough to deliver a gene into the cell nucleus fro successful transfection (Scheper et al., 2009). Praetorius *et al*. (2007) demonstrated that application of silica NPs via the RWM resulted in detection in the cochlea, vestibular organs, and brain stem, mainly in the central auditory nuclei such as dorsal cochlear nucleus and superior olivary complex. We did not detect liposomes or polymersomes in contralateral ear or in the brain after RWM application (data not shown), extracochlear localization of polylysine was not tested. Even though the NPs are biodegradable, no data is available regarding the metabolic processing of NP compounds. This is an especially important point when long-term treatment is required.

The application of drug or gene-loaded NPs to the middle ear cavity and their penetration to the cochlea through the RWM is a less invasive and safer alternative to direct intracochlear drug administration via a cochleostomy or microinjection through the RWM. A question that arises is, what are the possible routes of NP entry from the middle ear to the individual cochlear structures? From this study we conclude that after the application of the NP suspension onto the RWM, the NPs permeate to the ST. The RWM is comprised of three layers: the outer epithelium, a middle layer composed of connective tissue with blood vessels and lymphatic channels, and an inner layer of squamous cells (Goycoolea and Lundman, 1997). Substances as well as NPs usually cross the outer epithelium by pinocytosis or translocation between the cells; they are absorbed into the lymphatic and vascular spaces of the middle layer and then transported into the perilymph (Tanaka and Motomura, 1981). However, the transport of NPs through the RWM is variable and depends on the NP size, NP payload or tag, the duration that the NP suspension is in contact with the membrane and the concentration of the suspension. In this study, to prolong the contact time of the NPs with the RWM we delivered the NPs to gel foam placed on the RWM.

NPs passing through the RWM entered the ST. Based on the previous literature and our results we can propose a hypothetical distribution pathway for NPs within the cochlea (Figure 41). The osseous spiral lamina was found to be highly porous; the bony surface is separated from the perilymphatic space by a thin discontinuous sheet of mesothelial cells (Duckert and Duvall, 1978, Rask-Andersen et al., 2006). The osseous spiral lamina appears to

provide an open and extensive fluid communication channel between the ST and the Rosenthal canal (Figure 41, arrows 1). This pathway is probably responsible for the frequent finding of NPs in the SG in this study. A perineural and perivascular communication route was suggested as an important communication pathway between the perilymph and the tunnel of Corti (Masuda et al., 1971, Duckert and Duvall, 1978). Another route for the entry of NPs into the organ of Corti may be via the most lateral part of the osseous spiral lamina (Figure 41, arrow 2). The smallest numbers of NPs were found in the lateral wall. The possible routes of NP entry to the spiral ligament and stria vascularis may be from the ST (Figure 41, arrows 3 & 4). The longitudinal flow of perilymph in the ST has been shown to be relatively slow, if present at all, and drug distribution in the perilymph is dominated by passive diffusion (Sykova et al., 1987, Ohyama et al., 1988). However, NPs can pass into the more apical parts of the cochlea through the radial communication between the ST and scala vestibuli through the modiolar space (Figure 41, arrow 5) (Salt et al., 1991, Naganawa et al., 2008). Our results support the common hypothesis of mechanisms for NP distribution in the cochlea, but direct proof is still needed.

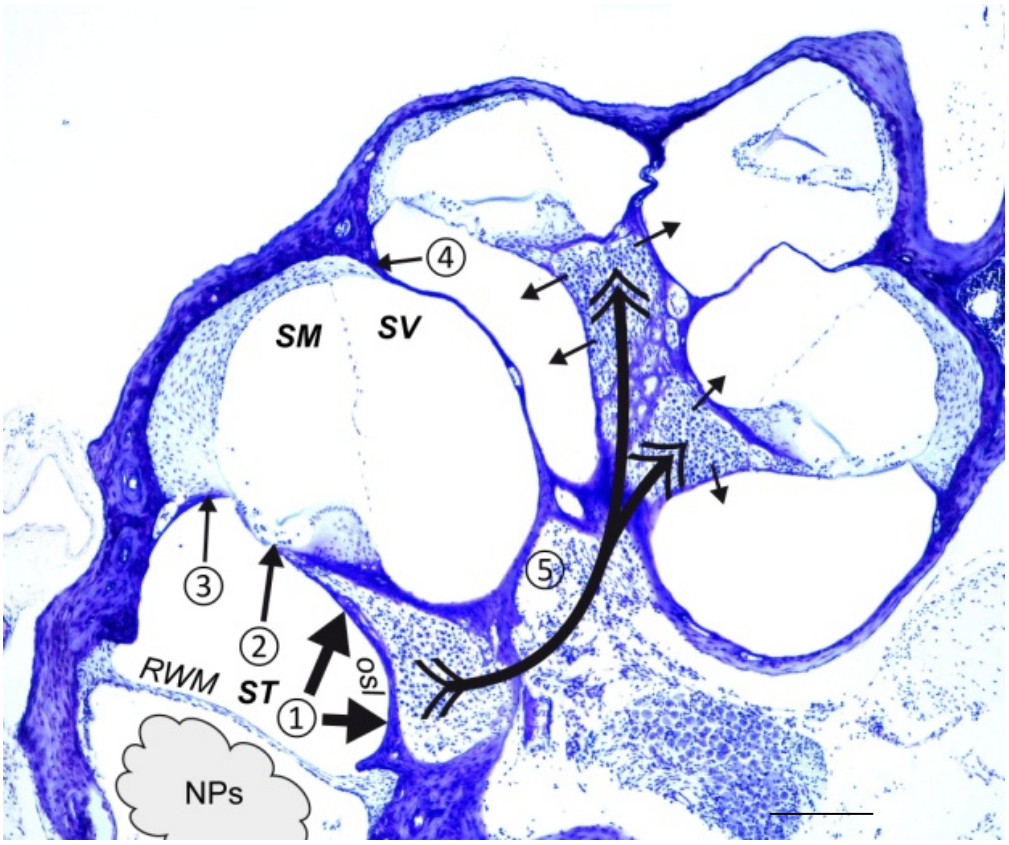

Figure 41. Hypothetical intracochlear routes for nanoparticles distribution.

A section through the cochlea showing hypothetical routes for nanoparticles permeation from the middle ear to the inner ear. Scale bar = 100 µm. NPs: Nanoparticles; RWM: Round window membrane; SM: Scala media; ST: Scala tympani; SV: Scala vestibule, osl: Osseous spiral lamina.

5.3.2. Use of nanoparticles as drug delivery tool

To determine the efficiency of drug delivery to the inner ear and the dose of the drug delivered in our model, we introduced experiments using nanoparticles loaded with an active agent.

Polylysine have been proposed as effective polymeric carrier for gene delivery *in vitro* (Zauner et al., 1998, Vanderkerken et al., 2000, Putnam et al., 2001, Zhang et al., 2010a, Kim, 2012, Zhao et al., 2016). To test transfection efficiency of polylysine-plasmid complex *in vivo* we used two plasmids: polylysine-plFL was tagged with fluorescent marker and was supposed to be used as a positive control of polylysine-plasmid intracochlear permeation, and polylysine- eGFP, contained plasmid, that in case of its intracellular delivery and successful transfection would be detected as green fluorescence. Unfortunately, we were not able to detect any specific fluorescence inside cochlea after RWM application of either polylysine-plasmid complex 1 and 3 days after injection. Experiments on intracochlear application of polylysine-plasmid complex would be needed to find out if failure in transfection was due to permeability issue.

As load for polymersomes and liposomes, neurotoxic drug disulfiram was selected. Several neurotoxic drugs such as ouabain (Schmiedt et al., 2002) or b-bungarotoxin (Palmgren et al., 2010) have been used in the previous studies to induce selective damage of neurons in the cochlea. However, in contrast to disulfiram, these drugs can transit alone through the RWM due to different physical parameters, which makes them unsuitable for testing a NP-based drug delivery system. When used clinically, disulfiram has several negative side effects including induction of a peripheral neuropathy (Tonkin et al., 2000, Bevilacqua et al., 2002, Tonkin et al., 2004). Recent *in vitro* studies demonstrated that disulfiram-induced apoptotic cell death is due to proteosomal inhibition (Chen et al., 2001, Chen et al., 2006, Wickstrom et al., 2007). The results of our study demonstrate that the amount of disulfiram transported by NPs into the cochlea was sufficient to produce a toxic effect in the SG, which corresponds to the site where the largest amount of NPs was detected. In other cochlear tissues including the lateral wall or the organ of Corti, the pathological changes were negligible. There is an issue as to whether disulfiram is released from the

particles within the cells, or prior to cellular uptake while the NPs are within the perilymph. We observed that fluorescently labeled NPs accumulated mainly within the SG, and as this is also where the toxic effects of disulfiram were also observed it is reasonable to assume that drug release occurred intracellularly. Undetectable morphological damage in the lateral wall or the organ of Corti may be due to the smaller amounts of disulfiram-loaded NPs transported to these tissues, and also due to the differential susceptibility of individual cell types to disulfiram toxicity (Chen et al., 2006, Wickstrom et al., 2007). Pronounced morphological alterations in the SG correspond with the significant hearing loss seen in the treated animals. Because SG cells project centrally to the brain as fibers of the auditory nerve, this type of hearing loss is regarded as 'neural' hearing loss, in contrast to 'sensory' hearing loss, caused by the loss of sensory hair cells or stria vascularis damage.

A similar degree of pathology was seen for both disulfiram-loaded liposomes and disulfiram-loaded polymersomes, leading us to conclude that similar amounts of disulfiram were delivered to the cochlea with both types of NPs.

The results of the present study demonstrate that the toxic effect in the inner ear was produced by disulfiram delivered to the cochlea in the NPs, since no damaging effect was obtained after the application of free disulfiram onto the RWM. This suggests that polymersome and liposome NPs are capable of carrying a payload into the inner ear that elicits a biological effect, with consequences measurable by a functional readout. Future research on NP-mediated therapeutic delivery to the SG cell population within the inner ear will be aimed at promoting cell survival, neurogenesis, maintenance of neurons and synaptogenesis in subjects after an acute injury or to ameliorate the effects of aging (Syka, 2002). With this in mind, liposomes and polymersomes are suitable delivery vehicles for neurotrophic factors, plasmid DNA and for antiapoptotic agent delivery (e.g., siRNA).

6. Summary

Sensorineural hearing loss is the most common sensory disorder in humans. Due to popularity of recreational activities accompanied by loud noise (music concerts, movie theaters, maximum levels in personal stereo systems) and ageing of the population the number of people with disabling hearing loss is expected to grow. Hearing loss affects human wellbeing as well as represents an economic burden on society.

Sensorineural hearing loss is most often caused by degeneration of main sound processing and transmitting parts in the cochlea- hair cells and spiral ganglion neurons. In mammals including human once these cells die they never regenerate. As no regenerative inner ear therapy is available by now people suffering hearing loss may benefit from supporting devices such as hearing aids and cochlear implantats. However, recent progress in research of developmental, degenerative and regenerative processes in the inner ear of different species open new perspectives. First experiments show that genes and factors active during inner ear development may have a potential for regenerative therapy. Inner ear, though, is a very complex organ with strict spatial and functional organization. Full understanding of the role and function of each player is needed to succeed in creation of new functional sensory epithelium or neurons after degeneration. Besides that, to induce and manipulate the regenerative process safe, efficient and targeted instruments for drug delivery are needed.

In this work we studied the role of potentially regenerative factors Islet1 and BDNF in development and function of the auditory system. We also tested three types of nanoparticles – liposomes, polymersomes and polylysine as a potential drug delivery tool for regenerative therapy.

Gain in embryonic development of Pax2-Isl1 transgenic mice

*Isl*1 has been shown to be expressed during early inner ear development in the otocyst and correlate with formation of the prosensory inner ear domain (Huang et al., 2008). In contrast to chicken inner ear, where Isl1 is prominently expressed in adult supporting and hair cells (Li et al., 2004) possibly contributing to spontaneous regeneration after damage, *Isl1* expression is shut down in adult mouse cochlea. Our hypothesis was that ISL1-expressing cells are the common precursors for both sensory epithelia and neurons; and by modulation the expression of *Isl1* we would be able to change the fate specification of cells in the inner ear.

As expected, Pax2Isl1 overexpression at the early stages of inner ear development leads to enlargement of the ISL1+ expression domain in the $Tg^{+/-}$ otocysts. The size of the cochlear-vestibular ganglion delaminating from the otic epithelium and differentiating into ganglion neurons is increased in $Tg^{+/-}$ embryos compared to WT littermates. Besides that increased expression levels of Isl1 in mutant embryos are associated with more rapid differentiation of afferents leading to their accelerated branching and extension.

Altogether this supports our hypothesis of significance of *Isl1* in cell fate specification in the inner ear during development.

ISL1 missexpression leads to medial olivocochlear bundle degeneration and accelerated age-related hearing loss in adult transgenic animals

Despite gains in early development, the overexpression of ISL1 impairs the maintenance and function of hair cells of the organ of Corti. Transgenic mice exhibit reduced DPOAE responses staring from 1 months of age and severely impaired by 9 months. As we found, this functional inefficiency of OHCs is caused by degeneration of terminals of medial olivocochlear bundle. Most likely Pax2Isl1 missexpression in the midbrain/hindbrain region early in the development (Pfeffer et al., 2002, Bohuslavova et al., 2016) affects medial olivocochlear budnle as well. For the first time, our results show that the genetic alteration of the medial olivocochlear efferent system induces an early onset of age-related hearing loss. Thus, the neurodegeneration of the MOC system could be a contributing factor to the pathology of age-related hearing loss. Our results support the idea of preventive role of the olivocochlear system in age related hearing loss (Fu et al., 2010, Liberman et al., 2014b).

BDNF in lower brain parts modifies auditory fiber activity to gain fidelity

In the previous study, reduced exocytosis in otherwise mature IHCs in high-frequency cochlear turns of 2–3-week-old BDNF^{Pax2}KO mice (Zuccotti et al. 2012) pointed out a critical role of BDNF for pre- and postsynaptic maturation of IHCs after onset of hearing. The alterations in ABR waves I and IV found in BDNF^{Pax2}KO (Zuccotti et al. 2012) but not BDNF^{Trk}CKO mice (Chumak et al. 2015) indicate that BDNF activities that are carried out independently of higher auditory brain regions improve sound sensitivity at least up to the level of the IC. To gain insight into “peripheral” BDNF role in the lower brain auditory structures we performed extracellular recording of neuronal activity in the IC of BDNF^{Pax2}KO and BDNF^{Pax2}WT mice.

We show here that response characteristics of IC neurons are altered in KO mice. Basic response properties such as neuronal thresholds and dynamic range were impaired in the IC of mutant mice. Responses of high frequency IC neurons exhibited prolonged latency and were lacking sharply tuned neuronal population. Decreased inhibitory strength together with reduced levels of parvalbumin expression in the IC indicates that after the onset of hearing BDNF in lower brain parts sharpens a very narrow tuning characteristic of IC neurons.

Most of found functional alterations affected behaviorally relevant frequency range. Altogether this suggests a significant role of "peripheral" BDNF in driving auditory fidelity along the entire ascending auditory pathway.

Nanoparticles are safe and able to penetrate into cochlea after middle ear application

Nanoparticles are among the most promising tools for minimally invasive delivery to the inner ear of active agents such as regenerative genes, transcription or neurotrophic factors. We aimed to test intracochlear distribution and ability to deliver payload of three types of nanoparticles: liposomes, polymersomes and polylysine. These nanoparticles have different chemical origin: liposomes are made of phospholipids, polymersomes contain amphiphilic block copolymers and polylysine is represented by a randomly branched polymer. Liposomes and polymersomes have similar vesicular structure with hydrophobic membrane and hydrophilic core. Polylysine is a dendrimer able to form complexes with DNA.

All three types of NPs were shown to be able to penetrate inside the cochlea after application on the RWM and enter identical cochlear structures (i.e., the SG, the organ of Corti and the lateral wall). Although due to its affinity to the bone and fibrous tissue polylysine is able to penetrate through the cochlear bone and oval window it does not affect significantly its intracochlear distribution. Within the cochlear tissues liposomes and polymersomes are localized mainly intracellularly and only rarely in the intercellular space (organ of Corti), while polylysines were detected both, intra- and extracellularly in all analysed structures.

Unloaded nanoparticles of all types do not cause any detectable harm to the inner ear structures.

Liposomes and polymersomes are able to deliver sufficient amount of drug inside cochlea

All types of nanoparticles were tested for their ability to deliver an active agent inside cochlea. Since polylysine have been proposed as effectlive polymeric carrier for gene delivery *in vitro* (Zauner et al. 1998, Vanderkerken et al. 2000, Putnam et al. 2001, Zhang et al. 2010, Kim 2012, Zhao et al. 2016) we applied two polylysine-plasmid complexes to the RWM *in vivo*. Unfortunately, we were unable to detect any specific fluorescence inside cochlea after RWM application.

As a load for polymersomes and liposomes, we selected disulfiram. Disulfiram does not permeate through the round window membrane by itself, which makes it suitable for testing a NP-based drug delivery system. Since it is a neurotoxic drug (Tonkin et al. 2000, Tonkin et al. 2004) we assumed that detection of its action should be easily detectable. Indeed, both disulfiram-loaded nanoparticles produced pronounced morphological alterations in the SG and significant hearing loss in the treated animals. Signs of morphological damage are evident in the SG cells of all cochlear turns as early as 2 days after NP application. Significant threshold shifts (20–35 dB) two weeks after the treatment are present at 8 and 16 kHz after liposome and at 8–25 kHz after polymersome application. The fact that application of free disulfiram onto the RWM do not result in damaging effect suggests that the toxic effect in the inner ear was produced by disulfiram delivered to the cochlea in the NPs.

Our results demonstrate that polymersome and liposome NPs are capable of carrying a payload into the inner ear that elicits a biological effect, with consequences measurable by a functional readout.

Clinical relevance of the experimental results

Our results provide details about the role of Islet1 and BDNF during auditory system development and function and confirm their potential importance as regenerative factors for the inner ear therapy. Besides that we suggest possible role of neurodegeneration in age related hearing loss and assume that decline in BDNF function with age may contribute to reduced temporal resolution of complex sound processing. We also show that nanoparticles may be a suitable tool for minimally invasive intracochlear drug delivery; however, some modifications to improve targeting would be beneficial.

7. Conclusions

Role of ISL1 in development and function of the auditory system

- The transgenic expression of Pax2-Isl1 results in an enlargement of ISL1+ expression domain with an increased number of ISL1+ cells in the otic epithelium and delaminating neuroblasts of the ganglion in the E10.5 mouse otocyst.
- The transgenic expression of Pax2-Isl1 is accompanied by rapid extension and branching of fibers connecting developing brainstem and inner ear in E12.5 embryos.
- The misexpression of Pax2-Isl1 in the MOC area is most likely the reason for MOC efferent system degeneration in $Tg^{+/-}$ mice that resulted in accelerated age-related hearing loss

Role of "peripheral" BDNF in the auditory system

- Pax2-BDNF deletion increases thresholds and constricts dynamic range of IC neurons
- Pax2-BDNF deletion alters latency and frequency selectivity of IC neurons suggesting that after the onset of hearing, BDNF in lower brain parts sharpens a very narrow tuning characteristic of IC neurons.
- Deletion of BDNF affects the inhibitory strength of IC neurons and reduces the density of PV-immunopositivity in IC and AC projecting neurons which may affect temporal processing of complex sound
- The source of BDNF that sharpens IC neuronal responses is not fully clear, however, it is surely not auditory cortex or hippocampus.

Use of nanoparticles as a potential drug delivery tool

- All three tested types of nanoparticles (liposomes, polymersomes and polylysine) penetrate through the RWM and enter cells within the cochlea after middle ear in mice
- All types of nanoparticles are found in the spiral ganglion, the organ of Corti and spiral ligament suggesting unsatisfied targeting of unlabeled nanoparticles
- Unloaded nanoparticles are not overtly toxic to cochlear structure or function.
- Although polylysine is claimed to be a suitable tool for gene delivery, in our experiment transfection was unsuccessful.

- Liposome and polymersome NPs loaded with neurotoxic drug are capable to deliver it inside cochlea in sufficient amount to produce an effect detectable functionally and morphologically.

8. References

Abdala C, Dhar S (2012) Maturation and Aging of the Human Cochlea: A View through the DPOAE Looking Glass. Jaro-J Assoc Res Oto 13:403-421.

Adams JC, Mugnaini E (1984) Dorsal Nucleus of the Lateral Lemniscus - a Nucleus of Gabaergic Projection Neurons. Brain Res Bull 13:585-590.

Adams JC, Schulte BA (1997) Histopathologic observations of the aging gerbil cochlea. Hear Res 104:101-111.

Adler HJ, Raphael Y (1996) New hair cells arise from supporting cell conversion in the acoustically damaged chick inner ear. Neurosci Lett 205:17-20.

Agterberg MJH, Versnel H, de Groot JCMJ, Smoorenburg GF, Albers FWJ, Klis SFL (2008) Morphological changes in spiral ganglion cells after intracochlear application of brain-derived neurotrophic factor in deafened guinea pigs. Hearing Res 244:25-34.

Aitkin LM, Dickhaus H, Schult W, Zimmermann M (1978) External Nucleus of Inferior Colliculus - Auditory and Spinal Somatosensory Afferents and Their Interactions. Journal of Neurophysiology 41:837-847.

Alvarez-Buylla A, Ling CY, Kirn JR (1990) Cresyl violet: a red fluorescent Nissl stain. J Neurosci Methods 33:129-133.

Atkinson PJ, Wise AK, Flynn BO, Nayagam BA, Hume CR, O'Leary SJ, Shepherd RK, Richardson RT (2012) Neurotrophin Gene Therapy for Sustained Neural Preservation after Deafness. Plos One 7.

Avila MA, Varelanieto I, Romero G, Mato JM, Giraldez F, Vandewater TR, Represa J (1993) Brain-Derived Neurotrophic Factor and Neurotrophin-3 Support the Survival and Neuritogenesis Response of Developing Cochleovestibular Ganglion Neurons. Dev Biol 159:266-275.

Ayala YA, Udeh A, Dutta K, Bishop D, Malmierca MS, Oliver DL (2015) Differences in the strength of cortical and brainstem inputs to SSA and non-SSA neurons in the inferior colliculus. Sci Rep-Uk 5.

Bajo VM, Merchan MA, Malmierca MS, Nodal FR, Bjaalie JG (1999) Topographic organization of the dorsal nucleus of the lateral lemniscus in the cat. Journal of Comparative Neurology 407:349-366.

Bemelmans AP, Horellou P, Pradier L, Brunet I, Colin P, Mallet J (1999) Brain-derived neurotrophic factor-mediated protection of striatal neurons in an excitotoxic rat model of Huntington's disease, as demonstrated by adenoviral gene transfer. Hum Gene Ther 10:2987-2997.

Berghuis P, Agerman K, Dobszay MB, Minichiello L, Harkany T, Ernfors P (2006) Brain-derived neurotrophic factor selectively regulates dendritogenesis of parvalbumin-containing interneurons in the main olfactory bulb through the PLC gamma pathway. J Neurobiol 66:1437-1451.

Bermingham-McDonogh O, Rubel EW (2003) Hair cell regeneration: winging our way towards a sound future. Curr Opin Neurobiol 13:119-126.

Bevilacqua JA, Diaz M, Diaz V, Silva C, Fruns M (2002) Disulfiram neuropathy. Report of three cases. Rev Med Chile 130:1037-1042.

Bhati M, Lee C, Nancarrow AL, Lee M, Craig VJ, Bach I, Guss JM, Mackay JP, Matthews JM (2008) Implementing the LIM code: the structural basis for cell type-specific assembly of LIM-homeodomain complexes. Embo J 27:2018-2029.

Bitsche M, Dudas J, Roy S, Potrusil T, Schmutzhard J, Schrott-Fischer A (2011) Neurotrophic Receptors as Potential Therapy Targets in Postnatal Development, in Adult, and in Hearing Loss-Affected Inner Ear. Otol Neurotol 32:761-773.

Bohuslavova R, Dodd N, Macova I, Chumak T, Horak M, Syka J, Fritzsch B, Pavlinkova G (2016) Pax2-Islet1 Transgenic Mice Are Hyperactive and Have Altered Cerebellar Foliation. Mol Neurobiol.

Bohuslavova R, Kolar F, Kuthanova L, Neckar J, Tichopad A, Pavlinkova G (2010) Gene expression profiling of sex differences in HIF1-dependent adaptive cardiac responses to chronic hypoxia. J Appl Physiol (1985) 109:1195-1202.

Bolte S, Cordelieres FP (2006) A guided tour into subcellular colocalization analysis in light microscopy. J Microsc-Oxford 224:213-232.

Borkholder DA (2008) State-of-the-art mechanisms of intracochlear drug delivery. Curr Opin Otolaryngo 16:472-477.

Bouchard M, de Caprona D, Busslinger M, Xu P, Fritzsch B (2010a) Pax2 and Pax8 cooperate in mouse inner ear morphogenesis and innervation. Bmc Dev Biol 10:89.

Bouchard M, de Caprona D, Busslinger M, Xu PX, Fritzsch B (2010b) Pax2 and Pax8 cooperate in mouse inner ear morphogenesis and innervation. Bmc Dev Biol 10.

Bramham CR, Panja D (2014) BDNF regulation of synaptic structure, function, and plasticity. Neuropharmacology 76:601-602.

Brigande JV, Heller S (2009) Quo vadis, hair cell regeneration? Nat Neurosci 12:679-685.

Brown MC, Levine JL (2008) Dendrites of medial olivocochlear neurons in mouse. Neuroscience 154:147-159.

Buran BN, Strenzke N, Neef A, Gundelfinger ED, Moser T, Liberman MC (2010) Onset coding is degraded in auditory nerve fibers from mutant mice lacking synaptic ribbons. J Neurosci 30:7587-7597.

Bures Z, Grecova J, Popelar J, Syka J (2010) Noise exposure during early development impairs the processing of sound intensity in adult rats. Eur J Neurosci 32:155-164.

Burns JC, Cox BC, Thiede BR, Zuo J, Corwin JT (2012a) In Vivo Proliferative Regeneration of Balance Hair Cells in Newborn Mice. Journal of Neuroscience 32:6570-6577.

Burns JC, Yoo JJ, Atala A, Jackson JD (2012b) MYC Gene Delivery to Adult Mouse Utricles Stimulates Proliferation of Postmitotic Supporting Cells In Vitro. Plos One 7.

Cai CL, Liang XQ, Shi YQ, Chu PH, Pfaff SL, Chen J, Evans S (2003) Isl1 identifies a cardiac progenitor population that proliferates prior to differentiation and contributes a majority of cells to the heart. Dev Cell 5:877-889.

Campbell JP, Henson MM (1988) Olivocochlear Neurons in the Brain-Stem of the Mouse. Hearing Res 35:271-274.

Carcea I, Froemke RC (2013) Cortical Plasticity, Excitatory-Inhibitory Balance, and Sensory Perception. Changing Brains Applying Brain Plasticity to Advance and Recover Human Ability 207:65-90.

Carvalho GJ, Lalwani AK (1999) The effect of cochleostomy and intracochlear infusion on auditory brain stem response threshold in the guinea pig. Am J Otol 20:87-90.

Casaccia-Bonnefil P, Carter BD, Dobrowsky RT, Chao MV (1996) Death of oligodendrocytes mediated by the interaction of nerve growth factor with its receptor p75. Nature 383:716-719.

Casseday JH, Ehrlich D, Covey E (2000) Neural measurement of sound duration: Control by excitatory-inhibitory interactions in the inferior colliculus. Journal of Neurophysiology 84:1475-1487.

Cizkova D, Nagyova M, Slovinska L, Novotna I, Radonak J, Cizek M, Mechirova E, Tomori Z, Hlucilova J, Motlik J, Sulla I, Jr., Vanicky I (2009) Response of ependymal progenitors to spinal cord injury or enhanced physical activity in adult rat. Cell Mol Neurobiol 29:999-1013.

Coote EJ, Rees A (2008) The distribution of nitric oxide synthase in the inferior colliculus of guinea pig. Neuroscience 154:218-225.

Copley CO, Duncan JS, Liu C, Cheng H, Deans MR (2013) Postnatal refinement of auditory hair cell planar polarity deficits occurs in the absence of Vangl2. J Neurosci 33:14001-14016.

Corwin JT, Cotanche DA (1988) Regeneration of Sensory Hair-Cells after Acoustic Trauma. Science 240:1772-1774.

Costalupes JA, Young ED, Gibson DJ (1984) Effects of Continuous Noise Backgrounds on Rate Response of Auditory-Nerve Fibers in Cat. Journal of Neurophysiology 51:1326-1344.

Covey E, Casseday JH (1991) The monaural nuclei of the lateral lemniscus in an echolocating bat: parallel pathways for analyzing temporal features of sound. J Neurosci 11:3456-3470.

Dallos P, Wu X, Cheatham MA, Gao J, Zheng J, Anderson CT, Jia S, Wang X, Cheng WH, Sengupta S, He DZ, Zuo J (2008) Prestin-based outer hair cell motility is necessary for mammalian cochlear amplification. Neuron 58:333-339.

Darrow KN, Maison SF, Liberman MC (2007) Selective removal of lateral olivocochlear efferents increases vulnerability to acute acoustic injury. Journal of Neurophysiology 97:1775-1785.

Darrow KN, Simons EJ, Dodds L, Liberman MC (2006) Dopaminergic innervation of the mouse inner ear: Evidence for a separate cytochemical group of cochlear efferent fibers. Journal of Comparative Neurology 498:403-414.

Davis KA (2002) Evidence of a functionally segregated pathway from dorsal cochlear nucleus to inferior colliculus. Journal of Neurophysiology 87:1824-1835.

Davis KA, Ramachandran R, May BJ (2003) Auditory processing of spectral cues for sound localization in the inferior colliculus. Jaro-J Assoc Res Oto 4:148-163.

De Ceulaer G, Johnson S, Yperman M, Daemers K, Offeciers FE, O'Donoghue GM, Govaerts PJ (2003) Long-term evaluation of the effect of intracochlear steroid deposition on electrode impedance in cochlear implant patients. Otol Neurotol 24:769-774.

Dechant G, Barde YA (2002) The neurotrophin receptor p75(NTR): novel functions and implications for diseases of the nervous system. Nat Neurosci 5:1131-1136.

Delacroix L, Malgrange B (2015) Cochlear afferent innervation development. Hear Res 330:157-169.

Deng M, Luo XJ, Pan L, Yang H, Xie XL, Liang GQ, Huang L, Hu F, Kiernan AE, Gan L (2014) LMO4 Functions As a Negative Regulator of Sensory Organ Formation in the Mammalian Cochlea. Journal of Neuroscience 34:10072-10077.

Despres G, Romand R (1994) Neurotrophins and the Development of Cochlear Innervation. Life Sci 54:1291-1297.

Diamond IT, Jones EG, Powell TPS (1969) Projection of Auditory Cortex Upon the Diencephalon and Brain Stem in Cat. Brain Res 15:305-&.

Diensthuber M, Zecha V, Wagenblast J, Arnhold S, Edge AS, Stover T (2014) Spiral ganglion stem cells can be propagated and differentiated into neurons and glia. Biores Open Access 3:88-97.

Druga R, Syka J (1984a) Ascending and Descending Projections to the Inferior Colliculus in the Rat. Physiol Bohemoslov 33:31-&.

Druga R, Syka J (1984b) Neocortical Projections to the Inferior Colliculus in the Rat - (an Experimental-Study Using Anterograde Degeneration Techniques). Physiol Bohemoslov 33:251-253.

Druga R, Syka J (1993) Nadph-Diaphorase Activity in the Central Auditory Structures of the Rat. Neuroreport 4:999-1002.

Druga R, Syka J, Rajkowska G (1997) Projections of auditory cortex onto the inferior colliculus in the rat. Physiol Res 46:215-222.

Duckert LG, Duvall AJ (1978) Cochlear Communication Routes in Guinea-Pig - Spiral Ganglia and Osseous Spiral Laminae - Electron-Microscope Study Using Microsphere Tracers. Otolaryngology 86:434-446.

Dworkin S, Darido C, Georgy SR, Wilanowski T, Srivastava S, Ellett F, Pase L, Han YC, Meng AM, Heath JK, Lieschke GJ, Jane SM (2012) Midbrain-hindbrain boundary patterning and morphogenesis are regulated by diverse grainy head-like 2-dependent pathways. Development 139:525-536.

Edge ASB, Chen ZY (2008) Hair cell regeneration. Curr Opin Neurobiol 18:377-382.

Eggermont JJ (2001) Between sound and perception: reviewing the search for a neural code. Hearing Res 157:1-42.

Egorova M, Ehret G, Vartanian I, Esser KH (2001) Frequency response areas of neurons in the mouse inferior colliculus. I. Threshold and tuning characteristics. Exp Brain Res 140:145-161.

El Kechai N, Agnely F, Mamelle E, Nguyen Y, Ferrary E, Bochot A (2015) Recent advances in local drug delivery to the inner ear. Int J Pharmaceut 494:83-101.

Elshatory Y, Everhart D, Deng M, Xie XL, Barlow RB, Gan L (2007) Islet-1 controls the differentiation of retinal bipolar and cholinergic amacrine cells. Journal of Neuroscience 27:12707-12720.

Endo T, Nakagawa T, Kita T, Iguchi F, Kim TS, Tamura T, Iwai K, Tabata Y, Ito J (2005) Novel strategy for treatment of inner ears using a biodegradable gel. Laryngoscope 115:2016-2020.

Ernfors P, Lee KF, Jaenisch R (1994) Mice Lacking Brain-Derived Neurotrophic Factor Develop with Sensory Deficits. Nature 368:147-150.

Eybalin M, Parnaud C, Geffard M, Pujol R (1988) Immunoelectron Microscopy Identifies Several Types of Gaba-Containing Efferent Synapses in the Guinea-Pig Organ of Corti. Neuroscience 24:29-38.

Faingold CL, Anderson CAB, Randall ME (1993) Stimulation or Blockade of the Dorsal Nucleus of the Lateral Lemniscus Alters Binaural and Tonic Inhibition in Contralateral Inferior Colliculus Neurons. Hearing Res 69:98-106.

Faingold CL, Boersma CA, Anderson, Caspary DM (1991) Involvement of Gaba in Acoustically-Evoked Inhibition in Inferior Colliculus Neurons. Hearing Res 52:201-216.

Fayelund H (1985) The Neocortical Projection to the Inferior Colliculus in the Albino-Rat. Anat Embryol 173:53-70.

Fayelund H, Osen KK (1985) Anatomy of the Inferior Colliculus in Rat. Anat Embryol 171:1-20.

Fechner FP, Nadol JB, Burgess BJ, Brown MC (2001) Innervation of supporting cells in the apical turns of the guinea pig cochlea is from type II afferent fibers. Journal of Comparative Neurology 429:289-298.

Forge A, Li L, Corwin JT, Nevill G (1993) Ultrastructural Evidence for Hair Cell Regeneration in the Mammalian Inner-Ear. Science 259:1616-1619.

Frade JM, RodriguezTebar A, Barde YA (1996) Induction of cell death by endogenous nerve growth factor through its p75 receptor. Nature 383:166-168.

Franklin KBJ, Paxinos G (2008) The mouse brain in stereotaxic coordinates. San Diego: Academic Press.

Fritzsch B, Beisel KW, Hansen LA (2006) The molecular basis of neurosensory cell formation in ear development: a blueprint for hair cell and sensory neuron regeneration? Bioessays 28:1181-1193.

Fritzsch B, Jahan I, Pan N, Elliott KL (2015) Evolving gene regulatory networks into cellular networks guiding adaptive behavior: an outline how single cells could have evolved into a centralized neurosensory system. Cell and Tissue Research 359:295-313.

Fritzsch B, Tessarollo L, Coppola E, Reichardt LF (2004) Neurotrophins in the ear: their roles in sensory neuron survival and fiber guidance. Prog Brain Res 146:265-278.

Fu B, Le Prell C, Simmons D, Lei DB, Schrader A, Chen AB, Bao JX (2010) Age-related synaptic loss of the medial olivocochlear efferent innervation. Mol Neurodegener 5.

Fukui H, Wong HT, Beyer LA, Case BG, Swiderski DL, Di Polo A, Ryan AF, Raphael Y (2012) BDNF gene therapy induces auditory nerve survival and fiber sprouting in deaf Pou4f3 mutant mice. Sci Rep-Uk 2.

Furman AC, Kujawa SG, Liberman MC (2013) Noise-induced cochlear neuropathy is selective for fibers with low spontaneous rates. J Neurophysiol 110:577-586.

Gao M, Maynard KR, Chokshi V, Song LH, Jacobs C, Wang H, Tran T, Martinowich K, Lee HK (2014) Rebound Potentiation of Inhibition in Juvenile Visual Cortex Requires Vision-Induced BDNF Expression. Journal of Neuroscience 34:10770-10779.

Ge XX, Jackson RL, Liu JZ, Harper EA, Hoffer ME, Wassel RA, Dormer KJ, Kopke RD, Balough BJ (2007) Distribution of PLGA nanoparticles in chinchilla cochleae. Otolaryng Head Neck 137:619-623.

Gillespie LN, Clark GM, Bartlett PF, Marzella PL (2003) BDNF-induced survival of auditory neurons in vivo: Cessation of treatment leads to accelerated loss of survival effects. J Neurosci Res 71:785-790.

Glendenning KK, Baker BN, Hutson KA, Masterton RB (1992) Acoustic Chiasm .5. Inhibition and Excitation in the Ipsilateral and Contralateral Projections of Lso. Journal of Comparative Neurology 319:100-122.

Glueckert R, Pritz CO, Roy S, Dudas J, Schrott-Fischer A (2015) Nanoparticle mediated drug delivery of rolipram to tyrosine kinase B positive cells in the inner ear with targeting peptides and agonistic antibodies. Front Aging Neurosci 7.

Golding NL, Oertel D (2012) Synaptic integration in dendrites: exceptional need for speed. J Physiol-London 590:5563-5569.

Goycoolea MV, Lundman L (1997) Round window membrane. Structure function and permeability: A review. Microsc Res Techniq 36:201-211.

Grant L, Yi EY, Glowatzki E (2010) Two Modes of Release Shape the Postsynaptic Response at the Inner Hair Cell Ribbon Synapse. Journal of Neuroscience 30:4210-4220.

Griffen TC, Maffei A (2014) GABAergic synapses: their plasticity and role in sensory cortex. Front Cell Neurosci 8.

Groff JA, Liberman MC (2003) Modulation of cochlear afferent response by the lateral olivocochlear system: Activation via electrical stimulation of the inferior colliculus. Journal of Neurophysiology 90:3178-3200.

Grothe B, Pecka M, McAlpine D (2010) Mechanisms of sound localization in mammals. Physiol Rev 90:983-1012.

Guimaraes P, Zhu XX, Cannon T, Kim SH, Frisina RD (2004) Sex differences in distortion product otoacoustic emissions as a function of age in CBA mice. Hearing Res 192:83-89.

Guinan JJ, Stankovic KM (1996) Medial efferent inhibition produces the largest equivalent attenuations at moderate to high sound levels in cat auditory-nerve fibers. Journal of the Acoustical Society of America 100:1680-1690.

Hafidi A (1999) Distribution of BDNF, NT-3 and NT-4 in the developing auditory brainstem. Int J Dev Neurosci 17:285-294.

Hafidi A, Moore T, Sanes DH (1996) Regional distribution of neurotrophin receptors in the developing auditory brainstem. Journal of Comparative Neurology 367:454-464.

Hage SR, Ehret G (2003a) Mapping responses to frequency sweeps and tones in the inferior colliculus of house mice. Eur J Neurosci 18:2301-2312.

Hage SR, Ehret G (2003b) Mapping responses to frequency sweeps and tones in the inferior colliculus of house mice. European Journal of Neuroscience 18:2301-2312.

Han YK, Kover H, Insanally MN, Semerdjian JH, Bao SW (2007) Early experience impairs perceptual discrimination. Nat Neurosci 10:1191-1197.

Handrock M, Zeisberg J (1982) The Influence of the Efferent System on Adaptation, Temporary and Permanent Threshold Shift. Arch Oto-Rhino-Laryn 234:191-195.

Hans S, Liu D, Westerfield M (2004) Pax8 and Pax2a function synergistically in otic specification, downstream of the Foxi1 and Dlx3b transcription factors. Development 131:5091-5102.

Havenith S, Versnel H, Agterberg MJH, de Groot JCMJ, Sedee RJ, Grolman W, Klis SFL (2011) Spiral ganglion cell survival after round window membrane application of brain-derived neurotrophic factor using gelfoam as carrier. Hearing Res 272:168-177.

Heil P, Neubauer H, Brown M, Irvine DRF (2008) Towards a unifying basis of auditory thresholds: Distributions of the first-spike latencies of auditory-nerve fibers. Hearing Res 238:25-38.

Heimel JA, van Versemdaal D, Levelt CN (2011) The Role of GABAergic Inhibition in Ocular Dominance Plasticity. Neural Plast.

Hernandez O, Espinosa N, Perez-Gonzalez D, Malmierca MS (2005) The inferior colliculus of the rat: A quantitative analysis of monaural frequency response areas. Neuroscience 132:203-217.

Hobert O, Westphal H (2000) Functions of LIM-homeobox genes. Trends Genet 16:75-83.

Hofstetter P, Ding D, Powers N, Salvi RJ (1997) Quantitative relationship of carboplatin dose to magnitude of inner and outer hair cell loss and the reduction in distortion product otoacoustic emission amplitude in chinchillas. Hear Res 112:199-215.

Hori R, Nakagawa T, Sakamoto T, Matsuoka Y, Takebayashi S, Ito J (2007) Pharmacological inhibition of Notch signaling in the mature guinea pig cochlea. Neuroreport 18:1911-1914.

Hoshaw BA, Malberg JE, Lucki I (2005) Central administration of IGF-I and BDNF leads to long-lasting antidepressant-like effects. Brain Res 1037:204-208.

Hoskison E, Daniel M, Al-Zahid S, Shakesheff KM, Bayston R, Birchall JP (2013) Drug delivery to the ear. Ther Deliv 4:115-124.

Hu H, Gan J, Jonas P (2014) Fast-spiking, parvalbumin(+) GABAergic interneurons: From cellular design to microcircuit function. Science 345:529-+.

Huang M, Sage C, Li H, Xiang M, Heller S, Chen ZY (2008) Diverse expression patterns of LIM-homeodomain transcription factors (LIM-HDs) in mammalian inner ear development. Dev Dyn 237:3305-3312.

Huang MQ, Kantardzhieva A, Scheffer D, Liberman MC, Chen ZY (2013) Hair Cell Overexpression of Islet1 Reduces Age-Related and Noise-Induced Hearing Loss. Journal of Neuroscience 33:15086-15094.

Chan DK, Hudspeth AJ (2005) Ca2+ current-driven nonlinear amplification by the mammalian cochlea in vitro. Nat Neurosci 8:149-155.

Chen D, Cui QZC, Yang HJ, Dou QP (2006) Disulfiram, a clinically used anti-alcoholism drug and copper-binding agent, induces apoptotic cell death in breast cancer cultures and xenografts via inhibition of the proteasome activity. Cancer Res 66:10425-10433.

Chen JC, Streit A (2013) Induction of the inner ear: Stepwise specification of otic fate from multipotent progenitors. Hearing Res 297:3-12.

Chen SH, Liu SH, Liang YC, Lin JK, Lin-Shiau SY (2001) Oxidative stress and c-Jun-amino-terminal kinase activation involved in apoptosis of primary astrocytes induced by disulfiram-Cu(2+) complex. Eur J Pharmacol 414:177-188.

Chikar JA, Colesa DJ, Swiderski DL, Di Polo A, Raphael Y, Pfingst BE (2008) Over-expression of BDNF by adenovirus with concurrent electrical stimulation improves cochlear implant thresholds and survival of auditory neurons. Hearing Res 245:24-34.

Chithrani BD, Stewart J, Allen C, Jaffray DA (2009) Intracellular uptake, transport, and processing of nanostructures in cancer cells. Nanomedicine-Uk 5:118-127.

Christophorou NA, Mende M, Lleras-Forero L, Grocott T, Streit A (2010) Pax2 coordinates epithelial morphogenesis and cell fate in the inner ear. Dev Biol 345:180-190.

Chumak T, Ruttiger L, Lee SC, Campanelli D, Zuccotti A, Singer W, Popelar J, Gutsche K, Geisler HS, Schraven SP, Jaumann M, Panford-Walsh R, Hu J, Schimmang T, Zimmermann U, Syka J, Knipper M (2015) BDNF in Lower Brain Parts Modifies Auditory Fiber Activity to Gain Fidelity but Increases the Risk for Generation of Central Noise After Injury. Mol Neurobiol.

Ingham NJ, McAlpine D (2005) GABAergic inhibition controls neural gain in inferior colliculus neurons sensitive to interaural time differences. J Neurosci 25:6187-6198.

Ito J, Endo T, Nakagawa T, Kita T, Kim TS, Iguchi F (2005) A new method for drug application to the inner ear. Orl J Oto-Rhino-Lary 67:272-275.

Izumikawa M, Minoda R, Kawamoto K, Abrashkin KA, Swiderski DL, Dolan DF, Brough DE, Raphael Y (2005) Auditory hair cell replacement and hearing improvement by Atoh1 gene therapy in deaf mammals. Nat Med 11:271-276.

Jahan I, Pan N, Elliott KL, Fritzsch B (2015) The quest for restoring hearing: Understanding ear development more completely. Bioessays 37:1016-1027.

Jahan I, Pan N, Kersigo J, Fritzsch B (2013) Beyond generalized hair cells: Molecular cues for hair cell types. Hearing Res 297:30-41.

Jero J, Mhatre AN, Tseng CJ, Stern RE, Coling DE, Goldstein JA, Hong K, Zheng WW, Hoque ATMS, Lalwani AK (2001) Cochlear gene delivery through an intact round window membrane in mouse. Hum Gene Ther 12:539-548.

Jiao YY, Zhang Z, Zhang CZ, Wang XJ, Sakata K, Lu B, Sun QQ (2011) A key mechanism underlying sensory experience-dependent maturation of neocortical GABAergic circuits in vivo. P Natl Acad Sci USA 108:12131-12136.

Jimenez AM, Stagner BB, Martin GK, Lonsbury-Martin BL (1999) Age-related loss of distortion product otoacoustic emissions in four mouse strains. Hearing Res 138:91-105.

Jonas P BG (2007) Neural inhibition. In: Scholarpedia, vol. 2(9):3286.

Jones JM, Montcouquiol M, Dabdoub A, Woods C, Kelley MW (2006) Inhibitors of differentiation and DNA binding (Ids) regulate Math1 and hair cell formation during the development of the organ of Corti. J Neurosci 26:550-558.

Kalra S, Genge A, Arnold DL (2003) A prospective, randomized, placebo-controlled evaluation of corticoneuronal response to intrathecal BDNF therapy in ALS using magnetic resonance spectroscopy: feasibility and results. Amyotroph Lateral Sc 4:22-26.

Karlsson O, Thor S, Norberg T, Ohlsson H, Edlund T (1990) Insulin gene enhancer binding protein Isl-1 is a member of a novel class of proteins containing both a homeo- and a Cys-His domain. Nature 344:879-882.

Kawase T, Liberman MC (1993) Antimasking effects of the olivocochlear reflex. I. Enhancement of compound action potentials to masked tones. Journal of neurophysiology 70:2519-2532.

Kelley MW (2006) Regulation of cell fate in the sensory epithelia of the inner ear. Nat Rev Neurosci 7:837-849.

Kelly JB, Caspary DM (2005) Pharmacology of the Inferior Colliculus. In: The Inferior Colliculus (Winer J. A., S. C. E., ed), pp 248-311 United States of America: Springer Science+Business Media, Inc.

Kennedy HJ, Crawford AC, Fettiplace R (2005) Force generation by mammalian hair bundles supports a role in cochlear amplification. Nature 433:880-883.

Kersigo J, D'Angelo A, Gray BD, Soukup GA, Fritzsch B (2011) The role of sensory organs and the forebrain for the development of the craniofacial shape as revealed by Foxg1-cre-mediated microRNA loss. Genesis 49:326-341.

Khalin I, Alyautdin R, Kocherga G, Abu Bakar M (2015) Targeted delivery of brain-derived neurotrophic factor for the treatment of blindness and deafness. Int J Nanomed 10:3245-3267.

Kiernan AE, Pelling AL, Leung KKH, Tang ASP, Bell DM, Tease C, Lovell-Badge R, Steel KP, Cheah KSE (2005) Sox2 is required for sensory organ development in the mammalian inner ear. Nature 434:1031-1035.

Kilgard MP, Pandya PK, Engineer ND, Moucha R (2002) Cortical network reorganization guided by sensory input features. Biol Cybern 87:333-343.

Kim SW (2012) Polylysine copolymers for gene delivery. Cold Spring Harb Protoc 2012:433-438.

King EB, Salt AN, Kel GE, Eastwood HT, O'Leary SJ (2013) Gentamicin administration on the stapes footplate causes greater hearing loss and vestibulotoxicity than round window administration in guinea pigs. Hearing Res 304:159-166.

Kirk EC, Smith DW (2003) Protection from acoustic trauma is not a primary function of the medial olivocochlear efferent system. Jaro-J Assoc Res Oto 4:445-465.

Knipper L, Van Dijk P, Nunes I, Ruttiger L, Zimmermann U (2013) Advances in the neurobiology of hearing disorders: Recent developments regarding the basis of tinnitus and hyperacusis. Prog Neurobiol 111:17-33.

Knipper M, Panford-Walsh R, Singer W, Ruttiger L, Zimmermann U (2015) Specific synaptopathies diversify brain responses and hearing disorders: you lose the gain from early life. Cell and Tissue Research 361:77-93.

Koehler KR, Mikosz AM, Molosh AI, Patel D, Hashino E (2013) Generation of inner ear sensory epithelia from pluripotent stem cells in 3D culture. Nature 500:217-+.

Konrad-Martin D, Dille MF, McMillan G, Griest S, McDermott D, Fausti SA, Austin DF (2012) Age-Related Changes in the Auditory Brainstem Response. J Am Acad Audiol 23:18-35.

Konrad-Martin DL, Rubsamen R, Dorrscheidt GJ, Rubel EW (1998) Development of single- and two-tone responses of anteroventral cochlear nucleus neurons in gerbil. Hear Res 121:35-52.

Kopp-Scheinpflug C, Dehmel S, Dorrscheidt GJ, Rubsamen R (2002) Interaction of excitation and inhibition in anteroventral cochlear nucleus neurons that receive large endbulb synaptic endings. J Neurosci 22:11004-11018.

Kotak VC, Pendola LM, Rodriguez-Contreras A (2012) Spontaneous Activity in the Developing Gerbil Auditory Cortex in Vivo Involves Gabaergic Transmission. Neuroscience 226:130-144.

Kujawa SG, Liberman MC (1997) Conditioning-related protection from acoustic injury: Effects of chronic deefferentation and sham surgery. Journal of Neurophysiology 78:3095-3106.

Kujawa SG, Liberman MC (2009) Adding Insult to Injury: Cochlear Nerve Degeneration after "Temporary" Noise-Induced Hearing Loss. Journal of Neuroscience 29:14077-14085.

Land RB, A.; Kral, A. (2016) The Contribution of Inferior Colliculus Activity to the Auditory Brainstem Response (ABR) in Mice. 39TH ANNUAL MIDWINTER MEETING OF THE ASSOCIATION FOR RESEARCH IN OTOLARINGOLOGY.

Landi S, Cenni MC, Maffei L, Berardi N (2007a) Environmental Enrichment Effects on Development of Retinal Ganglion Cell Dendritic Stratification Require Retinal BDNF. Plos One 2.

Landi S, Ciucci F, Maffei L, Berardi N, Cenni MC (2009) Setting the Pace for Retinal Development: Environmental Enrichment Acts Through Insulin-Like Growth Factor 1 and Brain-Derived Neurotrophic Factor. Journal of Neuroscience 29:10809-10819.

Landi S, Sale A, Berardi N, Viegi A, Maffei L, Cenni MC (2007b) Retinal functional development is sensitive to environmental enrichment: a role for BDNF. Faseb J 21:130-139.

Latchman DS (1997) Transcription factors: An overview. Int J Biochem Cell B 29:1305-1312.

Lauer AM, May BJ (2011) The medial olivocochlear system attenuates the developmental impact of early noise exposure. J Assoc Res Otolaryngol 12:329-343.

Lawoko-Kerali G, Milo M, Davies D, Halsall A, Helyer R, Johnson CM, Rivolta MN, Tones MA, Holley MC (2004) Ventral otic cell lines as developmental models of auditory epithelial and neural precursors. Dev Dyn 231:801-814.

Le Beau FE, Rees A, Malmierca MS (1996) Contribution of GABA- and glycine-mediated inhibition to the monaural temporal response properties of neurons in the inferior colliculus. J Neurophysiol 75:902-919.

Le Magueresse C, Monyer H (2013) GABAergic Interneurons Shape the Functional Maturation of the Cortex. Neuron 77:388-405.

Leake PA, Hradek GT, Hetherington AM, Stakhovskaya O (2011) Brain-Derived Neurotrophic Factor Promotes Cochlear Spiral Ganglion Cell Survival and Function in Deafened, Developing Cats. Journal of Comparative Neurology 519:1526-1545.

Lee FS, Kim AH, Khursigara G, Chao MV (2001) The uniqueness of being a neurotrophin receptor. Curr Opin Neurobiol 11:281-286.

Leto K, Rolando C, Rossi F (2012) The genesis of cerebellar GABAergic neurons: fate potential and specification mechanisms. Front Neuroanat 6.

Levivier M, Przedborski S, Bencsics C, Kang UJ (1995) Intrastriatal implantation of fibroblasts genetically engineered to produce brain-derived neurotrophic factor prevents degeneration of dopaminergic neurons in a rat model of Parkinson's disease. J Neurosci 15:7810-7820.

Li D, Henley CM, O'Malley BW, Jr. (1999) Distortion product otoacoustic emissions and outer hair cell defects in the hyt/hyt mutant mouse. Hear Res 138:65-72.

Li H, Liu H, Sage C, Huang M, Chen ZY, Heller S (2004) Islet-1 expression in the developing chicken inner ear. J Comp Neurol 477:1-10.

Li HW, Liu H, Heller S (2003a) Pluripotent stem cells from the adult mouse inner ear. Nat Med 9:1293-1299.

Li HW, Roblin G, Liu H, Heller S (2003b) Generation of hair cells by stepwise differentiation of embryonic stem cells. P Natl Acad Sci USA 100:13495-13500.

Li L, Forge A (1997) Morphological evidence for supporting cell to hair cell conversion in the mammalian utricular macula. Int J Dev Neurosci 15:433-446.

Liang XQ, Song MR, Xu ZG, Lanuza GM, Liu YL, Zhuang T, Chen YH, Pfaff SL, Evans SM, Sun YF (2011) Isl1 Is required for multiple aspects of motor neuron development. Mol Cell Neurosci 47:215-222.

Liberman MC (1978) Auditory-Nerve Response from Cats Raised in a Low-Noise Chamber. Journal of the Acoustical Society of America 63:442-455.

Liberman MC (1991) The olivocochlear efferent bundle and susceptibility of the inner ear to acoustic injury. Journal of neurophysiology 65:123-132.

Liberman MC, Gao J, He DZ, Wu X, Jia S, Zuo J (2002) Prestin is required for electromotility of the outer hair cell and for the cochlear amplifier. Nature 419:300-304.

Liberman MC, Liberman LD, Maison SF (2014a) Efferent feedback slows cochlear aging. J Neurosci 34:4599-4607.

Liberman MC, Liberman LD, Maison SF (2014b) Efferent Feedback Slows Cochlear Aging. Journal of Neuroscience 34:4599-4607.

Light JP, Silverstein H (2004) Transtympanic perfusion: indications and limitations. Curr Opin Otolaryngol Head Neck Surg 12:378-383.

Light JP, Silverstein H, Jackson LE (2003) Gentamicin perfusion vestibular response and hearing loss. Otol Neurotol 24:294-298.

Lin LZ, Bu L, Cai CL, Zhang XX, Evans S (2006) Isl1 is upstream of sonic hedgehog in a pathway required for cardiac morphogenesis. Dev Biol 295:756-763.

Lin V, Golub JS, Nguyen TB, Hume CR, Oesterle EC, Stone JS (2011) Inhibition Of Notch Activity Promotes Nonmitotic Regeneration of Hair Cells in the Adult Mouse Utricles. Journal of Neuroscience 31:15329-15339.

Liu W, Kinnefors A, Bostrom M, Rask-Andersen H (2011) Expression of TrkB and BDNF in human cochlea-an immunohistochemical study. Cell and Tissue Research 345:213-221.

Lockwood AH, Salvi RJ, Burkard RF (2002) Current concepts: Tinnitus. New Engl J Med 347:904-910.

Loftus WC, Malmierca MS, Bishop DC, Oliver DL (2008) The cytoarchitecture of the inferior colliculus revisited: A common organization of the lateral cortex in rat and cat. Neuroscience 154:196-205.

Lonsbury-Martin BL, Cutler WM, Martin GK (1991) Evidence for the Influence of Aging on Distortion-Product Otoacoustic Emissions in Humans. Journal of the Acoustical Society of America 89:1749-1759.

Lou XX, Nakagawa T, Nishimura K, Ohnishi H, Yamamoto N, Sakamoto T, Ito J (2013) Reprogramming of Mouse Cochlear Cells by Transcription Factors to Generate Induced Pluripotent Stem Cells. Cell Reprogram 15:514-519.

Lu Y, Jen PH (2001) GABAergic and glycinergic neural inhibition in excitatory frequency tuning of bat inferior collicular neurons. Exp Brain Res 141:331-339.

Maeda Y, Fukushima K, Kawasaki A, Nishizaki K, Smith RJH (2007) Cochlear expression of a dominant-negative GJB2(R75W) construct delivered through the round window membrane in mice. Neurosci Res 58:250-254.

Magariños MCJV-N, I. (2014) Early Development of the Vertebrate Inner Ear. In: Development of Auditory and Vestibular Systems (Romand, R. V.-N., I., ed): Elsevier Inc.

Maison SF, Adams JC, Liberman MC (2003) Olivocochlear innervation in the mouse: immunocytochemical maps, crossed versus uncrossed contributions, and transmitter colocalization. J Comp Neurol 455:406-416.

Maison SF, Luebke AE, Liberman MC, Zuo J (2002a) Efferent protection from acoustic injury is mediated via alpha9 nicotinic acetylcholine receptors on outer hair cells. J Neurosci 22:10838-10846.

Maison SF, Luebke AE, Liberman MC, Zuo J (2002b) Efferent protection from acoustic injury is mediated via alpha 9 nicotinic acetylcholine receptors on outer hair cells. Journal of Neuroscience 22:10838-10846.

Maison SF, Usubuchi H, Liberman MC (2013) Efferent Feedback Minimizes Cochlear Neuropathy from Moderate Noise Exposure. Journal of Neuroscience 33:5542-5552.

Makar TK, Bever CT, Singh IS, Royal W, Sahu SN, Sura TP, Sultana S, Sura KT, Patel N, Dhib-Jalbut S, Trisler D (2009) Brain-derived neurotrophic factor gene delivery in an animal model of multiple sclerosis using bone marrow stem cells as a vehicle. J Neuroimmunol 210:40-51.

Makary CA, Shin J, Kujawa SG, Liberman MC, Merchant SN (2011) Age-Related Primary Cochlear Neuronal Degeneration in Human Temporal Bones. Jaro-J Assoc Res Oto 12:711-717.

Malmierca MS (2003) The structure and physiology of the rat auditory system: An overview. Int Rev Neurobiol 56:147-211.

Malmierca MS, Hernandez O, Falconi A, Lopez-Poveda EA, Merchan M, Rees A (2003) The commissure of the inferior colliculus shapes frequency response areas in rat: an in vivo study using reversible blockade with microinjection of kynurenic acid. Experimental Brain Research 153:522-529.

Malmierca MS, Rees A, Lebeau FEN, Bjaalie JG (1995) Laminar Organization of Frequency-Defined Local Axons within and between the Inferior Colliculi of the Guinea-Pig. Journal of Comparative Neurology 357:124-144.

Malmierca MS, Ryugoy DK (2012) Auditory System. Mouse Nervous System 607-645.

Malmierca MS, Saint Marie RL, Merchan MA, Oliver DL (2005) Laminar inputs from dorsal cochlear nucleus and ventral cochlear nucleus to the central nucleus of the inferior colliculus: Two patterns of convergence. Neuroscience 136:883-894.

Maness LM, Kastin AJ, Weber JT, Banks WA, Beckman BS, Zadina JE (1994) The Neurotrophins and Their Receptors - Structure, Function, and Neuropathology. Neurosci Biobehav R 18:143-159.

Martin GK, Vazquez AE, Jimenez AM, Stagner BB, Howard MA, Lonsbury-Martin BL (2007) Comparison of distortion product otoacoustic emissions in 28 inbred strains of mice. Hear Res 234:59-72.

Masuda Y, Sando I, Hemenway WG (1971) Perilymphatic Communication Routes in Guinea Pig Cochlea - Experimental Autoradiographic Study. Archiv Otolaryngol 94:240-&.

May BJ, McQuone SJ (1995) Effects of Bilateral Olivocochlear Lesions on Pure-Tone Intensity Discrimination in Cats. 1:385-400.

Mccabe BF (1989) Autoimmune Inner-Ear Disease - Therapy. Am J Otol 10:196-197.

Meininger V, Pol D, Derer P (1986) The Inferior Colliculus of the Mouse - a Nissl and Golgi-Study. Neuroscience 17:1159-&.

Melcher JR, Kiang NY (1996) Generators of the brainstem auditory evoked potential in cat. III: Identified cell populations. Hear Res 93:52-71.

Merchan M, Aguilar LA, Lopez-Poveda EA, Malmierca MS (2005) The inferior colliculus of the rat: Quantitative immunocytochemical study of GABA and glycine. Neuroscience 136:907-925.

Merchanperez A, Gilloyzaga P, Lopezsanchez J, Eybalin M, Valderrama FJ (1993) Ontogeny of Gamma-Aminobutyric-Acid in Efferent Fibers to the Rat Cochlea. Dev Brain Res 76:33-41.

Mikulec AA, Plontke SK, Hartsock JJ, Salt AN (2009) Entry of Substances Into Perilymph Through the Bone of the Otic Capsule After Intratympanic Applications in Guinea Pigs: Implications for Local Drug Delivery in Humans. Otol Neurotol 30:131-138.

Mizutari K, Fujioka M, Hosoya M, Bramhall N, Okano HJ, Okano H, Edge ASB (2013) Notch Inhibition Induces Cochlear Hair Cell Regeneration and Recovery of Hearing after Acoustic Trauma. Neuron 77:58-69.

Moskowitz D, Lee KJ, Smith HW (1984) Steroid Use in Idiopathic Sudden Sensorineural Hearing-Loss. Laryngoscope 94:664-666.

Mou K, Hunsberger CL, Cleary JM, Davis RL (1997) Synergistic effects of BDNF and NT-3 on postnatal spiral ganglion neurons. Journal of Comparative Neurology 386:529-539.

Nagahara AH, Merrill DA, Coppola G, Tsukada S, Schroeder BE, Shaked GM, Wang L, Blesch A, Kim A, Conner JM, Rockenstein E, Chao MV, Koo EH, Geschwind D, Masliah E, Chiba AA, Tuszynski MH (2009) Neuroprotective effects of brain-derived neurotrophic factor in rodent and primate models of Alzheimer's disease. Nat Med 15:331-337.

Naganawa S, Satake H, Iwano S, Sone M, Nakashima T (2008) Communication between cochlear perilymph and cerebrospinal fluid through the cochlear modiolus visualized after intratympanic administration of Gd-DTPA. Radiat Med 26:597-602.

Nakagawa T (2014) Therapeutic Targets and Possible Strategies for Regenerative Medicine for the Inner Ear. In: Regenerative Medicine for the Inner Ear (Ito, J., ed) Japan: Springer Japan.

Nakaizumi T, Kawamoto K, Minoda R, Raphael Y (2004) Adenovirus-mediated expression of brain-derived neurotrophic factor protects spiral ganglion neurons from ototoxic damage. Audiol Neuro-Otol 9:135-143.

Nataraj K, Wenstrup JJ (2005) Roles of inhibition in creating complex auditory responses in the inferior colliculus: Facilitated combination-sensitive neurons. Journal of Neurophysiology 93:3294-3312.

Nichols DH, Pauley S, Jahan I, Beisel KW, Millen KJ, Fritzsch B (2008) Lmx1a is required for segregation of sensory epithelia and normal ear histogenesis and morphogenesis. Cell and Tissue Research 334:339-358.

Nordang L, Linder B, Anniko M (2003) Morphologic changes in round window membrane after topical hydrocortisone and dexamethasone treatment. Otol Neurotol 24:339-343.

Oesterle EC, Cunningham DE, Westrum LE, Rubel EW (2003) Ultrastructural analysis of [H-3]thymidine-labeled cells in the rat utricular macula. Journal of Comparative Neurology 463:177-195.

Ohyama K, Salt AN, Thalmann R (1988) Volume Flow-Rate of Perilymph in the Guinea-Pig Cochlea. Hearing Res 35:119-130.

Ohyama T, Groves AK (2004) Generation of Pax2-Cre mice by modification of a Pax2 bacterial artificial chromosome. Genesis 38:195-199.

Okano T, Kelley MW (2012) Stem Cell Therapy for the Inner Ear: Recent Advances and Future Directions. Trends Amplif 16:4-18.

Oshima K, Grimm CM, Corrales CE, Senn P, Moneder RM, Geleoc GSG, Edge A, Holt JR, Heller S (2007) Differential distribution of stem cells in the auditory and vestibular organs of the inner ear. Jaro-J Assoc Res Oto 8:18-31.

Oshima K, Shin K, Diensthuber M, Peng AW, Ricci AJ, Heller S (2010) Mechanosensitive Hair Cell-like Cells from Embryonic and Induced Pluripotent Stem Cells. Cell 141:704-716.

Ota Y, Oliver DL, Dolan DF (2004) Frequency-specific effects on cochlear responses during activation of the inferior colliculus in the guinea pig. Journal of Neurophysiology 91:2185-2193.

Paasche G, Bockel F, Tasche T, Lesinski-Schiedat A, Lenarz T (2006) Changes of postoperative impedances in cochlear implant patients: The short-term effects of modified electrode surfaces and intracochlear corticosteroids. Otol Neurotol 27:639-647.

Palmgren B, Jin Z, Ma HM, Jiao Y, Olivius P (2010) beta-Bungarotoxin application to the round window: An in vivo deafferentation model of the inner ear. Hearing Res 265:70-76.

Palombi PS, Caspary DM (1996) GABA inputs control discharge rate primarily within frequency receptive fields of inferior colliculus neurons. Journal of Neurophysiology 75:2211-2219.

Parham K (1997) Distortion product otoacoustic emissions in the C57BL/6J mouse model of age-related hearing loss. Hearing Res 112:216-234.

Parnes LS, Sun AH, Freeman DJ (1999) Corticosteroid pharmacokinetics in the inner ear fluids: An animal study followed by clinical application. Laryngoscope 109:1-17.

Perez-Gonzalez D, Malmierca MS, Covey E (2005) Novelty detector neurons in the mammalian auditory midbrain. European Journal of Neuroscience 22:2879-2885.

Pettingill LN, Wise AK, Geaney MS, Shepherd RK (2011) Enhanced Auditory Neuron Survival Following Cell-Based BDNF Treatment in the Deaf Guinea Pig. Plos One 6.

Pfaff SL, Mendelsohn M, Stewart CL, Edlund T, Jessell TM (1996) Requirement for LIM homeobox gene Isl1 in motor neuron generation reveals a motor neuron-dependent step in interneuron differentiation. Cell 84:309-320.

Pfaffl MW (2001) A new mathematical model for relative quantification in real-time RT-PCR. Nucleic Acids Res 29:e45.

Pfeffer PL, Payer B, Reim G, di Magliano MP, Busslinger M (2002) The activation and maintenance of Pax2 expression at the mid-hindbrain boundary is controlled by separate enhancers. Development 129:307-318.

Pinyon JL, Tadros SF, Froud KE, Wong ACY, Tompson IT, Crawford EN, Ko M, Morris R, Klugmann M, Housley GD (2014) Close-Field Electroporation Gene Delivery Using the Cochlear Implant Electrode Array Enhances the Bionic Ear. Sci Transl Med 6.

Pirvola U, Arumae U, Moshnyakov M, Palgi J, Saarma M, Ylikoski J (1994) Coordinated Expression and Function of Neurotrophins and Their Receptors in the Rat Inner-Ear during Target Innervation. Hearing Res 75:131-144.

Pirvola U, Ylikoski J, Palgi J, Lehtonen E, Arumae U, Saarma M (1992) Brain-derived neurotrophic factor and neurotrophin 3 mRNAs in the peripheral target fields of developing inner ear ganglia. Proc Natl Acad Sci U S A 89:9915-9919.

Poe DS, Pyykko I (2011) Nanotechnology and the treatment of inner ear diseases. Wires Nanomed Nanobi 3:212-221.

Pollak GD, Xie RL, Gittelman JX, Andoni S, Li N (2011) The dominance of inhibition in the inferior colliculus. Hearing Res 274:27-39.

Popelar J, Groh D, Pelanova J, Canlon B, Syka J (2006) Age-related changes in cochlear and brainstem auditory functions in Fischer 344 rats. Neurobiology of aging 27:490-500.

Popelar J, Nwabueze-Ogbo FC, Syka J (2003) Changes in neuronal activity of the inferior colliculus in rat after temporal inactivation of the auditory cortex. Physiol Res 52:615-628.

Popelar J, Rybalko N, Burianova J, Schwaller B, Syka J (2013) The effect of parvalbumin deficiency on the acoustic startle response and prepulse inhibition in mice. Neurosci Lett 553:216-220.

Popelar J, Suta D, Lindovsky J, Bures Z, Pysanenko K, Chumak T, Syka J (2016) Cooling of the auditory cortex modifies neuronal activity in the inferior colliculus in rats. Hearing Res 332:7-16.

Praetorius M, Brunner C, Lehnert B, Klingmann C, Schmidt H, Staecker H, Schick B (2007) Transsynaptic delivery of nanoparticles to the central auditory nervous system. Acta Oto-Laryngol 127:486-490.

Puschel AW, Westerfield M, Dressler GR (1992) Comparative-Analysis of Pax-2 Protein Distributions during Neurulation in Mice and Zebrafish. Mech Develop 38:197-208.

Putnam D, Gentry CA, Pack DW, Langer R (2001) Polymer-based gene delivery with low cytotoxicity by a unique balance of side-chain termini. P Natl Acad Sci USA 98:1200-+.

Radde-Gallwitz K, Pan L, Gan L, Lin X, Segil N, Chen P (2004) Expression of Islet1 marks the sensory and neuronal lineages in the mammalian inner ear. J Comp Neurol 477:412-421.

Radeloff A, Smolders JW (2006a) Brain-derived neurotrophic factor treatment does not improve functional recovery after hair cell regeneration in the pigeon. Acta Otolaryngol 126:452-459.

Radeloff A, Smolders JWT (2006b) Brain-derived neurotrophic factor treatment does not improve functional recovery after hair cell regeneration in the pigeon. Acta Oto-Laryngol 126:452-459.

Rajan R (2000) Centrifugal pathways protect hearing sensitivity at the cochlea in noisy environments that exacerbate the damage induced by loud sound. Journal of Neuroscience 20:6684-6693.

Ramekers D, Versnel H, Grolman W, Klis SFL (2012) Neurotrophins and their role in the cochlea. Hearing Res 288:19-33.

Rask-Andersen H, Schrott-Fischer A, Pfaller K, Glueckert R (2006) Perilymph/modiolar communication routes in the human cochlea. Ear Hearing 27:457-465.

Reif R, Zhi Z, Dziennis S, Nuttall AL, Wang RK (2013) Changes in cochlear blood flow in mice due to loud sound exposure measured with Doppler optical microangiography and laser Doppler flowmetry. Quant Imaging Med Surg 3:235-242.

Reimer K (1993) Simultaneous demonstration of Fos-like immunoreactivity and 2-deoxy-glucose uptake in the inferior colliculus of the mouse. Brain Res 616:339-343.

Rejali D, Lee VA, Abrashkin KA, Humayun N, Swiderski DL, Raphael Y (2007) Cochlear implants and ex vivo BDNF gene therapy protect spiral ganglion neurons. Hearing Res 228:180-187.

Rhode WS, Smith PH (1986) Encoding timing and intensity in the ventral cochlear nucleus of the cat. J Neurophysiol 56:261-286.

Rios M, Fan GP, Fekete C, Kelly J, Bates B, Kuehn R, Lechan RM, Jaenisch R (2001) Conditional deletion of brain-derived neurotrophic factor in the postnatal brain leads to obesity and hyperactivity. Mol Endocrinol 15:1748-1757.

Riquelme R, Saldana E, Osen KK, Ottersen OP, Merchan MA (2001) Colocalization of GABA and glycine in the ventral nucleus of the lateral lemniscus in rat: An in situ hybridization and semiquantitative immunocytochemical study. Journal of Comparative Neurology 432:409-424.

Robards MJ (1979) Somatic Neurons in the Brain-Stem and Neocortex Projecting to the External Nucleus of the Inferior Colliculus - Anatomical Study in the Opossum. Journal of Comparative Neurology 184:547-&.

Roberson DW, Alosi JA, Cotanche DA (2004) Direct transdifferentiation gives rise to the earliest new hair cells in regenerating avian auditory epithelium. J Neurosci Res 78:461-471.

Rowitch DH, Mcmahon AP (1995) Pax-2 Expression in the Murine Neural Plate Precedes and Encompasses the Expression Domains of Wnt-1 and En-1. Mech Develop 52:3-8.

Roy S, Johnston AH, Newman TA, Glueckert R, Dudas J, Bitsche M, Corbacella E, Rieger G, Martini A, Schrott-Fischer A (2010) Cell-specific targeting in the mouse inner ear using nanoparticles conjugated with a neurotrophin-derived peptide ligand: Potential tool for drug delivery. Int J Pharmaceut 390:214-224.

Rubel EW, Dew LA, Roberson DW (1995) Mammalian Vestibular Hair Cell Regeneration. Science 267:701-703.

Rubel EW, Fritzsch B (2002) Auditory system development: Primary auditory neurons and their targets. Annu Rev Neurosci 25:51-101.

Ruttiger L, Panford-Walsh R, Schimmang T, Tan J, Zimmermann U, Rohbock K, Kopschall I, Limberger A, Muller M, Fraenzer JT, Cimerman J, Knipper M (2007) BDNF mRNA expression and protein localization are changed in age-related hearing loss. Neurobiol Aging 28:586-601.

Ryals BM, Dent ML, Dooling RJ (2013) Return of function after hair cell regeneration. Hearing Res 297:113-120.

Ryals BM, Rubel EW (1988) Hair Cell Regeneration after Acoustic Trauma in Adult Coturnix Quail. Science 240:1774-1776.

Safieddine S, Eybalin M (1992) Triple Immunofluorescence Evidence for the Coexistence of Acetylcholine, Enkephalins and Calcitonin Gene-Related Peptide within Efferent (Olivocochlear) Neurons of Rats and Guinea-Pigs. European Journal of Neuroscience 4:981-992.

Safieddine S, Prior AMS, Eybalin M (1997) Choline acetyltransferase, glutamate decarboxylase, tyrosine hydroxylase, calcitonin gene-related peptide and opioid peptides coexist in lateral efferent neurons of rat and guinea-pig. European Journal of Neuroscience 9:356-367.

Saldana E, Feliciano M, Mugnaini E (1996) Distribution of descending projections from primary auditory neocortex to inferior colliculus mimics the topography of intracollicular projections. J Comp Neurol 371:15-40.

Sale A, Berardi N, Spolidoro M, Baroncelli L, Maffei L (2010) GABAergic inhibition in visual cortical plasticity. Front Cell Neurosci 4.

Salt AN, King EB, Hartsock JJ, Gill RM, O'Leary SJ (2012) Marker entry into vestibular perilymph via the stapes following applications to the round window niche of guinea pigs. Hearing Res 283:14-23.

Salt AN, Ohyama K, Thalmann R (1991) Radial Communication between the Perilymphatic Scalae of the Cochlea .1. Estimation by Tracer Perfusion. Hearing Res 56:29-36.

Salvi RJ, Saunders SS, Gratton MA, Arehole S, Powers N (1990) Enhanced Evoked-Response Amplitudes in the Inferior Colliculus of the Chinchilla Following Acoustic Trauma. Hearing Res 50:245-258.

Sanchez JT, Gans D, Wenstrup JJ (2008) Glycinergic "Inhibition" mediates selective excitatory responses to combinations of sounds. Journal of Neuroscience 28:80-90.

Semple MN, Aitkin LM (1980) Physiology of Pathway from Dorsal Cochlear Nucleus to Inferior Colliculus Revealed by Electrical and Auditory-Stimulation. Experimental Brain Research 41:19-28.

Sergeyenko Y, Lall K, Liberman MC, Kujawa SG (2013) Age-Related Cochlear Synaptopathy: An Early-Onset Contributor to Auditory Functional Decline. Journal of Neuroscience 33:13686-13694.

Serviere J, Webster WR, Calford MB (1984) Isofrequency labelling revealed by a combined [14C]-2-deoxyglucose, electrophysiological, and horseradish peroxidase study of the inferior colliculus of the cat. J Comp Neurol 228:463-477.

Shibata SB, Cortez SR, Beyer LA, Wiler JA, Di Polo A, Pfingst BE, Raphael Y (2010) Transgenic BDNF induces nerve fiber regrowth into the auditory epithelium in deaf cochleae. Exp Neurol 223:464-472.

Schabitz WR, Schwab S, Spranger M, Hacke W (1997) Intraventricular brain-derived neurotrophic factor reduces infarct size after focal cerebral ischemia in rats. J Cerebr Blood F Met 17:500-506.

Schaette R, McAlpine D (2011) Tinnitus with a Normal Audiogram: Physiological Evidence for Hidden Hearing Loss and Computational Model. Journal of Neuroscience 31:13452-13457.

Schecterson LC, Bothwell M (1994) Neurotrophin and neurotrophin receptor mRNA expression in developing inner ear. Hear Res 73:92-100.

Scheper V, Wolf M, Scholl M, Kadlecova Z, Perrier T, Klok HA, Saulnier P, Lenarz T, Stover T (2009) Potential novel drug carriers for inner ear treatment: hyperbranched polylysine and lipid nanocapsules. Nanomedicine-Uk 4:623-635.

Schimmang T, Tan J, Muller M, Zimmermann U, Rohbock K, Kopschall I, Limberger A, Minichiello L, Knipper M (2003) Lack of Bdnf and TrkB signalling in the postnatal cochlea leads to a spatial reshaping of innervation along the tonotopic axis and hearing loss. Development 130:4741-4750.

Schmiedt RA, Okamura HO, Lang H, Schulte BA (2002) Ouabain application to the round window of the gerbil cochlea: A model of auditory neuropathy and apoptosis. Jaro 3:223-233.

Schneggenburger R, Forsythe ID (2006) The calyx of Held. Cell Tissue Res 326:311-337.

Schoen CJ, Burmeister M, Lesperance MM (2013) Diaphanous homolog 3 (Diap3) overexpression causes progressive hearing loss and inner hair cell defects in a transgenic mouse model of human deafness. PLoS One 8:e56520.

Schofield BR (2009) Projections to the inferior colliculus from layer VI cells of auditory cortex. Neuroscience 159:246-258.

Schuknecht HF (1964) Further Observations on the Pathology of Presbycusis. Archives of otolaryngology 80:369-382.

Simmons D JD, DC de Caprona, B Fritzsch (2011) Development of the inner ear efferent system: Springer New York.

Singer W, Panford-Walsh R, Knipper M (2014) The function of BDNF in the adult auditory system. Neuropharmacology 76:719-728.

Sivaramakrishnan S, Sterbing-D'Angelo SJ, Filipovic B, D'Angelo WR, Oliver DL, Kuwada S (2004) GABA(A) synapses shape neuronal responses to sound intensity in the inferior colliculus. J Neurosci 24:5031-5043.

Sly DJ, Hampson AJ, Minter RL, Heffer LF, Li J, Millard RE, Winata L, Niasari A, O'Leary SJ (2012) Brain-Derived Neurotrophic Factor Modulates Auditory Function in the Hearing Cochlea. Jaro-J Assoc Res Oto 13:1-16.

Sobkowicz HM, August BK, Slapnick SM (2002) Influence of neurotrophins on the synaptogenesis of inner hair cells in the deaf Bronx waltzer (bv) mouse organ of Corti in culture. Int J Dev Neurosci 20:537-554.

Spandow O, Hellstrom S, Anniko M (1990) Structural-Changes in the Round Window Membrane Following Exposure to Escherichia-Coli Lipopolysaccharide and Hydrocortisone. Laryngoscope 100:995-1000.

Spirou GA, Davis KA, Nelken I, Young ED (1999) Spectral integration by type II interneurons in dorsal cochlear nucleus. J Neurophysiol 82:648-663.

Staecker H, Gabaizadeh R, Federoff H, Van de Water TR (1998) Brain-derived neurotrophic factor gene therapy prevents spiral ganglion degeneration after hair cell loss. Otolaryng Head Neck 119:7-13.

Staecker H, VanDeWater TR, Lefebvre PP, Liu W, Moghadassi M, GalinovicSchwartz V, Malgrange B, Moonen G (1996) NGF, BDNF and NT-3 play unique roles in the in vitro development and patterning of innervation of the mammalian inner ear. Dev Brain Res 92:49-60.

Sterio DC (1984) The unbiased estimation of number and sizes of arbitrary particles using the disector. J Microsc 134:127-136.

Stiebler I, Ehret G (1985) Inferior Colliculus of the House Mouse .1. A Quantitative Study of Tonotopic Organization, Frequency Representation, and Tone-Threshold Distribution. Journal of Comparative Neurology 238:65-76.

Stone JS, Cotanche DA (2007) Hair cell regeneration in the avian auditory epithelium. Int J Dev Biol 51:633-647.

Stover T, Yagi M, Raphael Y (1999) Cochlear gene transfer: round window versus cochleostomy inoculation. Hearing Res 136:124-130.

Suga A, Taira M, Nakagawa S (2009) LIM family transcription factors regulate the subtype-specific morphogenesis of retinal horizontal cells at post-migratory stages. Dev Biol 330:318-328.

Sugimoto S, Hosokawa Y, Horikawa J, Nasu M, Taniguchi I (2002) Spatial focusing of neuronal responses induced by asynchronous two-tone stimuli in the guinea pig auditory cortex. Cereb Cortex 12:506-514.

Sun YF, Dykes IM, Liang XQ, Eng SR, Evans SM, Turner EE (2008) A central role for Islet1 in sensory neuron development linking sensory and spinal gene regulatory programs. Nat Neurosci 11:1283-1293.

Syka J (2002) Plastic changes in the central auditory system after hearing loss, restoration of function, and during learning. Physiological Reviews 82:601-636.

Syka J, Popelar J (1984) Inferior Colliculus in the Rat - Neuronal Responses to Stimulation of the Auditory-Cortex. Neurosci Lett 51:235-240.

Syka J, Popelar J, Kvasnak E, Astl J (2000) Response properties of neurons in the central nucleus and external send dorsal cortices of the inferior colliculus in guinea pig. Experimental Brain Research 133:254-266.

Syka J, Popelář J, R. D, A. V (1988) Descending Central Auditory Pathway — Structure and Function. In: Auditory Pathway (Syka J., M. R. B., ed), pp 279-292: Springer US.

Sykova E, Syka J, Johnstone BM, Yates GK (1987) Longitudinal Flow of Endolymph Measured by Distribution of Tetraethylammonium and Choline in Scala Media. Hearing Res 28:161-171.

Tamura T, Kita T, Nakagawa T, Endo T, Kim TS, Ishihara T, Mizushima Y, Higaki M, Ito J (2005) Drug delivery to the cochlea using PLGA nanoparticles. Laryngoscope 115:2000-2005.

Tanaka K, Motomura S (1981) Permeability of the Labyrinthine Windows in Guinea-Pigs. Arch Oto-Rhino-Laryn 233:67-75.

Taranda J, Maison SF, Ballestero JA, Katz E, Savino J, Vetter DE, Boulter J, Liberman MC, Fuchs PA, Elgoyhen AB (2009) A Point Mutation in the Hair Cell Nicotinic Cholinergic Receptor Prolongs Cochlear Inhibition and Enhances Noise Protection. Plos Biol 7:71-83.

Terenghi G (1999) Peripheral nerve regeneration and neurotrophic factors. J Anat 194:1-14.

Tollin DJ, Koka K, Tsai JJ (2008) Interaural level difference discrimination thresholds for single neurons in the lateral superior olive. Journal of Neuroscience 28:4848-4860.

Tonkin EG, Erve JCL, Valentine WM (2000) Disulfiram produces a non-carbon disulfide-dependent Schwannopathy in the rat. J Neuropath Exp Neur 59:786-797.

Tonkin EG, Valentine HL, Milatovic DM, Valentine WM (2004) N,N-diethyldithiocarbamate produces copper accumulation, lipid peroxidation, and myelin injury in rat peripheral nerve. Toxicol Sci 81:160-171.

Torres M, Giraldez F (1998) The development of the vertebrate inner ear. Mech Develop 71:5-21.

Trautwein P, Hofstetter P, Wang J, Salvi R, Nostrant A (1996) Selective inner hair cell loss does not alter distortion product otoacoustic emissions. Hear Res 96:71-82.

Turgeon B, Meloche S (2009) Interpreting neonatal lethal phenotypes in mouse mutants: insights into gene function and human diseases. Physiol Rev 89:1-26.

Uchida Y, Ando F, Shimokata H, Sugiura S, Ueda H, Nakashima T (2008) The effects of aging on distortion-product otoacoustic emissions in adults with normal hearing. Ear Hearing 29:176-184.

Vanderkerken S, Vanheede T, Toncheva V, Schacht E, Wolfert MA, Seymour L, Urtti A (2000) Synthesis and evaluation of poly(ethylene glycol)-polylysine block copolymers as carriers for gene delivery. J Bioact Compat Pol 15:115-138.

Vogels TP, Froemke RC, Doyon N, Gilson M, Haas JS, Liu R, Maffei A, Miller P, Wierenga CJ, Woodin MA, Zenke F, Sprekeler H (2013) Inhibitory synaptic plasticity: spike timing-dependence and putative network function. Front Neural Circuits 7:119.

Waaijer L, Klis SFL, Ramekers D, Van Deurzen MHW, Hendriksen FGJ, Grolman W (2013) The Peripheral Processes of Spiral Ganglion Cells After Intracochlear Application of Brain-Derived Neurotrophic Factor in Deafened Guinea Pigs. Otol Neurotol 34:570-578.

Wan GQ, Gomez-Casati ME, Gigliello AR, Liberman MC, Corfas G (2014) Neurotrophin-3 regulates ribbon synapse density in the cochlea and induces synapse regeneration after acoustic trauma. Elife 3.

Wang HC, Bergles DE (2015) Spontaneous activity in the developing auditory system. Cell Tissue Res 361:65-75.

Whitney IE, Raven MA, Ciobanu DC, Poche RA, Ding Q, Elshatory Y, Gan L, Williams RW, Reese BE (2011) Genetic modulation of horizontal cell number in the mouse retina. Proc Natl Acad Sci U S A 108:9697-9702.

Wickstrom M, Danielsson K, Rickardson L, Gullbo J, Nygren P, Isaksson A, Larsson R, Lovborg H (2007) Pharmacological profiling of disulfiram using human tumor cell lines and human tumor cells from patients. Biochem Pharmacol 73:25-33.

Wiechers B, Gestwa G, Mack A, Carroll P, Zenner HP, Knipper M (1999) A changing pattern of brain-derived neurotrophic factor expression correlates with the rearrangement of fibers during cochlear development of rats and mice. Journal of Neuroscience 19:3033-3042.

Willingham MC (1999) Cytochemical methods for the detection of apoptosis. J Histochem Cytochem 47:1101-1109.

Wilson WR, Byl FM, Laird N (1980) The Efficacy of Steroids in the Treatment of Idiopathic Sudden Hearing-Loss - a Double-Blind Clinical-Study. Arch Otolaryngol 106:772-776.

Winer JA (2005a) Decoding the auditory corticofugal systems. Hearing Res 207:1-9.

Winer JA (2005b) Three systems of descending projections to the inferior colliculus. In: The inferior colliculus (Winer J.A., S. C. E., ed), pp 231–247 New York: Springer.

Winer JA, Larue DT, Diehl JJ, Hefti BJ (1998) Auditory cortical projections to the cat inferior colliculus. J Comp Neurol 400:147-174.

Winslow RL, Sachs MB (1987) Effect of electrical stimulation of the crossed olivocochlear bundle on auditory nerve response to tones in noise. Journal of neurophysiology 57:1002-1021.

Wise AK, Hume CR, Flynn BO, Jeelall YS, Suhr CL, Sgro BE, O'Leary SJ, Shepherd RK, Richardson RT (2010) Effects of Localized Neurotrophin Gene Expression on Spiral Ganglion Neuron Resprouting in the Deafened Cochlea. Mol Ther 18:1111-1122.

Wong ACY, Ryan AF (2015) Mechanisms of sensorineural cell damage, death and survival in the cochlea. Front Aging Neurosci 7.

Xia A, Song Y, Wang R, Gao SS, Clifton W, Raphael P, Chao SI, Pereira FA, Groves AK, Oghalai JS (2013) Prestin regulation and function in residual outer hair cells after noise-induced hearing loss. PLoS One 8:e82602.

Xu H, Kotak VC, Sanes DH (2010) Normal Hearing Is Required for the Emergence of Long-Lasting Inhibitory Potentiation in Cortex. Journal of Neuroscience 30:331-341.

Yamamoto N, Tanigaki K, Tsuji M, Yabe D, Ito J, Honjo T (2006) Inhibition of Notch/RBP-J signaling induces hair cell formation in neonate mouse cochleas. J Mol Med-Jmm 84:37-45.

Yan J, Ehret G (2001) Corticofugal reorganization of the midbrain tonotopic map in mice. Neuroreport 12:3313-3316.

Yates GK (1991) Auditory-nerve spontaneous rates vary predictably with threshold. Hear Res 57:57-62.

Ylikoski J, Pirvola U, Moshnyakov M, Palgi J, Arumae U, Saarma M (1993) Expression Patterns of Neurotrophin and Their Receptor Messenger-Rnas in the Rat Inner-Ear. Hearing Res 65:69-78.

Zauner W, Ogris M, Wagner E (1998) Polylysine-based transfection systems utilizing receptor-mediated delivery. Adv Drug Deliver Rev 30:97-113.

Zhang WK, Zhang Y, Lobler M, Schmitz KP, Ahmad A, Pyykko I, Zou J (2011) Nuclear entry of hyperbranched polylysine nanoparticles into cochlear cells. Int J Nanomed 6:535-546.

Zhang X, Oulad-Abdelghani M, Zelkin AN, Wang YJ, Haikel Y, Mainard D, Voegel JC, Caruso F, Benkirane-Jessel N (2010a) Poly(L-lysine) nanostructured particles for gene delivery and hormone stimulation. Biomaterials 31:1699-1706.

Zhang Y, Zhang WK, Johnston AH, Newman TA, Pyykko I, Zou J (2010b) Improving the visualization of fluorescently tagged nanoparticles and fluorophore-labeled molecular probes by treatment with CuSO4 to quench autofluorescence in the rat inner ear. Hearing Res 269:1-11.

Zhang Y, Zhang WK, Johnston AH, Newman TA, Pyykko I, Zou J (2012) Targeted delivery of Tet1 peptide functionalized polymersomes to the rat cochlear nerve. Int J Nanomed 7:1015-1022.

Zhao BW, Zhou ZX, Shen YQ (2016) Effects of chirality on gene delivery efficiency of polylysine. Chinese J Polym Sci 34:94-103.

Zheng JL, Gao WQ (2000) Overexpression of Math1 induces robust production of extra hair cells in postnatal rat inner ears. Nat Neurosci 3:580-586.

Zhou CH, Sun JJ, Gong SS, Gao G (2009) [Comparison of the antioxidants lipoic acid pharmacokinetics in inner ear between intravenous and intratympanic administration in guinea pigs.]. Zhonghua Er Bi Yan Hou Tou Jing Wai Ke Za Zhi 44:1034-1037.

Zhou JX, Shore S (2006) Convergence of spinal trigeminal and cochlear nucleus projections in the inferior colliculus of the guinea pig. Journal of Comparative Neurology 495:100-112.

Zou J, Poe D, Ramadan UA, Pyykko I (2012a) Oval Window Transport of Gd-DOTA From Rat Middle Ear to Vestibulum and Scala Vestibuli Visualized by In Vivo Magnetic Resonance Imaging. Ann Oto Rhinol Laryn 121:119-128.

Zou J, Saulnier P, Perrier T, Zhang Y, Manninen T, Toppila E, Pyykko I (2008) Distribution of lipid nanocapsules in different cochlear cell Populations after round window membrane permeation. J Biomed Mater Res B 87b:10-18.

Zou J, Sood R, Ranjan S, Poe D, Ramadan UA, Pyykko I, Kinnunen PKJ (2012b) Size-Dependent Passage of Liposome Nanocarriers With Preserved Posttransport Integrity Across the Middle-Inner Ear Barriers in Rats. Otol Neurotol 33:666-673.

Zuccotti A, Kuhn S, Johnson SL, Franz C, Singer W, Hecker D, Geisler HS, Kopschall I, Rohbock K, Gutsche K, Dlugaiczyk J, Schick B, Marcotti W, Ruttiger L, Schimmang T, Knipper M (2012) Lack of brain-derived neurotrophic factor hampers inner hair cell synapse physiology, but protects against noise-induced hearing loss. J Neurosci 32:8545-8553.

9. List of own publications

Publications related to the thesis and contributions of individual co-authors

1. **Chumak T**, Bohuslavova R, Macova I, Dodd N, Buckiova D, Fritzsch B, Syka J, Pavlinkova G: Deterioration of the Medial Olivocochlear Efferent System Accelerates Age-Related Hearing Loss in Pax2-Isl1 Transgenic Mice. *Mol. Neurobiol.*, 2016; 53(4): 2368-2383
   (IF 5.137)

   Contributions:
   Recording of ABRs and DPOAEs: Chumak T
   Immunohistochemistry, morphological analysis: Chumak T, Buckiova D, Bohuslavova R, Macova I,
   Data processing: Chumak T, Bohuslavova R, Macova I, Dodd N
   Statistical evaluation: Chumak T, Bohuslavova R, Macova I, Dodd N
   Lipophilic dye tracing: Fritzsch B, Dodd N
   Quantification of gene expression: Bohuslavova R, Macova I, Dodd N
   Experiment guidance, manuscript supervision: Fritzsch B, Syka J, Pavlinkova G.

2. **Chumak T**, Rüttiger L, Lee SC, Campanelli D, Zuccotti A, Singer W, Popelář J, Gutsche K, Geisler HS, Schraven SP, Jaumann M, Panford-Walsh R, Hu J, Schimmang T, Zimmermann U, Syka J, Knipper M: BDNF in Lower Brain Parts Modifies Auditory Fiber Activity to Gain Fidelity but Increases the Risk for Generation of Central Noise After Injury. *Mol. Neurobiol.*, 2015 [Epub ahead of print]
   (IF 5.137)

   Contributions:
   Recording of ABRs and DPOAEs: Chumak T
   Extracellular recording of neuronal activity in the inferior colliculus: Chumak T, Popelář J
   Data processing: Chumak T, Popelář J
   Immunohistochemistry: Singer W
   Statistical analysis: Chumak T, Zimmermann U
   Experiment guidance, manuscript supervision: Rüttiger L, Syka J, Knipper M.

3. Buckiová D, Ranjan S, Newman TA, Johnston AH, Sood R, Kinnunen PK, Popelář J, **Chumak T**, Syka J: Minimally invasive drug delivery to the cochlea through the application of nanoparticles to the round window membrane. *Nanomedicine (Lond)*, 2012; 7(9): 1339-54
   (IF 5.413)

Contributions:
Recording of ABRs and DPOAEs: Chumak T
RWM application: Chumak T
Immunohistochemistry: Chumak T, Buckiová D
Data processing: Chumak T, Buckiová D, Popelář J
Preparation of nanoparticles: Ranjan S, Newman TA, Johnston AH, Sood R, Kinnunen PK
Experiment guidance, manuscript supervision: Popelář J, Syka J

Other author's impacted publications:

Bohuslavova R, Dodd N, Macova I, **Chumak T**, Horak M, Syka J, Fritzsch B, Pavlinkova G: Pax2-Islet1 Transgenic Mice Are Hyperactive and Have Altered Cerebellar Foliation.
Mol. Neurobiol., 2016. [Epub ahead of print]
(IF 5.137)

Skoloudik L, Chrobok V, Kalfert D, Koci Z, Sykova E, **Chumak T**, Popelar J, Syka J, Laco J, Dedková J, Dayanithi G, Filip S: Human multipotent mesenchymal stromal cells in the treatment of postoperative temporal bone defect: an animal model.
Cell Transplant., 2015. [Epub ahead of print]
(IF 3.127)

Popelar J, Suta D, Lindovsky J, Bures Z, Pysanenko K, **Chumak T**, Syka J: Cooling of the auditory cortex modifies neuronal activity in the inferior colliculus in rats. *Hear. Res.* 2016; 332: 7-16
(IF 2.07)

Rybalko N, **Chumak T**, Bures Z, Popelar J, Suta D, Syka J: Development of the acoustic startle response in rats and its change after early acoustic trauma. *Behav. Brain Res.,* 2015; 286: 212-221
(IF 3.391)

Bures Z, Bartosova J, Lindovsky J, **Chumak T**, Popelar J, Syka J: Acoustical enrichment during early postnatal development changes response properties of inferior colliculus neurons in rats. *European J. Neurosci.,* 2014; 40(11): 3674-3683
(IF 3.181)